PSERC

Detection, Prevention and Mitigation of Cascading Events

Final Project Report

Power Systems Engineering Research Center

A National Science Foundation
Industry/University Cooperative Research Center
since 1996

Power Systems Engineering Research Center

Detection, Prevention and Mitigation of Cascading Events

Final Project Report

Project Team

Mani V. Venkatasubramanian, Project Leader, Washington State University

Mladen Kezunovic, Texas A&M University

Vijay Vittal, Arizona State University

PSERC Publication 08-18

September 2008

Information about this project

For information about this project contact:

Mani V. Venkatasubramanian
Professor
School of Electrical Engineering and Computer Science
Washington State University
Pullman WA 99164-2752
Tel: 509-335-6452
Fax: 509-335-3818
Email: mani@wsu.edu

Power Systems Engineering Research Center

The Power Systems Engineering Research Center (PSERC) is a multi-university Center conducting research on challenges facing the electric power industry and educating the next generation of power engineers. More information about PSERC can be found at the Center's website: http://www.pserc.org.

For additional information, contact:

Power Systems Engineering Research Center
Arizona State University
577 Engineering Research Center
Tempe, Arizona 85287-5706
Phone: 480-965-1643
Fax: 480-965-0745

Notice Concerning Copyright Material

Executive Summary

The risk of cascading outages in power systems manifests itself in a number of ways. With the advent of structured competitive power markets, and with the lack of needed investment in the transmission grid, electric power systems are increasingly being operated close to their limits. Potential terrorist threats raise concerns about power system being placed in unforeseen operating conditions. Recent blackouts in North America and in Europe show that the risk of cascading events is real with the cost of the 2003 North American blackout estimated to be around $10 Billion. As the power system becomes more stressed there are a host of reasons (such as weak connections, unexpected events, hidden failures in protection system, and human errors) for the loss of stability eventually leading to catastrophic failures.

When a power system is subjected to large disturbances control actions need to be taken to steer the system away from severe consequences and to limit the extent of the disturbance. This is particular true if system is in an operating condition that makes it unusually vulnerable to catastrophic failure. In a previous PSERC project (S-19 that ended in 2005), we developed novel algorithms for each of the following steps:

1. **Detection of major disturbances and protective relay operations leading to cascading events.** The detection algorithms improved capabilities of real-time fault detection and analysis to classify the impact of a fault towards initiating cascading outages.
2. **Wide-area measurement based detection and remedial control actions.** The wide-area mitigation algorithms include methods for reliably extracting modal information on critical wide-area modes through real-time wide-area Phasor Measurement Unit (PMU) measurements. They also provide specific control actions to damp out the oscillations when problems are detected.
3. **Adaptive islanding with selective under-frequency load shedding.** The adaptive islanding algorithms suggest methods for controlled islanding of the system should mitigation strategies fail.

The algorithms were shown to be effective using realistic computer models of test power systems. In this project, we focused on prototype implementations of those algorithms at collaborating PSERC member utilities.

Volume I: Detection of major disturbances and protective relay operations leading to cascading events (Lead: Mladen Kezunovic, Texas A&M University).

This research volume proposes a system-wide monitoring and control solution intended for use at control centers. The solution includes steady state and dynamic analysis tools. The tools may be used to check system stability, find the vulnerable elements, and send commands to the local tools for initiating detailed monitoring.

The local monitoring and control tools are intended for installation at substations. They have the capability for advanced fault analysis and relay monitoring using neural network

for fault detection and classification, synchronized sampling for fault location, and event tree analysis for relay operation verification. The local monitoring and control tools can characterize a disturbance and make a correction if there is an unintended relay operation. This information can be sent to a system monitoring and control tool for better security control.

Implementation of the proposed algorithms requires assessment of data handling requirements. Data handling includes obtaining, converting and storing data. Consideration must also be given to integrating data from various sources: Supervisory Control and Data Acquisition (SCADA) systems, Intelligent Electronic Devices, and other add-on high speed data acquisition systems. Data from system simulation packages is also needed to perform steady state analysis.

Steady state and dynamic analysis cases were studied using a model of the entire Entergy system. Vulnerability Index and Margin Index for each bus, generator, and transmission line were calculated to identify the vulnerability and security margin information for each individual power system element. A 500kV Extra High Voltage transmission line was modeled for evaluating local monitoring and analysis tools. The results indicate that when using adequate training sets and time synchronized data, the new algorithms are quite accurate and provide assessment of system conditions during cascades that are not feasible with any of the existing techniques.

Volume II: Wide-area measurement based detection and remedial control actions (Lead: Mani V. Venkatasubramanian, Washington State University)

If persistent over an extended period of time (e.g., 30 minutes), poorly damped oscillations in a power system can lead to permanent damage of expensive power system equipment and pose power quality issues. Negatively-damped oscillations can be even more problematic by resulting in sudden tripping of generators and/or widespread system blackout such as occurred in the August 10, 1996 western power system blackout.

In this research project, we designed, developed and implemented an Oscillation Monitoring System (OMS) that uses wide-area PMU measurements for automatically monitoring for poorly damped and/or negatively-damped oscillatory modes. OMS includes two complementary engines that provide real-time modal analysis: 1) an automatic Prony-type analysis of power system responses following routine events such as line tripping and generator outages; and 2) an engine for continuous estimation of poorly damped mode frequencies and their damping ratios from routine ambient noise PMU measurements. The algorithms were structured as a rule-based expert system for simplifying the Prony analysis of nonlinear PMU responses in real-time while avoiding false alarms and incorrect estimates. The OMS can issue operator alerts as well as initiate triggers to start appropriate control actions to improve damping of problematic oscillatory modes. A wide-area damping control strategy that uses Static VAR Compensators was developed in the previous PSERC project. Another damping control strategy was developed in this project. It uses HVDC modulation to improve the damping of inter-area oscillatory modes.

A prototype version of OMS has been integrated into real-time monitoring capability of the Phasor Data Concentrator at TVA. At present, it monitors PMU data from within TVA for estimating the frequency, damping, and mode shape of oscillatory modes. We are also collaborating with the Electric Power Group and Bonneville Power Administration (BPA) to implement a version of the Prony-type first engine of OMS at two PSERC companies: BPA and the California Independent System Operator. An off-line version of three Prony type algorithms from this project has been integrated into an event analysis software package being developed by Electric Power Group Inc., and the package aimed at off-line modal analysis of PMU measurements is available to PSERC members.

Volume III: Adaptive islanding with selective under-frequency load shedding (Lead: Vijay Vittal, Arizona State University)

The main objective of this portion of the research project was to develop a fast and accurate assessment tool to determine the timing of conducting controlled islanding scheme in real time for preventing cascading events that could lead to a large scale blackout. This work demonstrated an event-initiated controlled islanding scheme using phasor measurement units and decision trees to stabilize power systems following severe contingencies. The demonstration was performed on a test system provided by Entergy.

A control scheme for must be designed very carefully since the costs can be quite high for unneeded controlled separation operation and for failure to operate when needed. Normally, there are two major issues associated with the design of a controlled separation scheme:

i. **Where to island?** This issue mainly focuses on searching for the optimal cut set in the system to satisfy certain constraints, such as (a) coherent generators should stay in one island and (b) the load/generation imbalance of each island should be minimized. Much of the research effort of a previous PSERC project (S-19) focused on addressing this issue. Due to the large computational burden associated with this aspect, the controlled separation cut set is usually obtained offline.

ii. **When to island?** The second issue is to accurately determine the timing of controlled separation. This is the main focus of this research. The objective was to develop an online transient stability prediction scheme to determine whether certain contingencies can initiate severely unstable swings and cause cascading events. If so, controlled separation should be initiated to prevent a large scale blackout.

Taking advantage of synchronized phasor measurements, we developed a decision tree based transient stability assessment scheme for online application. The synchronized signals and high sampling frequency give PMUs the capability of observing different states across the whole system in a common time frame with great accuracy. System

transient behaviors can also be accurately captured compared to the traditional SCADA system. The decision tree technique is an effective data mining tool to solve the classification problems in high data dimensions. It can be used to uncover critical system attributes that contribute to an objective such as transient stability or voltage security. The splitting rules and the corresponding thresholds in the decision trees help to build a nomogram in terms of these critical system parameters and guide system operators effectively.

The project results indicate that out of step swings can be accurately predicted only a few cycles after the initial disturbance using properly trained decision trees. This is much faster than the traditional analysis method. The decision trees also identify transient stability indicators that are good candidates for new PMU locations. With an effective controlled islanding strategy, the system can be stabilized faster with less amount of load to be shed than the uncontrolled separation case.

We developed a software platform that implements the entire approach based on data provides the DSA^{Tools} suite of software from Powertech Labs. The approach also uses commercially-available software called CART developed by Salford Systems for decision tree training and testing.

Next Steps to Advancing this Research

At Texas A&M University, future steps to implementing algorithms for the detecting, classifying, and mitigating cascading events require selection of a utility test set-up. Currently discussions with several utilities under auspices of DOE-CERTS, EPRI, and ERCOT are under way to determine whether such arrangements for the final testing work can be made.

The Washington State University team will continue to work with PSERC utilities and software vendors for field implementations as well as testing, tuning and enhancement of OMS capabilities. Future research needs to focus on determining correct operator actions as well as automatic control actions to improve the damping of problematic oscillatory modes when such problems are detected by OMS.

At Arizona State University, future steps to implementing the controlled islanding work would require testing and implementation at an electric utility. Some of this work is being done in a CERTS project and discussions are under way to consider implementation at a specific company.

Detection, Prevention and Mitigation of Cascading Events:

Detection of Major Disturbances and Protective Relay Operations Leading to Cascading Events

Final Project Report
Part I

Part I Project Team

Mladen Kezunovic
Chengzong Pang
Texas A&M University

Information about Part I of the project report

For information contact:

Mladen Kezunovic, Ph.D., P.E.
Eugene E. Webb Professor
Texas A&M University
Department of Electrical Engineering
College Station, TX 77843-3128
Phone: 979-845-7509
Fax: 979-845-9887
Email: kezunov@ece.tamu.edu

Power Systems Engineering Research Center

The Power Systems Engineering Research Center (PSERC) is a multi-university Center conducting research on challenges facing the electric power industry and educating the next generation of power engineers. More information about PSERC can be found at the Center's website: http://www.pserc.org.

For additional information, contact:

Power Systems Engineering Research Center
Arizona State University
577 Engineering Research Center
Box 878606
Tempe, AZ 85287-8606
Phone: 480-965-1643
Fax: 480-965-0745

Notice Concerning Copyright Material

Acknowledgements

The Power Systems Engineering Research Center sponsored the research project titled "Detection, Prevention and Mitigation of Cascading Events-Prototype Implementation." This is Part I of the final project report.

We express our appreciation for the support provided by PSERC's industrial members and by the National Science Foundation under grants received under the Industry/University Cooperative Research Center program. We also thank Entergy Corporation for its additional support. Special thanks go to Floyd Galvan from Entergy Corporation for providing the case data and technical advice related to Entergy test cases. Other Entergy personnel that provided assistance are: Sujit Mandal, Cesar A. Rincon, Sze Mei Wong, and James A. Cunningham.

Table of Contents

List of Figures

List of Tables

1. Introduction

1.1 Introduction

With the development of flexible electricity markets operation under the deregulation rules, power system became more stressed and power network security and reliability criteria became more complex. The power system cascading outage is quite often a complicated phenomenon, which may finally result in a large area blackout. Different research efforts are aimed at understanding and finding ways for preventing cascading outages. A new interactive scheme of system-wide and local monitoring and control tools for efficiently dealing with cascading outages is introduced by Texas A&M University (TAMU) group earlier, which is presented in part I of PSerc project S-19: Detection of Major Disturbances and Protective Relay Operations Leading to Cascading Events [1].

This research effort focuses on implementing the application of the tools developed and reported earlier [1]. A detailed model of Entergy system is targeted for the demonstration as discussed in related sections of this report. The major objectives of this project are:

- Investigate the data requirements for implementation of the proposed system-wide and local substation algorithms.
- Develop the methods to convert the substation and system-wide data into information and get it ready for the use in related algorithms.
- Develop the implementation framework for system-wide and local monitoring and control tools based on the studied power system.

In this chapter, the background of the problem, as well review of literature dealing with detecting and preventing the cascading events in modern power systems are introduced. The algorithms used as the system-wide and local monitoring and control tools introduced by TAMU earlier are also reviewed in this section.

1.2 Background

Electric power system is one of the most complex man-made systems. Fig. 1.1 shows the conceptual structure of the electric power system [2]. Power system has many special characteristics:

- It is a *complex system* comprised of different kinds of power apparatus such as generators, transformers, transmission lines, substations, various loads and extensive infrastructure of measurements, communication and control equipment.
- It is a *large system* where the equipment used in a given power system is distributed across a large area, and are linked tightly in a network.
- It has a *hierarchy structure*, which determines how the influence of different disturbance propagates to the various levels of monitoring and control.
- It is a *dynamic system*, which means that the system states vary with time including changes in the voltage, angle, active and reactive power, etc.
- It is an *exposed system* subjected to various disturbances due to whether or other causes and as such requires real-time means for monitoring and control to mitigate disturbances

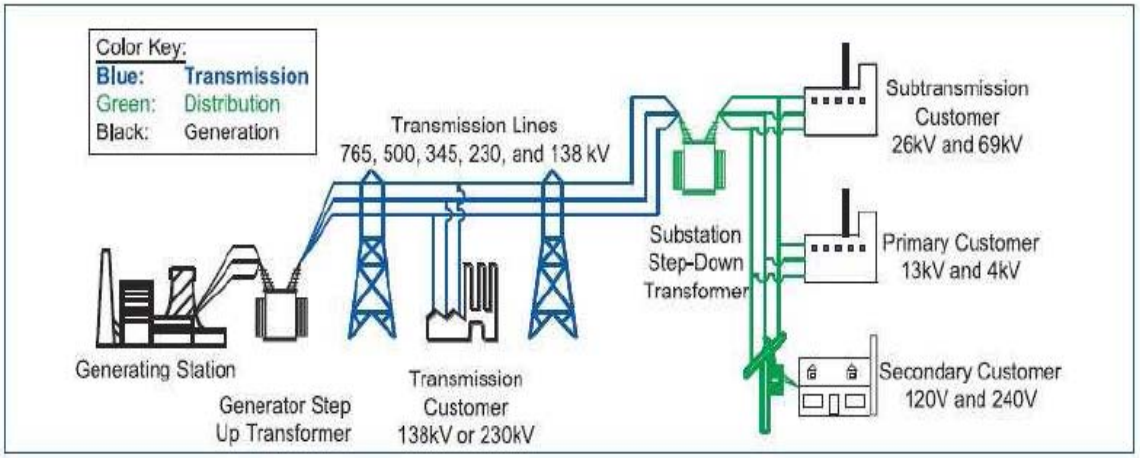

Figure 1.1. Conceptual structure of the electric power system

Since the reliability of power system operation may affect everyone's life, there are continuous attempts to develop the best control and monitoring methods to ensure the

security and stability of power systems. Since power systems are exposed to many kinds of disturbances, which may come from animal contacts, human errors, equipment malfunction, natural disasters, intentional sabotage, etc., and some of these disturbances may cause major power service interruption [2]. Protective relays and other control actions may be invoked to steer the system away from severe consequences, and to limit the extent of the disturbance. This way, most disturbances can be mitigated without power service interruption. But there are small part of disturbances may cause service interruption. Among the disturbances, cascading outage, especially the large-scale cascading outage, draws special attention since it can cause great economic loss to utility companies and other businesses and devastating impact on people's life. For example, Northeastern System Blackout in 2003 led to the load loss of 61.8GW, which influenced more than 50 million people [2]. To illustrate the severity of possible impacts, Table 1-1 shows the summary of some major cascading outages throughout the world. [2-14]

Considering the power system characteristics discussed above, it is very difficult to define a high accuracy mathematical model to describe and fully analyze the system blackout so that it can be predicted and avoided. Hence, we may resort to real time monitoring of such events and developing on-line techniques for detecting, classifying and mitigating such disturbances. Monitoring major disturbances causing unintended protective relay operations leading to cascading events is very important part of preventing and mitigating the cascading events.

Many solutions proposed so far are aimed at understanding and finding ways for detecting, preventing, and mitigating the cascading events. Some of the proposed techniques include dynamic and probabilistic study of the cascade model, application of dynamic decision-event tree analysis, expert systems for wide area back-up protection, inclusion of relay hidden failure analysis, application of special protection schemes, controlled islanding, generalized line outage distribution factors calculation, etc. [15-21] Cascade model study tries to learn the cascading characteristics from the system dynamics, probability, and power system historical data. Dynamic event tree analysis combines the probability and event tree technique for prediction and mitigation of cascading events. It is still very difficult to generate comprehensive event trees due to the complexity and large number of components of the power system. For the wide area back

up protection expert system, it may be easy to apply it in the radial system, but this is not easy to do in a large and mashed transmission network. System Integrity Protection Scheme is typically hardware based and designed for particular conditions. It is not flexible and cannot adapt to the dynamic changing conditions in the competitive market environment. As a result of the review of the background literature, it may be concluded that there are no effective interactive monitoring and control tools developed so far for detecting and mitigating the cascading outage.

TABLE 1-1: Summary of cascading outages around the world

	Location	**Data**	**Lost of MW**	**Affected People**	**Collapse Time**	**Restoration Time**
1	US-Northeastern	Nov. 9, 1965	20000	30 million	13mins	13 hrs
2	New York	July 13, 1977	6000	9 million	1 hr	26 hrs
3	France	Dec. 19, 1978	29000		26mins	5 hrs
4	US-Western	Dec. 22, 1982	12350	5 million		
5	Sweden	Dec. 27, 1983	67% of total load		53 secs	About 5 hrs
6	Tokyo (Japan)	July 23, 1987	8200	2.8 million	20 mins	About 75 mins
7	US-Western	July 2, 1996	11850	2 million	36 secs	a few mins to several hrs
8	US-Western	Aug. 10, 1996	30500	7.5 million	>6 mins	A few mins to 9 hrs
9	Brazil	Mar. 11, 1999	25000	75 million	30 secs	30 mins to 4 hrs
10	US- Northeastern	Aug. 14, 2003	61800	50 million	> 1hr	Up to 4 days
11	Denmark/Sweden	Sept. 23, 2003	6550	4.85 million	7 mins	Average 2 to 4.3 hrs
12	Italy	Sept. 28, 2003	27700	57 million	27 mins	2.5 to 19.5 hrs

It appears that relaying problems and inadequate understanding of unfolding events are two major contributing factors in inability to predict or prevent cascading events. This is discussed in the reports for the August 1996 US West Coast System Blackout and August

2003 US Northeast System Blackout [2,22]. Regarding protective relays, relay failure or unintended operation contribute the most to the inadequate handling of power system disturbances. According to historical data, relaying problems were the contributing factor in almost 70% of the US disturbances from 1984 to 1991 [23]. Another problem is that power system operators lack sufficient analysis and decision support tools to take quick corrective actions needed to mitigate unfolding events. Considering the above factors, a novel interactive scheme of system-wide and local substation monitoring and control tools for detection, prevention and mitigation of cascading events was recently introduced [24-37]. This scheme is aimed at on-line identifying the disturbance leading to cascading events and providing real-time control means for preventing further unfolding of the cascading events while keeping the stability of the power system. The scheme determines system vulnerability and initiates local monitoring to verify correctness of protective relay operations that may contribute to the unfolding vulnerability.

1.3 Organization of the Report

The report is organized into four chapters. Chapter One introduces the project background. The research efforts related to cascading events, as well as the approach proposed in this report and summary of results are discussed in this chapter. Chapter Two reviews the approach proposed by the TAMU group earlier, which is based on the interactive scheme of system-wide and local monitoring and control tools, and is designed to help detect, prevent, and mitigate the cascading outages. Chapter Three presents the implementation of developed system-wide and local analysis tools based on steady state analysis and dynamic analysis. The case studies of neural network based fault detection and classification (NNFDC), synchronized sampling based fault location (SSFL), and event tree analysis (ETA) combined together into an advanced real time fault analysis tool and relay monitoring tool is presented. Conclusion of this report is given in Chapter Four.

2. The Proposed Approach: Review

2.1 Introduction

This chapter reviews the proposed approach for detection, prevention and mitigation of the power system cascading outages, which coordinates system-wide and local monitoring and control tools. The interactive coordination scheme is presented in section 2.2. The system-wide monitoring and control tools are based on routine and event-based security analyses. The local monitoring and control tools are based on advanced fault analysis and relay operation monitoring. Section 2.3 gives the conclusion.

2.2 The Interactive Scheme for coordination of System-Wide and Local Monitoring and Control Tools

The proposed monitoring and control scheme for detection, prevention and mitigation of cascading events coordinates the system-wide and local substation algorithms. The overall interaction is conceptually shown in Fig. 2.1.

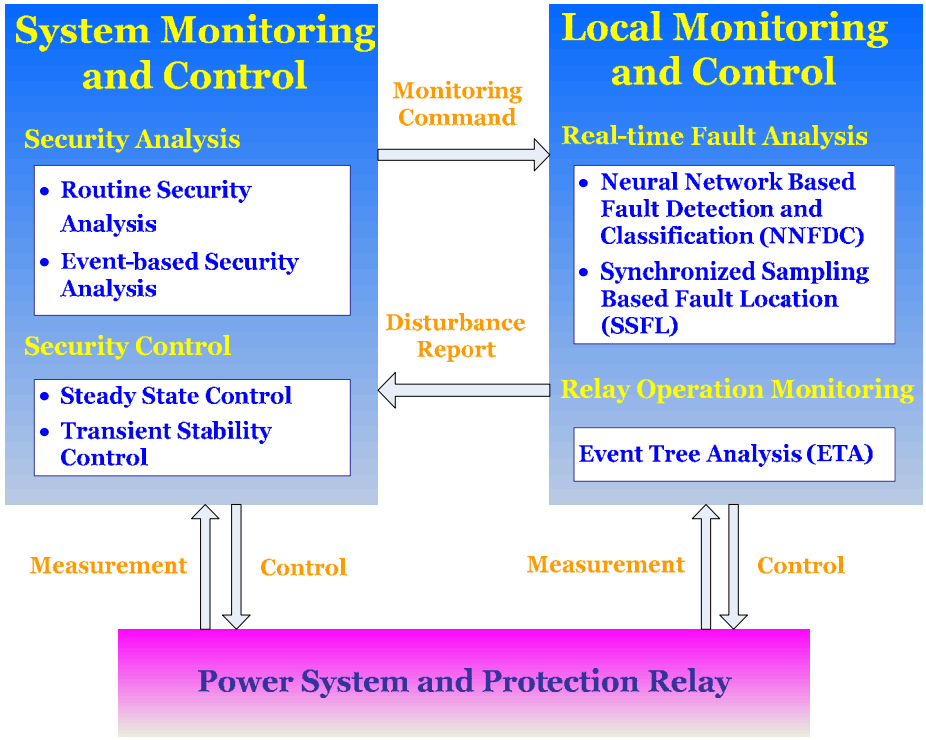

Figure 2.1. Overall interactive monitoring and control scheme

2.2.1 The System-Wide Monitoring and Control Tool

The proposed system-wide monitoring and control tool is intended for installation at the control center. The system tool consists of the routine and event-based security analyses based on the power flow method and topology processing method, along with the security control schemes for expected and unexpected events. Vulnerable elements are identified using calculated Vulnerability Index and Margin Index [24] while related relays are closely monitored. The event-based security analysis is triggered when an unexpected disturbance occurs. It indicates whether the emergency control is needed to mitigate the transient stability problem or not. Steady state control tools are based on Network Contribution Factor (NCF) [26], Generator Distribution Factor (GDF) [38], Load Distribution Factor (LDF) [38], and Selected Minimum Load Shedding (SMLS) used for early detection and prevention of cascading outages as analyzed utilizing steady state method. Transient stability control tools are based on Potential Energy Boundary Surface (PEBS) method [39], Admittance-based Control (ABC) and Generator-input-based Control (GIBC).

Vulnerability Index (VI) and Margin Index (MI) are a good way to assess the vulnerability and security margin of individual element and the whole system. The comprehensive concept of VI as well as MI is developed to give precise vulnerability and margin information for individual system element and the whole system-wide performance. For the generation part, vulnerability indices for real power output, reactive power output and generation loss and margin indices for real and reactive power outputs are given. For the bus part, vulnerability indices for bus voltage performance, loadability and load loss and margin indices for bus voltage performance and loadability are determined. Islanding and isolating buses due to the line outages is considered for the load loss part. For the transmission line part, vulnerability indices for line real power, reactive power, line charging, line bus voltage angle difference, line distance relay performance, and line switch-off influence are given. The margin indices for line flow, line bus voltage angle difference and line distance relay are also given. Different weights of different elements are considered based on their importance and power system operating practice.

For a small size system, one or two line outages may lead to system islanding. Even for a big size system, different control areas may have limited number of tie-lines. If they are disconnected, the whole system may split into several smaller systems and cascading outages may occur in those smaller systems if they are unbalanced. Thus, some critical lines must be identified. The relays on these lines need to be monitored. If they misoperate, system security may be decreased. After the system operation condition is identified as being vulnerable by examining the VI and MI, the topology processing method is used to find single-line connection, single-line connected load bus, and double-line connection, which is based on the node-branch incidence matrix search method. The results could generate the list that can be used in N-1 contingency analysis. Loss of connection of those critical elements may isolate one or several buses from the other part of the system. Thus the lines vulnerable to relay operations can be chosen for detailed monitoring and control by the local tool.

The NCF, GDF, and LDF are the different control methods for power system security control, which are used for the purpose of relieving overload, improving voltage, controlling emergency, etc. NCF method is developed to analyze the influence on branch flow and bus voltage due to power system network parameter variance. GDF and LDF are presented to determine the parameters contributing to the largest variance based on the network topology information and base power flow conditions. The ultimate aim is to give good guidance for solving steady state overload and low voltage problems faster and more accurately without many trials of running the load flow. For example, NCF method can find the most contributing parameter variance which can relieve the line overload or improve the bus voltage by using the base load flow condition and network topology information. Line on/off switching, line parameter change due to TCSC insertion, bus shunt capacitor/reactor on/off switching, can all be considered. Not only single parameter but also multi-parameter analysis and control can be achieved. All these results can be verified by the full AC load flow.

2.2.2 The Local Monitoring and Control Tool

The local monitoring and control tool is intended for installation at local substations. It consists of an advanced real time fault analysis tool and a relay operation monitoring tool utilizing neural network based fault detection and classification algorithm (NNFDC), synchronized sampling based fault location algorithm (SSFL), and event tree analysis (ETA) [33-37], which is shown in Fig. 2.2. The advanced on-line fault analysis tool detects the disturbance by analyzing local measurements. Once the disturbance is detected and classified, event tree analysis process will be invoked to validate relay operations. The combination of the two algorithms performs a more accurate fault analysis than conventional relays do on their own. This provides a reference for monitoring and verification of the distance relay operations. The substation-based solution can provide the system-wide tool with local disturbance information and diagnostic support so that the system-wide tool can utilize local information to take better control action to ensure the secure operation.

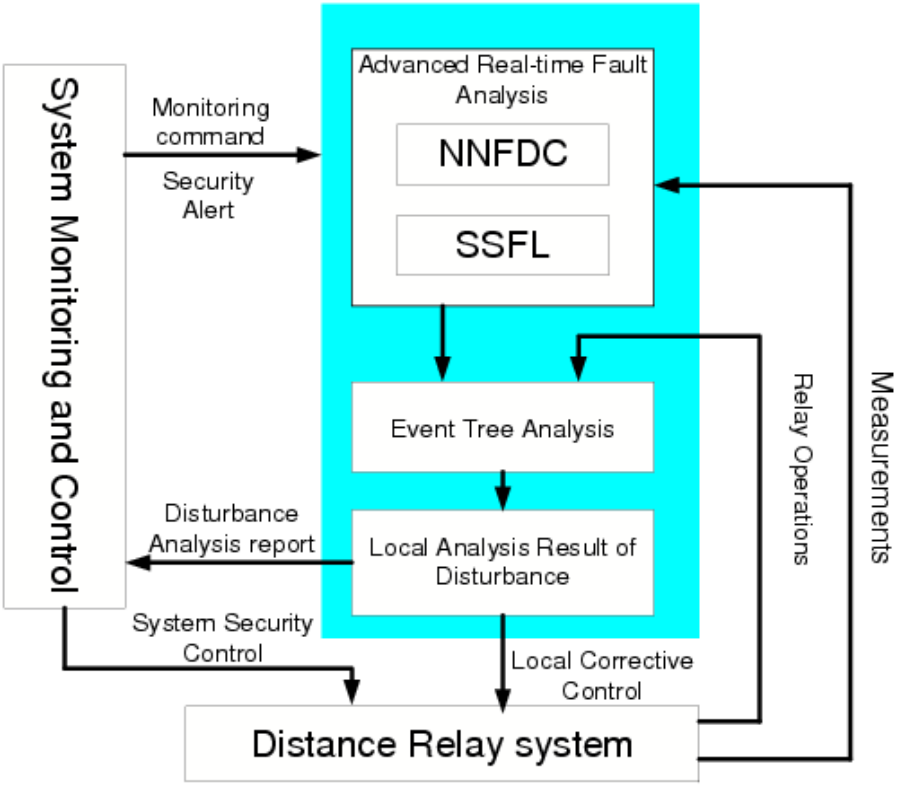

Figure 2.2. Framework of local monitoring and control tools

As mentioned before, the local monitoring and control consists of an advanced real time fault analysis tool and a relay operation monitoring tool. The main technologies used in the local monitoring tool are a neural network based fault detection and classification algorithm, a synchronized sampling based fault location algorithm, and event tree analysis.

- *Neural Network Based Fault Detection and Classification:* Neural network is one of artificial intelligence techniques. The neural network based algorithm classifier is used to detect and classify the disturbances that require protective relay action. Comparing with traditional method, neural network based fault diagnosis algorithms usually uses the time-domain voltage and current signals directly as patterns instead of calculating phasors. The technique compares the input voltage and current signals with well-trained prototypes instead of predetermined settings. Thus accuracy of phasor measurement and relay setting coordination are not an issue in neural network based algorithms as they are in the traditional methods. This provides an advantage of the proposed solution vs the traditional methods. A self-organized, fuzzy ART neural network based fault detection and classification algorithm has been developed, which is conceptually shown in Fig. 2.3. Voltage and current signals from the local measurement are formed as patterns by certain data processing method. Thousands of such patterns obtained from power system simulation or substation database of field recordings are used to train the neural network offline and then the pattern prototypes are used to analyze faults on-line by using the Fuzzy K-NN classifier. The use of multiple neural networks can also enhance the capability of dealing with large data set.

- *Synchronized Sampling Based Fault Location:* Synchronized sampling based fault location algorithm uses raw samples of voltage and current data synchronously taken from two ends of the transmission line, which provides a very high accuracy in fault detection, classification, and location. Compared to the fault location algorithms that use one end or two end phasor data, synchronized sampling based fault location algorithm makes no assumptions

about fault condition and system operating state, so it is immune from power swing, overload, and other non-fault situation. This gives an accuracy and robustness advantage of the proposed scheme vs. the traditional one.

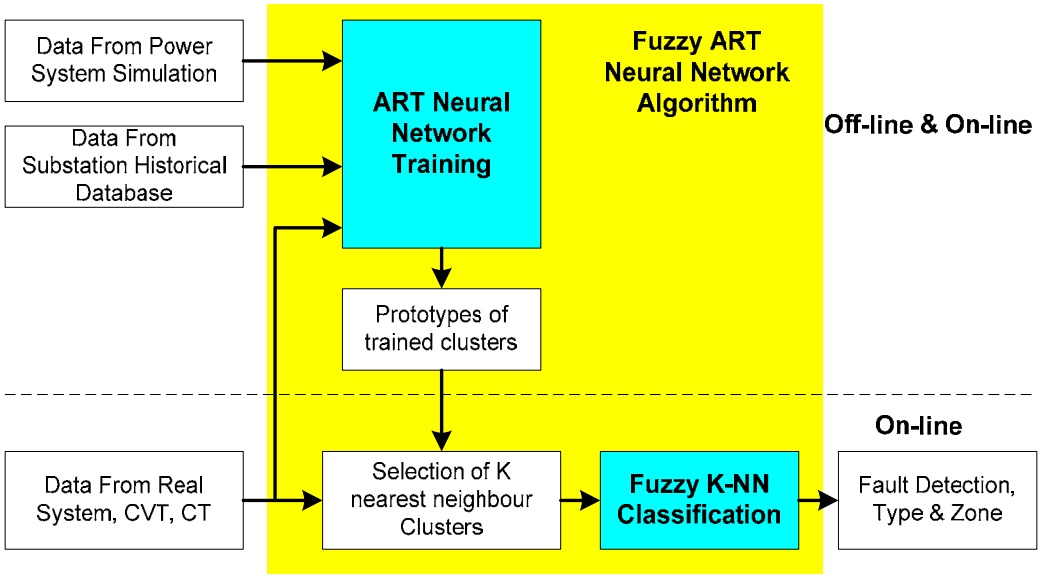

Figure 2.3. Fuzzy ART neural network algorithm

- *Event Tree Analysis:* Event tree analysis is a commonly used event/response technique in industry for identifying the consequences following an occurrence of an initial event. The Event Tree Analysis takes the structure of a forward (bottom-up) symbolic logic modeling technique. This technique explores system responses to an initial "challenge" and enables assessment of the probability of an unfavorable or favorable outcome. In our case, the design of event trees is distributed to each single relay system, and it provides an efficient way for real time observation of relay operations and an effective local disturbance diagnostic support.

2.3 Conclusion

Power system is the most complex man-made system, which is exposed to all kinds of disturbances. Some of the disturbances may induce the cascading outages, which are very difficult to control and complex to analyze. The new approach proposed by the TAMU

group is based on an interactive scheme of system-wide and local monitoring and control tools, which is designed to help detect, prevent, and mitigate the cascading outages.

The system-wide monitoring and control tool can find the vulnerable elements and send request to the local tool for detailed monitoring. The vulnerability and security margin information can be obtained by VI and MI. Emergency control approaches for expected events can be found by the routine security analysis and activated when such events occur. Emergency control approaches for unexpected events can be found by event-based security analysis and activated to mitigate the disturbance and keep the system secure.

The local monitoring and control tool can find the exact disturbance information and make a correction if there is relay failure or unintended operation. Further information can be sent to the system-wide monitoring and control tool for better security control.

The detailed explanation of the proposed approach can be found in literature [1].

3. The Implementation of Proposed Algorithms

3.1 Introduction

This chapter focuses on the implementation of the proposed algorithms. They are used to detect and prevent the cascading events by coordinating the system-wide and local monitoring and control tools. The concept is tested using scenarios from the Entergy system. The modeling of Entergy power system is explained first. The data requirements for all the system-wide and local level algorithms are discussed in detail next. The methods for obtaining the needed data are presented, which includes data acquisition through traditional Supervisory Control and Data Acquisition (SCADA) system, modern Intelligent Electronic Devices (IEDs), or other add-on high speed data acquisition system. Cases are demonstrated showing how the data are extracted and used in the specific applications.

3.2 The Implementation Framework

System-wide tool uses wide-area information to generate a comprehensive view of the system security and vulnerability conditions. It can notify the local tool to engage in detailed monitoring of vulnerable elements during abnormal conditions. Local tool collects the exact real-time local disturbance information. It has the ability to detect, classify and locate the fault with high accuracy and provide good reference for evaluating relay operation. Both the system-wide and local tools work together to fulfill the major task: help detect, and classify the cascading outages. The block diagram of the implementation is shown in Fig. 3.1.

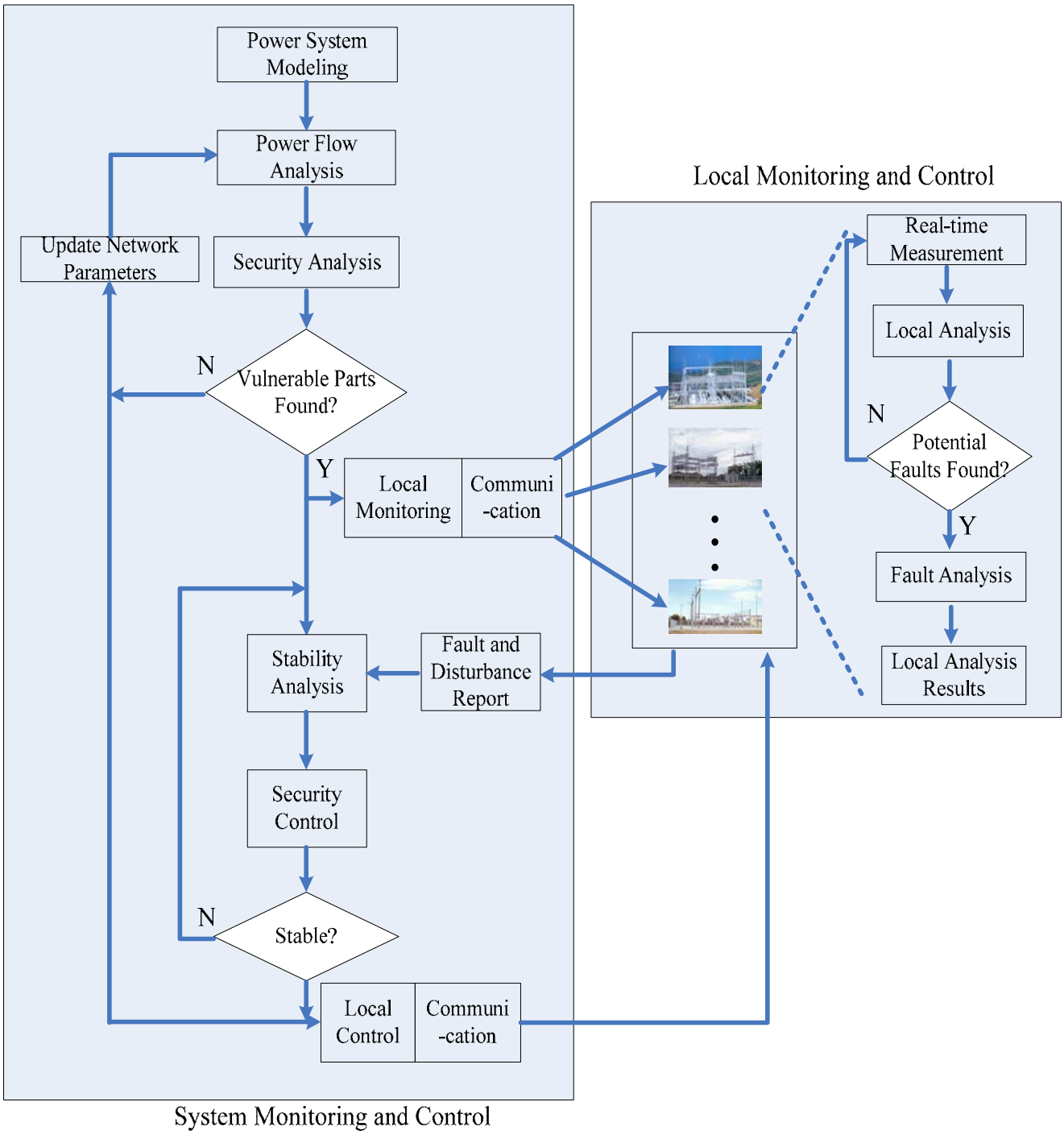

Figure 3.1. Block diagram of the implementation

3.3 The Implementation of System-wide Algorithm

3.3.1 Entergy System Model

Entergy Corporation is an integrated energy company engaged primarily in electric power production and retail distribution operations, which covers a large area including Arkansas, Louisiana, Mississippi, and Texas. Five major operation areas constitute the whole Entergy system: Northern Region, Eastern Region, Central Region, Southwest Region, and Metro Region, which are shown in Fig. 3.2. [40] Entergy owns and operates power plants with approximately 30,000 megawatts of electric generating capacity, and it owns the second-largest nuclear generation in the United States. The Entergy System delivers electricity to 2.7 million utility customers in its area. Entergy has annual revenues of more than $11 billion and approximately 14,300 employees [41]. Entergy system is interconnected with the surrounding areas, and it is an important part of the Southeast Electric Reliability Council (SERC) system, which is one of nine regional electric reliability councils under North American Electric Reliability Corporation (NERC) authority shown in Fig. 3.3. [42]

The power flow data provided by Entergy shows that there are 16117 buses, 3263 generators, and 20211 transmission lines in the SERC System. Entergy is one of the largest parts in the SERC system, which consists of more than 2100 buses, 240 generators and 2600 transmission lines. The Extra High Voltage System consists of 55 buses at 500 kV, which play the roles of the tie lines for the five regions.

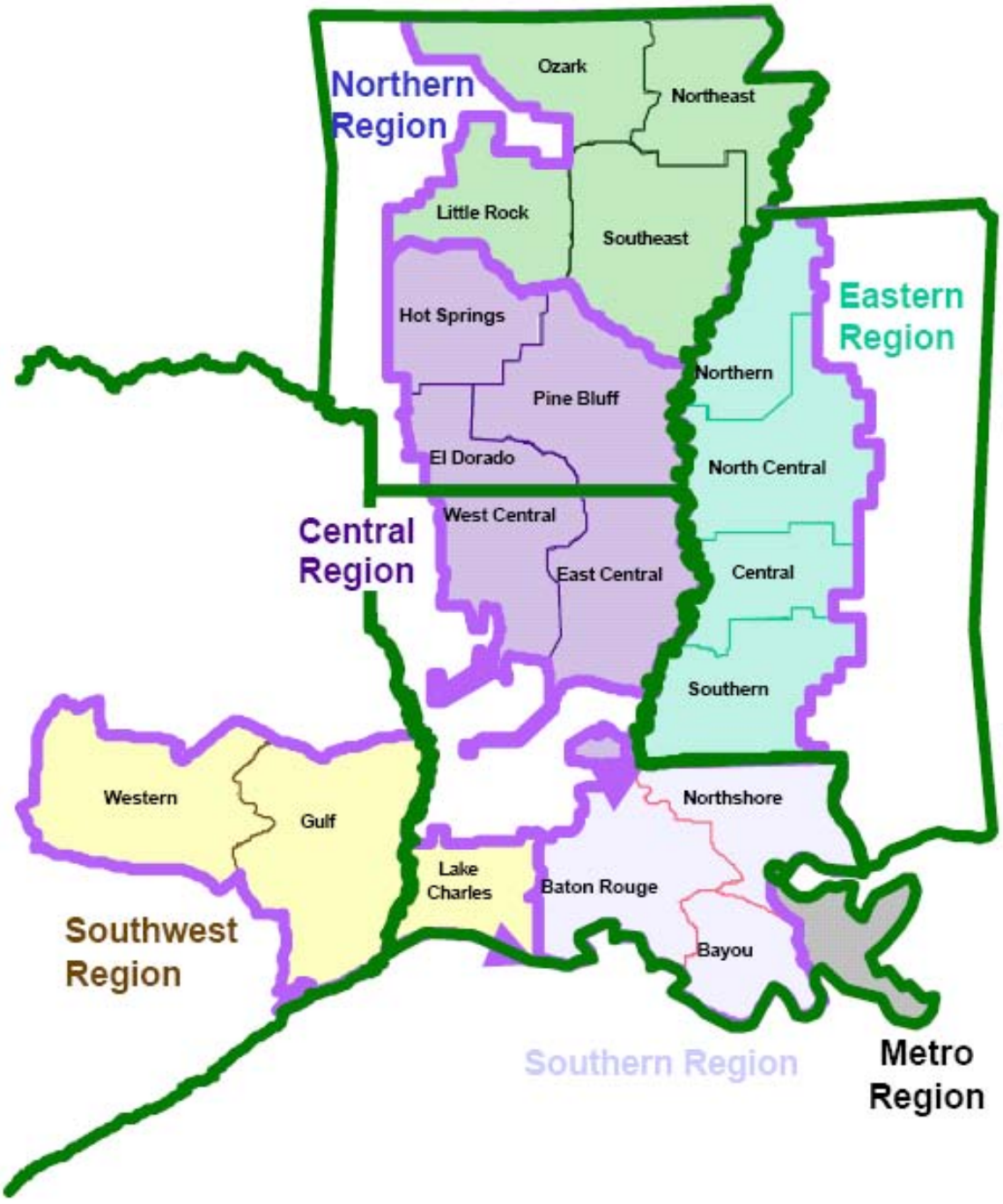

Figure 3.2. Five Operating Areas in the Entergy System

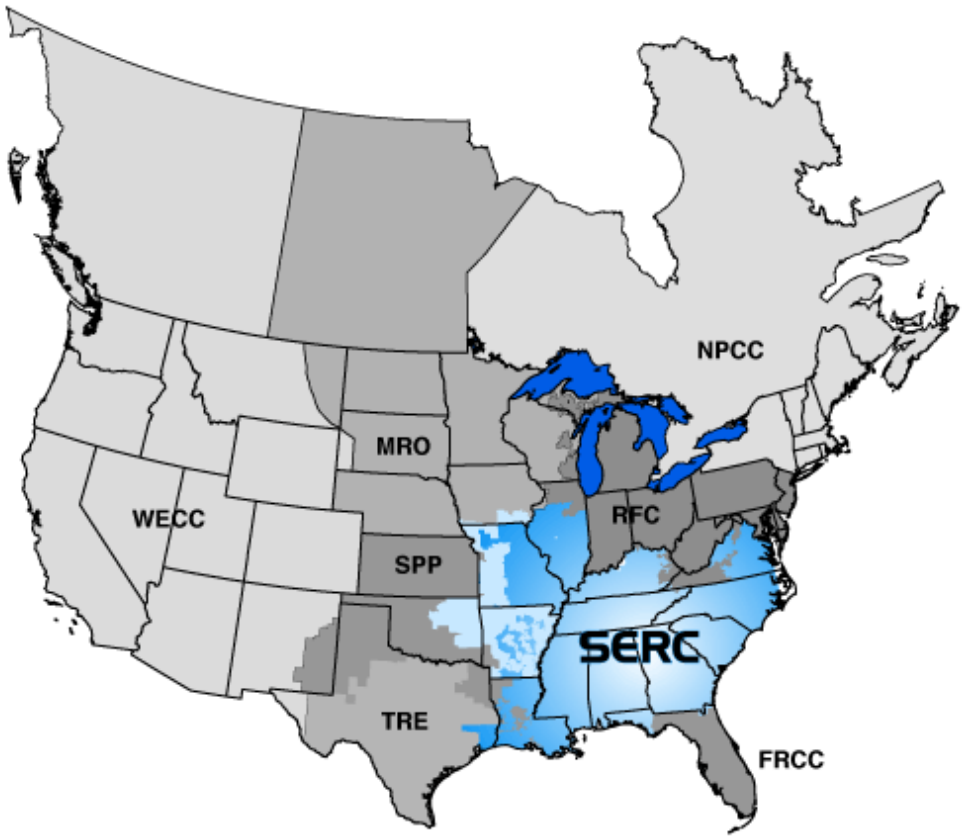

Figure 3.3. Regional Entities with Delegated Authority from NERC

3.3.2 Data Requirement

Data availability is the main factor in making the automatic monitoring and control feasible. In order to implement the proposed algorithms for system-wide and local level, two issues needed to be cleared: what type of data is needed and how to extract the useful information from obtained data. To solve these issues, different types of data from various sources are needed, which are naturally divided into two classes: system level data and substation data.

The data requirement for system level is discussed in this section. The data required for system level analysis aims at defining the power system network topology and establishing the steady state status. The power system model and real time network

topology change information are also needed. Different utilities may use various commercial programs for power system analysis but the main functions of those programs are the same. To meet the data requirement for system-wide analysis and control tools, the following detailed data are necessary:

- *Power Flow Analysis Data*

  This data contains the basic power system network topology. It is used to run the power flow analysis to establish the steady state status of the whole system.

- *Short Circuit Analysis Data*

  This data is needed for running short circuit calculation. It needs to be updated whenever the system topology changes.

- *Dynamic Analysis Data*

  This data contains all the dynamic models for generators, exciters, compensators, stabilizers, etc, which is used to perform dynamic analysis to check system dynamic stability under various disturbances.

3.3.3 Data Handling

After the data requirements are clarified, the next issue is how to collect the desired data or information. It may be relatively easy to get the system-wide data to build power system model. No matter what kind of operation programs the utilities used, they will definitely cover the power flow analysis, short circuit analysis and dynamic analysis. The only differences are coming from the data formats, which depend on the adopted programs.

In this project, we choose Siemens PTI Power System Simulator for Engineering (PSS/E) as the base program to implement the system level tools. The static power system is modeled using PSS/E. Table 3.1 shows an example of data obtained for the system-wide analysis. PSS/E software is an integrated program for simulating, analyzing, and optimizing power system transmission network and generation performance. Based on the power system analysis calculation, PSS/E program can handle power flow and related network analysis functions, balanced and unbalanced fault analysis, network equivalent construction, and dynamic simulation. By applying the functions of interest in the appropriated sequence, most of the system planning and operation problems can be

investigated and handled. Two master program modules included in PSS/E are steady-state analysis and dynamic simulation. The steady state analysis includes load flow calculation, fault analysis, optimal power flow, network equivalence, switching studies and open access. The dynamic simulation program includes transient, dynamic and long term stability analysis [43].

TABLE 3-1: Required data and related sources for the system-wide analysis

Function Module	Detailed Data	Related Source	Description
Security Analysis	Power Flow Raw Data	Input Data Files for PSS/E (*.raw)	This file contains power flow system specification data for the establishment of an initial case. This data is used by PSS/E to get the initialization values which will be utilized for security analysis.
	Slider Binary Data or Drawing Coordinate Data	Input Data Files for PSS/E (*.sld for V30 or *.drw for V2x)	This file is used to create and modify one-line diagrams and to display a variety of results.
Stability Analysis	Sequence Impedance Data	Input Data Files for PSS/E (*.seq)	This file contains the negative and zero sequence impedance data needed for unbalanced fault analysis. It is used by PSS/E to add the impedance data to the case of interest.
	Dynamics Data	Input Data Files for PSS/E (*.dyr)	This file is used by the PSS/E Dynamics program. It contains synchronous machines and other system components data for input to the PSS/E dynamic simulation working memory.

3.3.4 Case Studies

The study cases for steady state analysis and dynamic stability analysis are given based on Entergy System. The power flow raw data files and the dynamic data file are provided by Entergy to implement the case studies. The modeling and description of Entergy system has been introduced in section 3.3.1.

3.3.4.1 System Steady State Analysis Case Study

Power flow raw data files of PSS/E are used to build up the system model. The network topology, load level, generations, buses, and transmission lines are include in the raw data files. The system steady state can be extracted from the basic power flow analysis. The data formats of PSS/E raw data files of various versions are different, though the information they included are the same. Thus the data conversion is needed before using those raw data files.

The steady states operating conditions show the bus voltages in the Entergy area are within reasonable levels. No over loading problems exist on the major transmission lines. For vulnerability index calculation, all the weight factors for different parameters are assigned as 1 for general conditions. These weight factors can be assigned based on the importance of corresponding equipment. Large value of weight factor shows the need for more concern than for others. For the loadability of the bus vulnerability index calculation, Thevenin equivalent impedance method is used. The detail theory can be found in literature [44]. The bus voltage angle difference limit of transmission line is assigned as 40^{o}. The base power is assigned as 100MVA.

The highest load level case in January 2007 of SERC System is studied. Here we choose Entergy system as one subsystem for the steady state analysis. All the other parts of SERC System are removed from the Entergy model. Some islanding buses are generated by doing this separating action. These buses are not included in the steady state analysis in this study case. By vulnerability analysis, the vulnerability of individual elements and whole system can be assigned values. The results of the vulnerability analysis can be used as supplemental criteria for performance index analysis. Those most vulnerable elements need to be monitored to detect the sign of cascading outages, especially the elements in Extra High Voltage (EHV) system. The complete calculation results are given in Appendix A. Two examples are given here:

Table 3.2 shows the results of top 20 of individual bus voltage magnitudes. From the literature [1], we know that the equation for calculation of Vulnerability Index (VI) for an individual bus voltage magnitude is:

$$VI_{V,i} = \frac{W_{V,i}}{2N}\left(\frac{V_i - V_i^{sche}}{\Delta V_{i,\lim}}\right)^{2N} \qquad (3.1)$$

where

$VI_{V,i}$: *VI* of individual bus voltage magnitude

$W_{V,i}$: weight factor of individual bus voltage influence, here it is assigned as 1.0 for all buses

V_i : bus voltage magnitude

V_i^{sche} : scheduled bus voltage magnitude

$\Delta V_{i,\lim}$: voltage variance limit, here it is assigned as 1.0 p.u.

N : 1 in general by definition

TABLE 3-2: Top 20 of VI for individual bus voltage magnitude

	Bus Number	**VI_V**
1	97634	0.319787
2	97690	0.119463
3	97463	0.099756
4	97567	0.0978
5	97691	0.097035
6	97467	0.091935
7	97566	0.091535
8	97569	0.090171
9	97455	0.086473
10	97478	0.079521
11	97515	0.077934
12	97570	0.077146
13	97551	0.07579
14	97468	0.075686
15	97531	0.074087
16	97534	0.06944
17	97465	0.069043
18	97473	0.065522
19	97459	0.062328
20	97544	0.058847

Thus we can see that under the same parameters $W_{V,i}$, $\Delta V_{i,\lim}$, and N, the more the bus voltage magnitude deviates from the scheduled bus voltage magnitude, no matter whether increasing or decreasing, the bigger the VI for the bus voltage magnitude.. The sum of all the bus VI values of voltage magnitude can demonstrate the condition of the overall voltage magnitude situation. As mentioned above, the weight factor is a key parameter to determine the importance of the buses, which could be decided by historical experiences of power system operation.

Table 3.3 shows the results of top 20 VI of individual transmission line real power. From the literature [1], we know that the equation of calculation VI for individual transmission line real power:

$$VI_{Pf,i} = \frac{W_{Pf,i}}{2N}\left(\frac{Pf_i}{S_{i,\max}}\right)^{2N} \tag{3.2}$$

where

$VI_{Pf,i}$: *VI* of individual line real power

$W_{Pf,i}$: weight factor of individual line real power influence, here it is assigned as 1.0 for all transmission lines

Pf_i : transmission line real power

$S_{i,\max}$: individual transmission line transmission limit, which can be either thermal limit or transfer limit due to security constraints, here it is assigned as the same as the line thermal limit in the raw data files.

N : 1 in general by definition

Thus we can see that under the same parameters $W_{Pf,i}$, $S_{i,\max}$, and N, the bigger the transmission line real power flow at the transmission line, the bigger the VI value of the transmission line real power. Similar with VI of individual bus voltage magnitude, the value of the weighting factor $W_{Pf,i}$ is also a key parameter to determine the importance of the transmission lines of interest, which will influence the results through major contributions.

3.3.4.2 System Dynamic Analysis Case Study

System dynamic analysis is based on the model built from power flow raw data files. It is used to determine the response of the system to the prescribed stimuli. In PSS/E, the dynamic analysis is a straightforward simulation for an increasing time step. The behavior of a system is described by a set of differential equations. The time derivative of each state variable in the system is calculated under the constant and variable parameters, which is determined by the element models. Those state variables describe the condition of the system at exactly each time step. The state variable values at the next time step are calculated based on the present value of each state variable and its time derivative. The process is repeated step by step, and the dynamic simulation is advanced and finished [43].

TABLE 3-3: Top 20 of VI for individual line real power

	From Bus Number	To Bus Number	VI_Pl
1	98232	98234	1151.474
2	97745	97770	1054.963
3	97770	97868	811.4757
4	97982	98048	625.565
5	99738	99849	596.4457
6	97672	97745	567.5446
7	99344	99421	551.2517
8	99637	99640	508.2397
9	99485	99509	498.011
10	98482	98484	469.9219
11	99592	99660	456.3646
12	99323	99338	455.9427
13	99338	99384	444.0721
14	99485	99510	424.4625
15	99618	99646	423.6988
16	99508	99510	409.7863
17	98249	98434	402.2396
18	97583	97588	395.2331
19	99137	99146	389.0926
20	97920	98046	384.8288

The dynamic data file of PSS/E consists of models for the system equipment, including generators, compensators, stabilizers, excitation systems, loads, relays, DC lines, and FACTS. The detailed description of those models can be found in [43]. Entergy staff provided one dynamic data file for their system, which includes the data of SERC System. However, the models in this dynamic data file could not cover all the generators in service described in the power flow data. Similar with steady state analysis, only the Entergy system is considered for this case study.

N-1 contingency analysis is performance requirement for all the EHV system. None of the N-1 contingency cases has a stability problem, which satisfies the NERC requirement. Here we choose a N-2 contingency case (Mt. Olive - Hartburg 500 kV line; Richard - Wells 500 kV line) from the N-2 contingency list which is shown in Table 3.4. The Mt. Olive - Hartburg 500 kV transmission line is a tie line connecting the Central region and Southwest region. The Richard – Wells 500 kV transmission line is also a tie line connecting Southwest region and Southern region.

TABLE 3-4: N-2 contingency list for Entergy system

	First Contingency		**Second Contingency**	
	Line Name	**Voltage Level**	**Line Name**	**Voltage Level**
1	China - Sabine	230 kV	China - Amelia	230 kV
2	Mt. Olive - Hartburg	500 kV	Richard - Wells	500 kV
3	Franklin - Mcknight	500 kV	Webre - Wells	500 kV
4	Nelson - Moss Bluff	230 kV	Calcasieu - Pecan Grove	230 kV
5	WhiteBluff - Keo	500 kV	White Bluff - Sheridan	500 kV

First the dynamic analysis is run from -0.167s to 0.1s, which shows the system steady state. Then one 500 kV transmission line is taken out of service: Hatburg (Line 97717) to Mt. Olive (99162). After 0.4s, a fault is introduced on another transmission line: Richard (Line 98107) to Wells (Line 98109). The whole dynamic analysis lasts 4.5second. Various states can be set for monitoring, including machine rotor angle, machine/bus real

and reactive power, machine/bus terminal voltage, machine field voltage, machine speed deviation, frequency deviation, branch plow, real and reactive power load, etc. The dynamic analysis is based on step-by-step method. It will be quite time-consuming if all the system variables are monitored. Here we picked the rotor angles for some machines to demonstrate dynamic stability performance. The results are shown in Fig. 3.4.

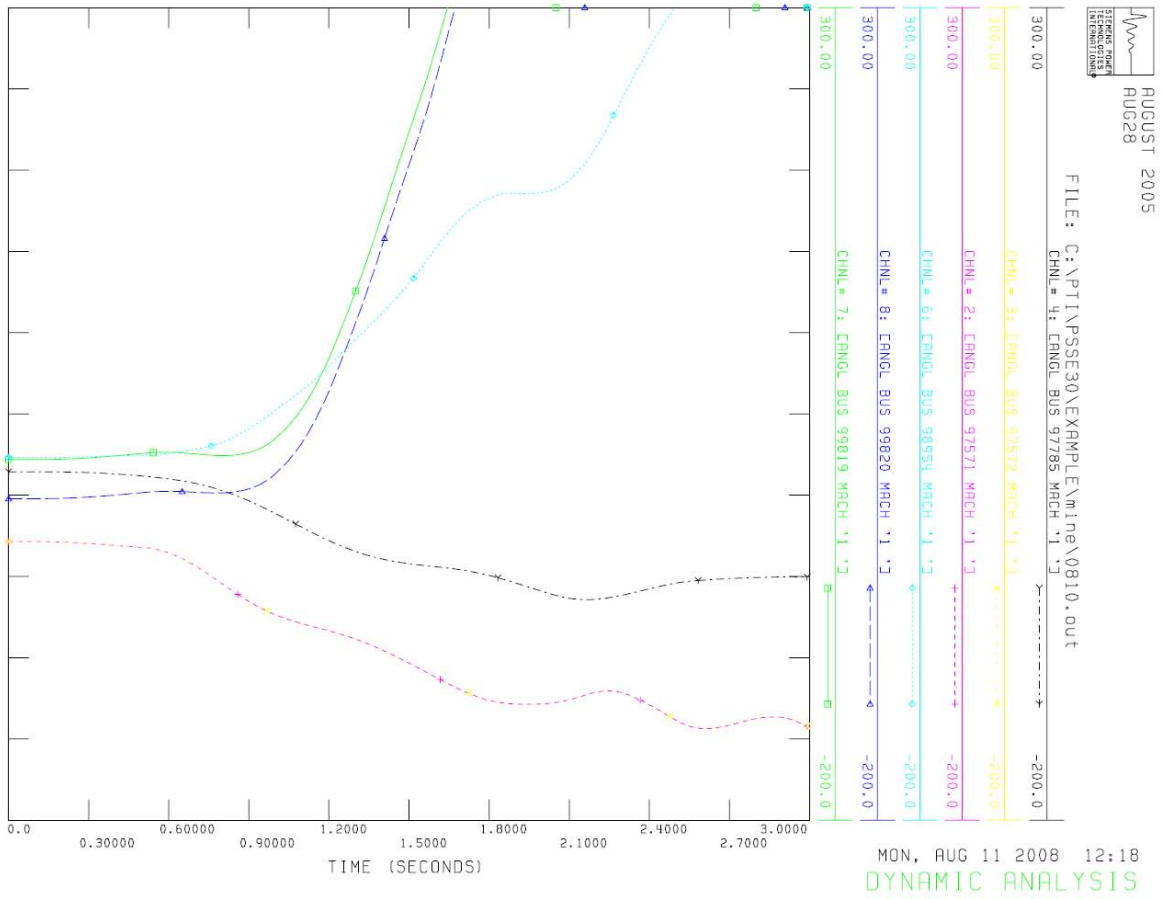

Figure 3.4. System dynamic analysis result

3.4 The Implementation of Local Level Algorithm

3.4.1 Data Requirement

The data required for local level analysis aims at getting detailed configuration for each substation, as well as measured data for any disturbance. To meet the data requirement for local fault analysis and control tool, the following detailed data are necessary:

- *Relay Setting and Event Reporting Data*

Data for relay setting contains the relay configuration information. Data for relay event reporting contains the results of relay operation under disturbances. This data is used for reconstructing relay operation by simulating relay behavior under given disturbances.

- *Fault Record Data*

Fault record data contains analog and digital sample values for all input channels for a specific fault or disturbance. It is used for the training set and testing set of fault scenarios for Neural Network based Fault Detection and Classification (NNFDC) Algorithm.

- *Synchronized Samples of Fault Voltages and Currents*

The synchronized sample data of fault voltages and currents contains time stamps from the Global Positioning System (GPS) of satellites on all the pre- and during-fault sample signals [38]. This data is used to verify the results of the Synchronized Sampling based Fault Location (SSFL) Algorithm.

3.4.2 Data Handling

Regarding the special requirement of each algorithm, two different ways for obtaining the desired data for the local level analysis are discussed.

3.4.2.1 Obtaining Data from Recording Equipment

Methods for obtaining data from the local level devices vary from one site to the other. With the new technologies and equipment used in substations, utilities keep upgrading or constructing their substations according to their operating needs and strategic importance of the substation. The data recording equipment is very versatile, since it typically comes from various vendors and it is installed in different time periods [45]

SCADA systems are being used to provide the real time information about power system states and they are in use since the late sixties. The introduction of SCADA solutions improved the performance of energy management systems (EMS) functions. Traditionally the substation data are acquired using remote terminal units (RTUs) of SCADA and sent to the EMS in every two to ten seconds. The acquired data are typically

bus voltages, flows (amps, MW, MVAR), frequency, breaker status, transformer tap position), etc. But, the measured data based on SCADA system does not have the characteristics needed to implement the proposed local analysis and control tools due to the lack of sampled waveform data [46].

Nowadays, most of the substations are equipped with Intelligent Electronic Devices (IEDs), which can collect huge amounts of sampled data in addition to performing their basic functions. The modern day IEDs can record and store a huge amount of data (both operational and non-operational) with a periodicity depending upon the intended purpose of the device, such as digital protective relays (DFRs) capturing data during fault occurrence, or phasor measurement units (PMUs) capturing continuous time-synchronized data. Although the IEDs are not standardized regarding the functions they perform, they are indeed a good addition to the data recording infrastructure needed for a comprehensive analysis to be performed related to substation equipment operation [47]. The integration and use of IED data has been discussed in literature [45], which offers a background for building the information management system for monitoring the cascading events.

Table 3.5 shows the data obtained from the local level considering the data integration from SCADA system and IEDs.

3.4.2.2 Obtaining Data from Simulation

NNFDC algorithm needs large number of fault and non-fault cases to complete the process of training and testing for neural network tuning. Those training and testing cases are quite different for various transmission lines due to the selection of different simulation parameters and settings. To perform comprehensive tests, it may not be possible to acquire enough fault cases from the field. Alternative solution is to generate the needed data files by simulation. Fig. 3.5 shows a block diagram for the fault and non-fault scenarios generation program which is based on ATP/ATPDraw [48] and Matlab [49]. The power system of interest is first modeled in ATP/ATPDraw. Then User can define the desired fault or non-fault cases by initializing the simulation setting parameters in Matlab. The measured three-phase voltage and current samples, which could also include time stamp, are extracted in the data format files defined by user.

TABLE 3-5: Required Data and related sources for the local analysis

Function Module	Detailed Data	Related Source	Description
Neural Network based Fault Detection and Classification (NNFDC)	Event File	Event File output from Relays	The relay event file is used to get the report of relay operations.
	Data Recorded During Faults	DFR and DPR files	This fault data file is used to check the results of relay operations using NNFDC
Synchronized Sampling based Fault Location (SSFL)	Synchronized Samples of Voltage and Current Data during Faults	GPS-Synchronized DFRs	This synchronized data file is used for evaluation of SSFL

NNFDC algorithm can be evaluated based on the simulated data. The data from simulation can be used for training procedure, by which the parameters of neural network can be set. The data captured by the recording equipment can be used to evaluate the algorithm.

3.4.3 Case Studies

A case study is given to demonstrate the process of the advanced fault analysis tools for the local level: NNFDC, SSFL and ETA. Different fault scenarios are generated to test the accuracy of the algorithms. A 500 kV transmission line from Entergy system is chosen as the base model for data generation: Hatburg (Line 97717) to Mt. Olive (99162), which is a tie line connecting the Central region and Southwest region of Entergy system.

3.4.3.1 Neural Network Based Fault Detection and Classification

According to the simulation block diagram, the simulation system for the 500 kV transmission line, Hatburg (Line 97717) to Mt. Olive (99162), is built based on the ATP/ATPDraw and Matlab. A large number of fault and non-fault cases has been generated, which includes different fault types, fault locations, fault resistance, and fault angles. The fault is initiated at 0.02s into the simulation process, and cleared at 0.45s.

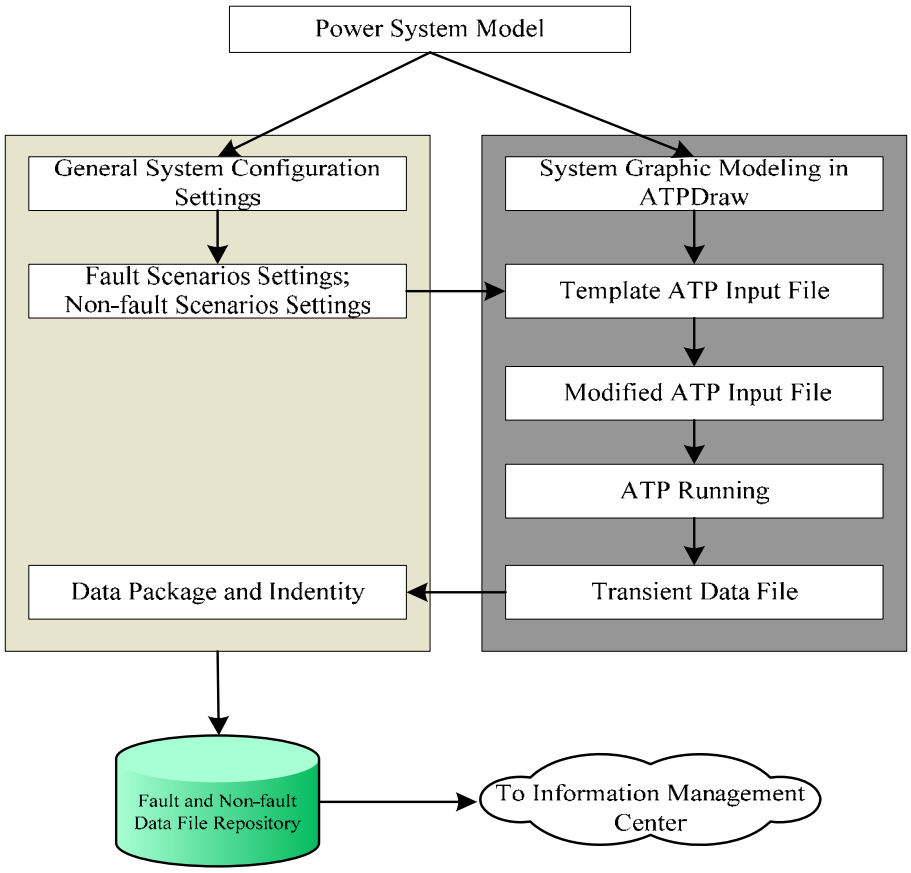

Figure 3.5. Block Diagram of simulations for fault and non-fault scenarios

The proposed neural network is trained by using the simulated fault and non-fault cases. There are 209 clusters altogether determined with labels of different fault types. Then 5000 cases are tested for the trained neural network. Two classification algorithms are used when performing the test procedures: the nearest neighbor algorithm and fuzzy k-nearest neighbor algorithm. Fig. 3.6 shows the errors for the fault classification for basic nearest neighbor algorithm and fuzzy 4-nearest neighbor algorithm. From Fig. 3.6, we can see that the error for fuzzy 4-NN is stable at about 1.5%.

3.4.3.2 Synchronized Sampling Based Fault Location

SSFL algorithm is also tested based on the same simulated transmission line: Hatburg (Line 97717) to Mt. Olive (99162). 140 fault cases are generated by random setting of parameters. The generated data includs the fault voltages and currents from two sides of

the transmission lines, which covers different cases of fault types, fault angles, fault resistance, and fault locations.

Table 3.6 shows 10 cases of the results for SSFL algorithm. For all the tests, the maximum error for fault classification is 3.6992%; the minimum error is 0.0234%.

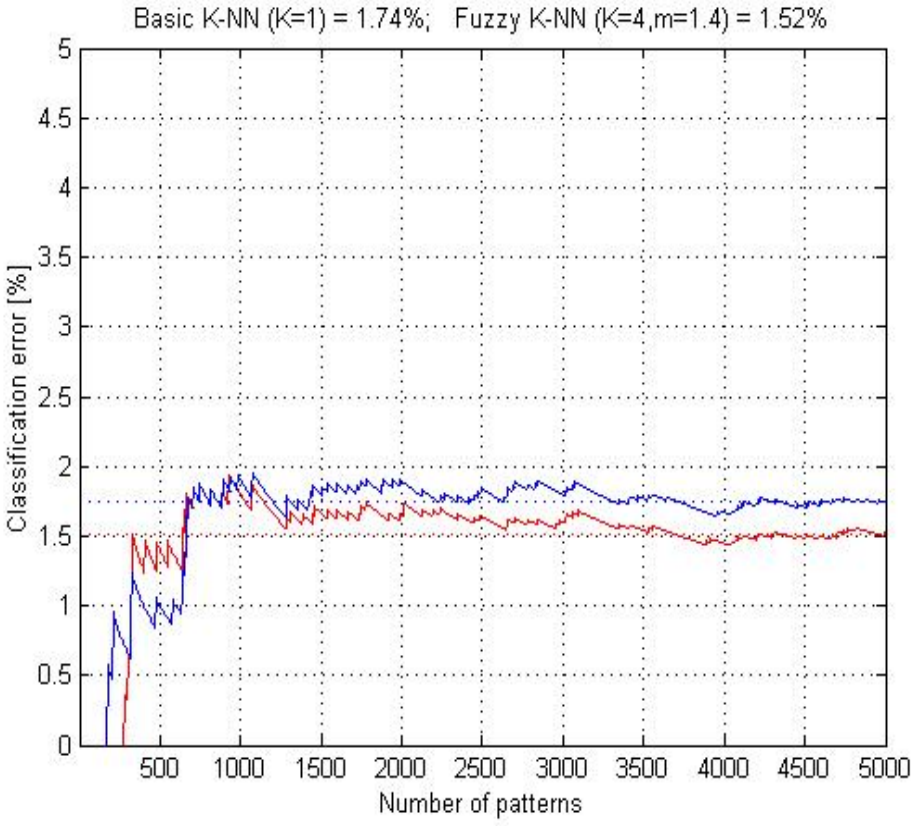

Figure 3.6. Error results of neural network fault classification tools

3.4.3.3 Event Tree Analysis

Event tree analysis is coming from the idea of dynamic decision event tree (DDET) analysis [50], which is in our case used to prevent system blackouts. The occurrences of power system events are really random. It is not possible to predict all the initial events and their unfolding contingencies. Therefore, implementing the idea in a real large scale system is becoming very difficult. However, for a simple protection system such as the single relay system on a given transmission line consisting of a distance relay, its

associated circuit breaker and communication equipment, it is feasible to list all the possible contingencies and foresee their corresponding actions.

For the case study, we built the event trees for transmission line from Hatburg (Line 97717) to Mt. Olive (99162). This system is simplified to represent a single relay system for the case study. The possible initial events and their following actions are predicted. Fig. 3.7 shows the event tree for the fault conditions detected in the primary zone. The corresponding reference actions are described in Table 3.7.

In the event tree, the nodes stand for the events or actions, where the white nodes represent correct actions and the black nodes represent incorrect actions. Following a set of events or actions from the root node (initial event), the event tree reaches an outcome that indicates whether the overall action for a corresponding disturbance. is appropriate or not If the event sequence is heading to or has already reached a “black” node, a corrective action must be taken. For the cases we built for NNFDC and SSFL, the activity path on the event tree for each fault will be *1-2-4-10-whit*. If any black node is detected, the local monitoring tool will initiate alarm signals to the operator and also provide the reference action for correction of the relay operation.

TABLE 3-6: Results of SSFL algorithm

	Fault Type	**Fault Distance (mile)**	**Fault Resistance (Ω)**	**Fault Angle (degree)**	**Fault Location (mile)**	**Error (%)**
1	CAG	85.2	3.1	199.9	85.25	0.0234
2	ABG	151.1	11.9	121.6	150.19	0.4706
3	ABCG	23.1	13.1	38.2	22.51	0.2870
4	AG	135.2	11.7	49.8	136.30	0.5693
5	CAG	116.2	1.3	217.0	115.61	0.3037
6	AB	38.3	15.1	3.8	37.48	0.3933
7	BCG	19.6	2.5	239.7	21.57	1.0016
8	CG	120.0	4.3	110.0	122.14	1.0656
9	AG	176.4	9.2	98.5	174.60	0.8917
10	ABCG	68.0	2.3	102.8	66.60	3.6992

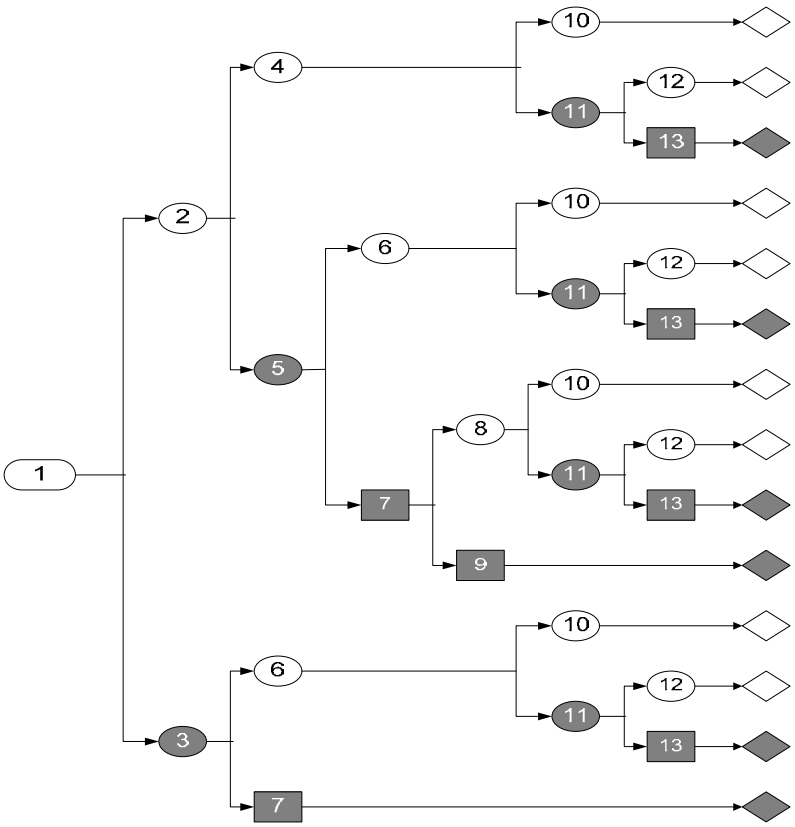

Figure 3.7. Event tree for a fault occurring in primary zone

3.5 Conclusion

Based on the proposed algorithms for detecting, preventing and mitigating the cascading events, discussed in chapter 2, this chapter introduced the implementation of the discussed algorithms, and present the implementation framework coordinating the system-wide and local monitoring tools. Aiming at carrying out the implementation issue, the data requirements for each algorithm of system-wide and local level tools to detect and prevent the cascading events are discussed in detail. How to obtain the desired data and information is also presented in this chapter. This data integration is taking into account data from SCADA system combined with data from IEDs, or data from add-on high speed data acquisition system, Case studies of system-wide and local level scenarios have been performed to test the proposed algorithms and show how the data are used and handled, which is based on the Entergy system model.

TABLE 3-7: Node explanation and reference corrective actions

Node	Scenarios	Reference Action.
1	Fault occurs in a primary zone.	Keep Monitoring
2	Relay detects the fault	Keep Monitoring
3	Relay does not detect the fault	Check defects in relay algorithm and settings
4	Relay sees the fault in a correct zone	Keep Monitoring
5	Relay sees the fault in an incorrect zone	Check defects in relay algorithm and settings
6	Transfer trip signal is received	Keep Monitoring
7	Transfer trip signal is not received	Check communication channel Send Trip Signal if necessary
8	Relay trips the breaker	Keep Monitoring
9	Relay does not trip the breaker; Fault is cleared by other breakers	Try to open the breaker associated with this relay and correct other redundant trips
10	Circuit breaker opened by a trip signal	Keep Monitoring
11	Circuit breaker fails to open	Check the breaker circuit
12	Breaker failure protection trips all the breakers at the substation	Keep Monitoring
13	No breaker failure protection or it does not work	Check the circuit of the breaker failure protection

4. Conclusions and Future Work

4.1 Conclusions

This final report reviewed implementation requirements for an interactive scheme comprising system-wide and local monitoring and control tools, and designed to help detect, prevent, and mitigate the cascading outages.

The system-wide monitoring and control approach includes steady state and dynamic analysis tools, which can find the vulnerable elements, check steady state and dynamic stability, and send command to the local tool for detailed monitoring. The local monitoring and control approach includes the advanced fault analysis and relay monitoring tools, which are based on a neural network based fault detection and classification, synchronized sampling based fault location, and event tree based analysis of relay operations. The local monitoring and control tool can accurately confirm properties of a disturbance and make a correction if there is an unintended relay operation. Further information can be sent to the system monitoring and control tool for better security control.

The main contributions of this project are:

- Apply the theoretical research results into practical application. The implementation framework of the proposed algorithms is presented by coordinating the system and local level monitoring and analysis tools.
- Data requirements for each system/local algorithm are discussed in detail in order to carry out the implementation issue.
- Data handling for obtaining the desired data and information is presented. In order to cover the data requirements, integration of data from Supervisory Control and Data Acquisition (SCADA) system, substation Intelligent Electronic Devices (IEDs), possibly some add-on high speed data acquisition system, as well as data from simulations is needed.

- Case studies are used to demonstrate the feasibilities of the proposed algorithms. Entergy system model is utilized for this purpose. Different cases of system-wide and local level analysis tool application to the Entergy system are tested.

4.2 Suggestions for Future Work

When performing the steady state analysis to find the vulnerability of system elements, the weight factors for all the equations are assigned with value of one. The value of the weight factor determines the importance for system vulnerability. Further research on how to determine the weight factors will be beneficial for the steady state analysis. All the software in this project is developed using ATP/ATPDraw, Matlab, and PSS/E. In order to improve the calculation speed, it is highly desirable to substitute Matlab by C++/Java. Performing the large amount of matrix calculations in C++/Java may also be a problem. Development of parallel computing techniques may also be needed for faster computations and real-time applications.

Project Publications

[1] M. Kezunovic, C. Pang, "Improved Transmission Line Protection During Cascading Events," *CIGRE B5 Colloquium*, Madrid, Spain, October 2007

[2] M. Kezunovic, C. Pang, J. Ren, Y. Guan, "New Solutions for Improved Transmission Line Protective relay Performance Analysis," *The 14th Medditerranean Electrotechnical Conference-MELECON 08*, Ajaccio, France, April 2008.

[3] C. Pang, M. M. Kezunovic, "Wavelet-Based Method for Fault Detection and Classification of Transmission Lines during Power Swing," *The 6th Mediterranean Conference and Exhibition on Power Generation, Transmission and Distribution (MedPower 2008)*, Thessaloniki, Greece, Nov. 2008. (Accepted)

[4] C. Pang, M. M. Kezunovic, "A New Approach to PID Controller Design of STATCOM," *2008 North American Power symposium (NAPS 2008)*, Calgary, Canada, Sept. 2008.

[5] C. Pang, M. M. Kezunovic, "Information Management System for Detecting Cascading Events," *PowerCon 2008 & 2008 IEEE Power India Conference*, New Delhi, India, Oct. 2008.

References

[1] PSerc Projcet S19 Final Report - Part I, "Detection, Prevention and Mitigation of Cascading Events," PSerc Publication 05-59. [Online] Available: http://www.pserc.org

[2] U.S.-Canada Power System Outage Task Force, "Final Report on the August 14, 2003 Blackout in the United States and Canada: Causes and Recommendations", April 5, 2004, [Online] Available: http://www.nerc.com

[3] C. S. Joseph, D. S. Black, R. Charles, and et al., "Report to the President by the Federal Power Commission On the Power Failure in the Northeastern United States and the Province of Ontario on November 9-10, 1965," Tech. Rep., Washington, D.C., Dec. 1965, [Online] Available: http://blackout.gmu.edu/archive/a_1965.html.

[4] Federal Power Commission U.S. Department of Energy, "The Con Edison Power Failure of July 13 and 14, 1977," Tech. Rep., Washington, D.C., June 1978, [Online] Available: http://blackout.gmu.edu/archive/a_1977.html.

[5] C. W. Taylor, Power system voltage stability, McGraw-Hill, New York, 1994.

[6] Evert Agneholm, "The Restoration Process Following a Major Breakdown in a Power System," Tech. Rep., Goteborg, Sweden, May 1996, [Online] Available: http://www.elkraft.chalmers.se/Publikationer/EKS.publ/Abstract/Agneholm_Lic.pdf.

[7] G. Doorman, G. Kjolle, K. Uhlen, and et al., "Report to the Nordic Council of Ministers: Vulnerability of the Nordic Power System," Tech. Rep., May 2004, [Online] Available: http://www.ksg.harvard.edu/hepg/Papers/Doorman.vul.nordic.system.0504.pdf.

[8] A. Kurita and T. Sakurai, "The power system failure on July 23, 1987 in Tokyo," in Proc. 27th Conference on Decision and Control, Austin, USA, Dec. 1988, pp. 2093–2097.

[9] V.X. Filho, L.A.S. Pilotto, N. Martins, and et al., "Brazilian Defense Plan Against Extreme Contingencies," in *Proc. of IEEE 2001 Power Engineering Society Summer Meeting*, July 2001, vol. 2, pp. 834–839.

[10] NERC Disturbance Analysis Working Group, "NERC Disturbance Reports," Tech. Rep., New Jersey, USA, 1996, [Online] Available: http://www.nerc.com.

[11] Hazel R. O'Leary, "DOE's Report to the President: The Electric Power Outages in the Western United States, July 2-3, 1996," Tech. Rep., Washington, D.C., Aug. 1996, [Online] Available: http://www.nerc.com.

[12] Elkraft System, "Power Failure in Eastern Denmark and Southern Sweden on 23 September 2003, Final report on the course of events," Tech. Rep., Nov. 2003, [Online] Available: http://www.pserc.org.

[13] Union for the Co-ordination of Transmission of Electricity, "Interim Report of the Investigation Committee on the 28 September 2003 Blackout in Italy," Tech. Rep., Oct. 2003.

[14] U. Knight, Power Systems in Emergencies, John Wiley and Sons, Inc., Chicester, England, 2004.

[15] Q. Chen, K. Zhu, and J.D. McCalley, "Dynamic Decision-event Trees for Rapid Response to Unfolding Events in Bulk Transmission Systems", in *IEEE 2001 Power Tech Proceedings*, Vol. 2 , Sept 2001

[16] B.A. Carreras, V.E. Lynch, and I. Dobson, "Dynamical and Probabilistic Approaches to the Study of Blackout Vulnerability of the Power Transmission Grid", in *2004 Proc. of the 37th Annual Hawaii International Conference on System Sciences*, Jan. 2004, pp. 55 – 61

[17] J.C. Tan, P.A. Crossley, and P.G. McLaren, "Application of a Wide Area Backup Protection Expert System to Prevent Cascading Outages", *IEEE Transactions on Power Delivery*, vol. 17, no. 2, pp. 375 – 380, April 2002

[18] D. C. Elizondo, J. de La Ree, A. G. Phadke, and S. Horowitz, "Hidden Failures in Protection Systems and their Impact on Wide-area Disturbances", in *Proc. of IEEE 2001 PES Winter Meeting*, vol. 2, pp. 710 – 714, Jan/Feb 2001

[19] B. Yang, V. Vittal, and G. T. Heydt, "Slow-coherency-based Controlled Islanding--a Demonstration of the Approach on the August 14, 2003 Blackout Scenario," *IEEE Transactions on Power Systems*, vol. 21, no. 4, pp. 1840-1847, Nov. 2006

[20] T. Guler, G. Cross, and M. Liu, "Generalized Line Outage Distribution Factors," *IEEE Transactions on Power Systems*, vol. 22, no. 2, pp. 879-881, May 2007

[21] S. Lim, C. Liu, S. Lee, M. Choi, and S. Rim, "Blocking of Zone 3 Relays to Prevent Cascaded Events," *IEEE Trans. on Power System*, vol. 23, no. 2, pp. 747-754, May 2008.

[22] NERC Disturbance Analysis Working Group, "Western Interconnection (WSCC) System Disturbance — August 10, 1996", NERC 1996 System Disturbances Report, Aug 2002, [Online] Available: http:// www.nerc.com

[23] NERC System Disturbances Reports, North American Electric Reliability Council, New Jersey, 1984-1991

[24] H. Song, and M. Kezunovic, "Static Security Analysis based on Vulnerability Index (VI) and Network Contribution Factor (NCF) Method", *2005 IEEE PES T&D Asia Pacific*, Dalian, China, August, 2005.

[25] H. Song, M. Kezunovic, "Relieving Overload and Improving Voltage by the Network Contribution Factor (NCF) Method", *NAPS2004, 36th Annual North American Power Symposium*, Moscow, Idaho, August, 2004

[26] H. Song, and M. Kezunovic, "A New Analysis Method for Early Detection and Prevention of Cascading Events," *Electric Power Systems Research*, Vol. 77, Issue 8, Pages 1132-1142, June 2007

[27] H. Song, M. Kezunovic, "A Comprehensive Contribution Factor Method for Congestion Management", *2004 IEEE Power Systems Conference & Exposition (PSCE)*, New York, October, 2004

[28] H. Song, M. Kezunovic, “Stability Control using PEBS Method and Analytical Sensitivity of the Transient Energy Margin”, *2004 IEEE PES Power Systems Conference & Exposition (PSCE)*, New York, October, 2004

[29] H. Song, M. Kezunovic, “Static Analysis of Vulnerability and Security Margin of the Power System”, *2005 IEEE PES T&D Conference*, New Orleans, Oct. 2005

[30] M. Kezunovic, and C. Pang, "Improved Transmission Line Protection During Cascading Events," CIGRE B5 Colloquium, Madrid, Spain, October 2007.

[31] N. Zhang, and M. Kezunovic, "A Real Time Fault Analysis Tool for Monitoring Operation of Transmission Line Protective Relay," *Electric Power Systems Research Journal*, Vol. 77, No. 3-4, pp. 361-370, March 2007

[32] N. Zhang, H. Song, M. Kezunovic, “New Monitoring and Control Scheme for Preventing Cascading Outage”, NAPS2005, *37th Annual North American Power Symposium*, Ames, Iowa, October, 2005

[33] N. Zhang, M. Kezunovic, “Verifying the Protection System Operation Using an Advanced Fault Analysis Tool Combined with the Event Tree Analysis”, *NAPS2004, 36th Annual North American Power Symposium*, Moscow, Idaho, August, 2004

[34] N. Zhang, M. Kezunovic, “A Study of Synchronized Sampling Based Fault Location Algorithm Performance under Power Swing and Out-of-step Conditions”, *PowerTech 2005*, St. Petersburg, Russia, June, 2005

[35] N. Zhang, M. Kezunovic, “Coordinating Fuzzy ART Neural Networks to Improve Transmission Line Fault Detection and Classification”, *2005 IEEE PES General Meeting*, San Francisco, June, 2005

[36] N. Zhang, M. Kezunovic, “Implementing an Advanced Simulation Tool for Comprehensive Fault Analysis”, *2005 IEEE PES T&D Aisa & Pacific Conference*, Dalian, China, Aug. 2005

[37] N. Zhang, M. Kezunovic, “Improving Real-time Fault Analysis and Validating Relay Operations to Prevent or Mitigate Cascading Blackouts”, *2005 IEEE PES T&D Conference*, New Orleans, Oct. 2005

[38] J. Bialek, “Topological Generation and Load Distribution Factors for Supplement Charge Allocation in Transmission Open Access,” *IEEE Trans. Power Systems*, vol. 12, no. 3, pp. 1185–1193, Aug. 1997.

[39] V. Vittal, E.Z. Zhou, C. Hwang, and A.-A. Fouad, “Derivation of Stability Limits using Analytical Sensitivity of the Transient Energy Margin,” *IEEE Trans. Power Systems*, vol. 4, no. 4, pp. 1363–1372, Nov. 1989.

[40] S. Kolluri and K. Tinnium, ”Impact of Independent Power Producers and Cogenerations on the Entergy’s Transmission System in a Deregulated Environment,” IEEE/PES Winter Power Meeting, Feb. 1, 2001, Columbus, Ohio. [Online] Available: http://www.eeh.ee.ethz.ch/downloads/psl/research/psdpc/ipp_presentation-kolluri.pdf

[41] Entergy Cooperation, [Online] Available: http://www.entergy.com/about_entergy/

[42] SERC Reliability Corporation, [Online] Available: http://www.serc1.org/Application/HomePageView.aspx

[43] Siemens Power Transmission & Distribution, Inc, Power Technologies International, User Manual for PSS/E 30.2, [Online] Available: http://www.pti-us.org/pti/software/psse/sitemap.cfm

[44] M. Larsson, C. Rehtanz, and J. Bertsch, "Monitoring and Operation or Transmission Corridors," *Proceeding of the IEEE Power Tech Conference*, vol. 3, June 2003.

[45] A. Newbold, et. al., " Use of Intelligent Systems within Substations," Electra, no. 181, pp. 93-111, December 1998.

[46] M. Kezunovic, C. Liu, J. R. McDonald, and L. Smith, Automated Fault Analysis, IEEE Tutorial, IEEE PES, 2000

[47] A.G. Phadke, et. al., "Synchronized Sampling and Phasor Measurements for Relaying and Control," *IEEE Transactions on Power Delivery*, Vol. 9, No. 1, pp. 442-452, January 1994.

[48] L. Priker and H.K. Hoidalen, ATPDraw Version 4.0 for Windows9X/NT/2000/XP, SINTEF Energy Research AS, Norway. Available: http://www.eeug.org/files/secret/atpdraw

[49] The MathWorks, Matlab 7 Getting Started Guide. [Online] Available: http://www.mathworks.com/access/helpdesk/help/pdf_doc/matlab/getstart.pdf

[50] Qiming Chen; Kun Zhu; McCalley, J.D.; "Dynamic decision-event trees for rapid response to unfolding events in bulk transmission systems," in *Proc. of the IEEE Power Tech Conference*, Porto, Portugal, Sept. 2001.

TABLE A-2: Top 20 of VI for individual load bus loadbility

	Bus Number	VI_loadab
1	97594	309.7008
2	97630	21.19049
3	97610	20.6713
4	97515	15.27361
5	97623	6.913426
6	97516	2.081536
7	97503	1.936339
8	97501	0.469092
9	97622	0.273054
10	97684	0.137867
11	97525	0.08768
12	97527	0.079701
13	97523	0.066198
14	97674	0.033403
15	97606	0.03032
16	97640	0.027512
17	97689	0.024629
18	97517	0.021372
19	97679	0.005349
20	97587	0.004751

TABLE A-3: Top 20 of MI for individual bus voltage magnitude

	Bus Number	MI_V
1	97634	0.200267
2	97690	0.5112
3	97463	0.553333
4	97567	0.557733
5	97691	0.559467
6	97467	0.5712
7	97566	0.572133
8	97569	0.575333
9	97455	0.584133
10	97478	0.6012
11	97515	0.6052
12	97570	0.6072
13	97551	0.610667
14	97468	0.610933
15	97531	0.615067
16	97534	0.627333
17	97465	0.6284
18	97473	0.638
19	97459	0.646933
20	97544	0.656933

TABLE A-4: Top 20 of VI for individual load bus load loss

	Bus Number	MI_loadab
1	97515	0.314466
2	97610	0.473249
3	97630	0.497737
4	97623	0.706945
5	97503	0.729686
6	97516	0.748849
7	97501	0.864369
8	97622	0.941578
9	97525	0.951646
10	97527	0.954501
11	97523	0.957413
12	97684	0.964757
13	97517	0.974742
14	97606	0.97955
15	97674	0.982248
16	97640	0.982418
17	97689	0.985269
18	97587	0.991316
19	97679	0.992979
20	97638	0.993227

A.2 Generator Vulnerability Results

TABLE A-5: Top 20 of VI for individual generator real power output

	Bus Number	VI_Pg
1	98457	2.491231
2	99343	2.168502
3	99434	1.063368
4	99435	1.063368
5	99436	0.812812
6	99432	0.78125
7	99433	0.78125
8	98954	0.516578
9	97704	0.5
10	97781	0.5
11	97828	0.5
12	97829	0.5
13	97830	0.5
14	98089	0.5
15	98090	0.5
16	98091	0.5
17	98100	0.5
18	98101	0.5
19	98102	0.5
20	98300	0.5

TABLE A-6: Top 20 of VI for individual generator reactive power output

	Bus Number	**VI_Qg**
1	99343	0.512912
2	98100	0.5
3	98101	0.5
4	98102	0.5
5	98300	0.5
6	98839	0.5
7	99166	0.5
8	99213	0.5
9	99504	0.5
10	98473	0.5
11	99356	0.5
12	98922	0.5
13	99357	0.5
14	99443	0.5
15	99488	0.5
16	98838	0.5
17	98313	0.5
18	98577	0.5
19	99567	0.5
20	99568	0.5

TABLE A-7: Top 20 of MI for individual generator real power output

	Bus Number	MI_V
1	98457	-1.23214
2	99343	-1.08255
3	99434	-0.45833
4	99435	-0.45833
5	99436	-0.275
6	99432	-0.25
7	99433	-0.25
8	98954	-0.01644
9	97704	0
10	97781	0
11	97828	0
12	97829	0
13	97830	0
14	98089	0
15	98090	0
16	98091	0
17	98100	0
18	98101	0
19	98102	0
20	98300	0

TABLE A-8: Top 20 of MI for individual generator reactive power output

	Bus Number	MI_loadab
1	97708	0.100267
2	98320	0.112773
3	98321	0.112773
4	97911	0.129816
5	97912	0.129816
6	99383	0.18425
7	99593	0.200925
8	98458	0.2288
9	99392	0.2862
10	99391	0.3194
11	99204	0.353027
12	99205	0.353027
13	99206	0.353027
14	99207	0.353027
15	98828	0.3716
16	98829	0.3716
17	98830	0.3716
18	98243	0.394137
19	97571	0.401436
20	97572	0.401436

A.3 Branch Vulnerability Results

TABLE A-9: Top 20 of VI for individual line real power

	From Bus Number	To Bus Number	VI_Pl
1	98232	98234	1151.474
2	97745	97770	1054.963
3	97770	97868	811.4757
4	97982	98048	625.565
5	99738	99849	596.4457
6	97672	97745	567.5446
7	99344	99421	551.2517
8	99637	99640	508.2397
9	99485	99509	498.011
10	98482	98484	469.9219
11	99592	99660	456.3646
12	99323	99338	455.9427
13	99338	99384	444.0721
14	99485	99510	424.4625
15	99618	99646	423.6988
16	99508	99510	409.7863
17	98249	98434	402.2396
18	97583	97588	395.2331
19	99137	99146	389.0926
20	97920	98046	384.8288

TABLE A-10: Top 20 of VI for individual line reactive power

	From Bus Number	To Bus Number	VI_Ql
1	97516	97527	89.54636
2	97515	97527	82.72929
3	99592	99660	66.92146
4	99618	99646	63.86051
5	99323	99338	56.84085
6	97982	98048	51.20045
7	99023	99035	42.84916
8	99615	99698	41.53738
9	97989	98048	38.24065
10	97745	97770	37.93719
11	99637	99698	37.30821
12	98041	98042	37.19817
13	98779	98780	36.91867
14	99033	99034	36.65245
15	98025	98032	35.32703
16	97835	97842	35.10533
17	99662	99666	32.92319
18	97663	97679	31.56741
19	98026	98027	30.43017
20	98132	98200	29.62247

TABLE A-11: Top 20 of VI for individual line charging

	From Bus Number	To Bus Number	VI_Qc
1	97717	99162	0.239509
2	99627	99788	0.09708
3	99486	99565	0.058764
4	99627	99818	0.05864
5	99742	99818	0.049337
6	99295	99333	0.045385
7	99309	99441	0.036494
8	98487	99027	0.032424
9	98937	99203	0.031234
10	97916	98107	0.024489
11	98808	98935	0.022694
12	98235	99027	0.021931
13	98930	99027	0.021184
14	99148	99295	0.019967
15	99162	99295	0.01836
16	98246	98539	0.015748
17	98952	99027	0.011762
18	99295	99309	0.011593
19	98109	98430	0.011018
20	98930	98937	0.007813

TABLE A-12: Top 20 of VI for individual line voltage angle difference

	From Bus Number	To Bus Number	VI_line_ang
1	97965	97966	40.4111
2	97528	97536	40.08467
3	97647	97765	40.07057
4	98770	98771	39.64087
5	98867	98868	39.51216
6	97737	97751	39.31885
7	97930	97949	39.28075
8	98767	98773	39.21349
9	97930	97947	39.15643
10	97535	97552	39.08168
11	97589	97591	38.89195
12	97930	97952	38.83512
13	99226	99234	38.80736
14	97930	97940	38.65229
15	97658	97668	38.64978
16	97630	97647	38.63089
17	99248	99296	38.59942
18	97470	97539	38.41589
19	99234	99268	38.21401
20	97995	97996	38.12265

TABLE A-13: Top 20 of VI for individual line distance relay

	From Bus Number	To Bus Number	VI_Relay
1	98481	99060	4.023602
2	99799	99807	4.003577
3	98718	99651	4.000304
4	98526	98528	4.000104
5	99197	99486	3.999766
6	98235	99027	3.995915
7	98930	98937	3.968904
8	99029	99070	3.965894
9	99034	99035	3.953131
10	99517	99519	3.94626
11	98529	98530	3.944212
12	99507	99508	3.942299
13	99114	99193	3.94105
14	99043	99044	3.937048
15	99112	99174	3.936976
16	99627	99818	3.933892
17	99627	99788	3.93258
18	98537	98566	3.931335
19	99797	99811	3.923051
20	99626	99787	3.916801

TABLE A-14: Top 20 of MI for individual line flow

	From Bus Number	To Bus Number	MI_Sf
1	98232	98234	-47.0939
2	97745	97770	-45.7525
3	97770	97868	-40.0138
4	97982	98048	-35.7904
5	99738	99849	-33.7424
6	97672	97745	-33.2464
7	99344	99421	-32.204
8	99592	99660	-31.3508
9	99637	99640	-31.2326
10	99485	99509	-31.1818
11	99323	99338	-31.0245
12	99618	99646	-30.2269
13	98482	98484	-29.6878
14	99338	99384	-28.933
15	99485	99510	-28.6961
16	99508	99510	-28.202
17	98249	98434	-27.6007
18	97583	97588	-27.5333
19	99137	99146	-27.041
20	97920	98046	-27.0287

TABLE A-15: Top 20 of MI for individual line voltage angle difference

	From Bus Number	To Bus Number	MI_line_ang
1	97965	97966	-7.99012
2	97528	97536	-7.95373
3	97647	97765	-7.95216
4	98770	98771	-7.90403
5	98867	98868	-7.88956
6	97737	97751	-7.86779
7	97930	97949	-7.86349
8	98767	98773	-7.8559
9	97930	97947	-7.84946
10	97535	97552	-7.841
11	97589	97591	-7.81952
12	97930	97952	-7.81307
13	99226	99234	-7.80992
14	97930	97940	-7.7923
15	97658	97668	-7.79202
16	97630	97647	-7.78987
17	99248	99296	-7.78629
18	97470	97539	-7.76537
19	99234	99268	-7.74231
20	97995	97996	-7.73186

TABLE A-16: Top 20 of MI for individual line distance relay at sending ends

	From Bus Number	To Bus Number	MI_Relay_ft
1	99155	99157	-1.65194
2	99631	99634	-1.48746
3	98934	98936	-1.48256
4	99614	99662	-1.47599
5	99822	99847	-1.4749
6	99578	99628	-1.47359
7	99173	99249	-1.46565
8	99498	99499	-1.45416
9	99590	99646	-1.44087
10	97695	97704	-1.43708
11	97518	97685	-1.43369
12	99397	99403	-1.42361
13	98624	98625	-1.40807
14	99230	99310	-1.40063
15	99624	99630	-1.39692
16	98806	98934	-1.3934
17	97490	97493	-1.39035
18	99032	99033	-1.36062
19	97752	97840	-1.35967
20	98778	98779	-1.35445

TABLE A-17: Top 20 of MI for individual line distance relay at receiving ends

	From Bus Number	To Bus Number	MI_Relay_tf
1	99155	99157	-1.64128
2	99631	99634	-1.48656
3	98934	98936	-1.47838
4	99578	99628	-1.47055
5	99614	99662	-1.46365
6	99173	99249	-1.46187
7	99498	99499	-1.4428
8	99590	99646	-1.43327
9	97695	97704	-1.4317
10	97518	97685	-1.42836
11	99397	99403	-1.41129
12	98624	98625	-1.40113
13	99624	99630	-1.39942
14	99032	99033	-1.39408
15	99230	99310	-1.39369
16	98806	98934	-1.39102
17	97490	97493	-1.38668
18	99822	99847	-1.37316
19	97752	97840	-1.36765
20	98108	98130	-1.35832

Detection, Prevention and Mitigation of Cascading Events:

Wide-Area Measurement Based Detection and Remedial Control Actions

Final Project Report
Part II

Part II Project Team

Mani V. Venkatasubramanian
Guoping Liu
Qiang Zhang
Washington State University

Information about Part II of the final project report

For information about this project contact:

Mani V. Venkatasubramanian
Professor
School of Electrical Engineering and Computer Science
Washington State University
Pullman WA 99164-2752
Tel: 509-335-6452
Fax: 509-335-3818
Email: mani@wsu.edu

Power Systems Engineering Research Center

The Power Systems Engineering Research Center (PSERC) is a multi-university Center conducting research on challenges facing the electric power industry and educating the next generation of power engineers. More information about PSERC can be found at the Center's website: http://www.pserc.org.

For additional information, contact:

Power Systems Engineering Research Center
Arizona State University
577 Engineering Research Center
Box 878606
Tempe, AZ 85287-8606
Phone: 480-965-1643
FAX: 480-965-0745

Notice Concerning Copyright Material

Acknowledgements

This is the final report for the Power Systems Engineering Research Center (PSERC) research project S-29, titled “Detection, Prevention and Mitigation of Cascading Events.” We express our appreciation for the support provided by PSERC’s industrial members and by the National Science Foundation under grants received through the Industry/University Cooperative Research Center program. Co-funding of this project from Entergy and Tennessee Valley Authority (TVA) is gratefully acknowledged. Specifically, the project team thanks Floyd Galvan (Entergy) and Lisa Beard (TVA) who have encouraged and supported us throughout this project.

Project team at Washington State University (WSU) has consisted of three Ph.D. students:

1) Jaime Quintero first started on the oscillation monitoring work at WSU in the previous PSERC project S-19 and Jaime's Ph.D. dissertation work led to this current PSERC project S-29.
2) Guoping Liu has been the principal contributor to this report.
3) Qiang Zhang is continuing the development of the Oscillation Monitoring System at WSU.

The project has greatly benefited from collaborations with engineers from several Pserc member companies including Sujit Mandal (Entergy), Kolluri Sharma (Entergy), Gary Kobet (TVA), and William Mittelstadt (Bonneville Power Administration (BPA)). Also, a special note of thanks is reserved for Ritchie Carroll (TVA). Ricthie's expertise on Phasor Data Concentrator (PDC) capabilities has been vital to the prototype real-time implementation of our Oscillation Monitoring System into the PDC at TVA. We also thank Manu Parashar at Electric Power Group (EPG) for collaborative efforts in a related continuing project at WSU that is co-funded by BPA and the California Energy Commission (CEC).

Table of Contents

List of Figures

List of Tables

1 Introduction

This PSERC S29 project is primarily focused on prototype implementations of the algorithms that were previously developed in the PSERC S19 project that ended in 2005. In the S19 project, we had proposed the framework of a wide-area oscillation monitoring and control system that uses systemwide synchrophasor measurements for early detection and mitigation of poorly damped electromechanical oscillations in the power system. In this S29 project, we have extended the oscillation monitoring framework into an Oscillation Monitoring System (OMS) and we have implemented a prototype version of OMS into the real-time monitoring capability of the Phasor Data Concentrator at TVA. This report introduces the algorithms used within OMS and the expert system like rules that are employed within OMS for reliable automatic extraction of modal properties using real-time data.

Small-signal stability problem of power systems has remained a concern for power engineers for the past several decades. With growing loads, the power transfers over long geographical distances among different power companies have been increasing steadily. The power transfers have also become more unpredictable because of market deregulation. Large power exchanges over long transmission lines are major contributing factors for instability phenomena in power systems including oscillations [1], [2]. Growing inter-area oscillations from negatively damped inter-area modes can result in widespread blackouts such as the August 10, 1996 WECC blackout [3], [4]. It is important that we are able to detect these poorly damped or growing oscillations in the early stages of the disturbance. Then, we can initiate appropriate controls to damp out the oscillations before they become critical.

All over the world, efforts are underway to use synchrophasor measurement-based information networks to bring the Phasor Measurement Units (PMU) measurements into the control center from different parts of a large power system to determine the current state of the system [5]. These networks are called Wide Area Measurement Systems (WAMS). In WAMS, the data from the PMUs are sent to Phasor Data Concentrators (PDC) located in control centers through digital communication channels. From these real-time wide-area PMU data, we can extract dynamic information of the system such as the presence of oscillatory modal responses.

The real time measurements can be categorized into two types. The ambient type data corresponds to stationary normal operating condition, and the small variations in measurements are caused by highly distributed random load changes across the whole system. Since this type of measurements is non-intrusive and always available, many researchers have pursued analysis of ambient data recently [6]-[8]. The post-disturbance type data is observed when some changes occur in the system, e.g. a transmission line tripping or a generator tripping, etc. As discussed in [6], the ambient type methods are mainly suited for identifying the dominant oscillatory modes for the current system condition. In most cases, problematic oscillations are triggered by some radical changes in the system, and the post-disturbance type methods are more appropriate for identifying

sudden changes in damping of oscillatory modes. In our proposed Oscillation Monitoring System (OMS) being developed at Washington State University (WSU), these two types of methods work in a complementary manner [6]. A prototype version of our OMS has already been implemented into the Phasor Data Concentrator at Tennessee Valley Authority [9].

This report discusses the post-disturbance type methods, and extends the earlier work by Jaime Quintero in his doctoral dissertation [10] at WSU. In this report, we summarize efforts to develop an automatic oscillation monitoring system which is a rule based expert system that monitors PMU measurements in real-time to detect the danger of growing or poorly damped oscillations in the early stages of the event. Three modal analysis methods from signal processing theory are used in this report, namely, Prony's Method, Matrix Pencil method and Hankel Total Least Square (HTLS) method. All these methods try to fit a sum of exponential terms to the uniformly sampled data.

The Prony analysis of real-time data or event recordings in power systems is especially challenging because the power system responses contain both linear and nonlinear phenomena. Moreover, presence of noise in the measurements can upset the accuracy of results. Typically, there are also many discrete switching events that occur during a routine disturbance event, and these damping of the modes can change after each of these switching events. In the oscillation monitoring system developed at WSU, three types of rules have been developed to crosscheck results from a) moving time-window analysis, b) multiple signal groups that contain modal responses, and c) different types of signal processing engines, in order to ensure consistency of the modal analysis.

This report is organized as follows. Section 2 provides the common mathematical model for all the following algorithms. In section 3, Prony's method, Matrix Pencil Method and Hankel Total Least Squares (HTLS) are introduced and compared. Section 4 presents the framework of the Oscillation Monitoring System. The application of modal analysis engine following large disturbances is discussed in Section 5, followed by actual testing cases from real power system measurements in Section 6. Section 7 briefly discusses HVDC modulation type damping control strategies that could be triggered by OMS for improving the damping of inter-area modes.

2 Linear Analysis of Power System Small-Signal Stability

The power system is a high-order nonlinear system. However, for analyzing small disturbances, we can linearize a system around its operation point (or the equilibrium point). The linearized system can be simplified into the following form:

$$\begin{aligned} \Delta\dot{x} &= A\Delta x + b\Delta u \\ \Delta y_i &= c_i \Delta x \end{aligned}, \; i = 1,2,..., m \tag{1}$$

where Δx are the state vector, *b* and *c* are the input and output vectors respectively, Δu is the input and Δy_i is the output. As shown in [1], the transfer functions between the input and output has the following form,

$$G_i(s) = \frac{\Delta y_i(s)}{\Delta u(s)} = \sum_{i=1}^{n} \frac{R_i}{s - \lambda_i} \tag{2}$$

where $R_i = c_i \phi_i \psi_i b$, ϕ_i and ψ_i are right eigenvector and left eigenvector corresponding to λ_i respectively.

If we apply an impulse as input to the system, the m outputs are

$$y_j(t) = \sum_{i=1}^{n} R_i \exp(\lambda_i t), \; j = 1,2,..m \tag{3}$$

If the input is not an impulse, e.g. a step input, the linearized system response will still be a sum of exponential terms. This is the form that our methods can be applied to for modal estimation. When $y_j(t)$ is sampled at a constant sampling period Δt, we get the following discrete form.

$$y(k) = \sum_{i=1}^{n} R_i z_i^k \tag{4}$$

where $z_i = \exp(\lambda_i \Delta t)$, $\lambda_i = \sigma_i + j\varpi_i$. *n* is called the model order, which is not known for real power system measurements.

3 Engines for Modal Analysis

We summarize the three signal processing engines in this section mainly aimed at providing an introduction. Each method has its own advantages and weaknesses.

3.1 Prony's Method

Prony's Method tries to fit a sum of exponential terms to the uniformly sampled data. It was originally developed by Baron de Prony in 1795 to explain the expansion of various gases [11]. Prony analysis and classical eigenanalysis have become two standard approaches to study the problem of power system small signal stability [12]-[14]. The main steps are summarized below.

First, (4) can be written in the following form.

$$\begin{bmatrix} y(0) \\ y(1) \\ \\ y(N-1) \end{bmatrix} = \begin{bmatrix} 1 & 1 & \dots & 1 \\ z_1 & z_2 & \dots & z_n \\ \dots & \dots & \dots & \dots \\ z_1^{N-1} & z_2^{N-1} & \dots & z_n^{N-1} \end{bmatrix} \begin{bmatrix} R_1 \\ R_2 \\ \dots \\ R_n \end{bmatrix} \tag{5}$$

The z_i s are necessarily the roots of a nth-order polynomial with unknown coefficients a_i , and thus satisfy

$$z^n - (a_1 z^{n-1} + a_2 z^{n-2} + \dots + a_n z^0) = 0 \tag{6}$$

If we left-multiply $[-a_n, -a_{n-1}, \dots, -a_1, 1, 0, \dots 0]$ to the both sides of (5), then we get the following equation using (6).

$$[-a_n, -a_{n-1}, \dots, -a_1, 1, 0, \dots 0] \begin{bmatrix} y(0) \\ y(1) \\ \\ y(N-1) \end{bmatrix} = 0 \tag{7}$$

We can left-multiply $[0, -a_n, -a_{n-1}, \dots, -a_1, 1, 0, \dots 0]$ to the both sides of (5) and the resulting right hand side is also zero. Next, (7) can be repeated to get the following form.

$$\begin{bmatrix} y(n) \\ y(n+1) \\ \\ y(N-1) \end{bmatrix} = \begin{bmatrix} y(n-1) & y(n-2) & \dots & y(0) \\ y(n) & y(n-1) & \dots & y(1) \\ \dots & \dots & \dots & \dots \\ y(N-2) & y(N-3) & \dots & y(N-n-1) \end{bmatrix} \begin{bmatrix} a_1 \\ a_2 \\ \dots \\ a_n \end{bmatrix} \tag{8}$$

We can summarize the procedure of Prony's Method in the following three steps.

Step 1. Solve (8) to get the coefficients a_i .

Step 2. Calculate the roots of (6) to get z_i .

Step 3. Solve (5) for complex residues R_i .

Prony's Method can be extended to analyze multiple signals simultaneously. In step 1, we stack equations for each signal in (8). Consider a set of m signals $y_j(t)$, $j = 1, 2, \dots m$. Now we have a total of $(N-n)\times m$ equations with n unknown coefficients a_i in (8). The coefficients a_i are solved in the least-square sense. After calculating roots z_i , Step 3 becomes solving the following equations.

$$\begin{bmatrix} y_1(0) & y_2(0) & \dots & y_m(0) \\ y_1(1) & y_2(1) & \dots & y_m(1) \\ \dots & \dots & \dots & \dots \\ y_1(N-1) & y_2(N-1) & \dots & y_m(N-1) \end{bmatrix}$$

$$= \begin{bmatrix} 1 & 1 & \dots & 1 \\ z_1 & z_2 & \dots & z_n \\ \dots & \dots & \dots & \dots \\ z_1^{N-1} & z_2^{N-1} & \dots & z_n^{N-1} \end{bmatrix} \begin{bmatrix} R_1^1 & R_1^2 & \dots & R_1^m \\ R_2^1 & R_2^2 & \dots & R_2^m \\ \dots & \dots & \dots & \dots \\ R_n^1 & R_n^2 & \dots & R_n^m \end{bmatrix} \tag{9}$$

A practical issue in Prony's Method is to determine the unknown model order n. The common procedure is to fit a high order model to the data, and the modes corresponding to the noise have small residue magnitudes that can be filtered out from the result.

3.2 Matrix Pencil Method

The idea of Matrix Pencil method comes from the pencil-of-function approach. It is used in the areas like system identification and spectrum estimation [15]-[18]. The main steps of Matrix Pencil method are shown below.

First, define two matrices as follows.

$$[Y_1]=\begin{bmatrix} x(0) & x(1) & \dots & x(L-1) \\ x(1) & x(2) & \dots & x(L) \\ \dots & \dots & \dots & \dots \\ x(N-L-1) & x(N-L) & \dots & x(N-2) \end{bmatrix} \tag{10}$$

$$[Y_2]=\begin{bmatrix} x(1) & x(2) & \dots & x(L) \\ x(2) & x(3) & \dots & x(L+1) \\ \dots & \dots & \dots & \dots \\ x(N-L) & x(N-L+1) & \dots & x(N-1) \end{bmatrix} \tag{11}$$

where *x(k)* are the noise-free data points. *L* is the pencil parameter.

Using (4), we can write (10) and (11) as

$$[Y_2]=[Z_1][R][Z_0][Z_2] \tag{12}$$

$$[Y_1]=[Z_1][R][Z_2] \tag{13}$$

where

$$[Z_2]=\begin{bmatrix} 1 & z_1 & \dots & z_1^{L-1} \\ 1 & z_2 & \dots & z_2^{L-1} \\ \dots & \dots & \dots & \dots \\ 1 & z_n & \dots & z_n^{L-1} \end{bmatrix}_{n\times L},$$

$$[Z_1]=\begin{bmatrix} 1 & 1 & \dots & 1 \\ z_1 & z_2 & \dots & z_n \\ \dots & \dots & \dots & \dots \\ z_1^{N-L-1} & z_2^{N-L-1} & \dots & z_n^{N-L-1} \end{bmatrix}_{(N-L)\times n},$$

$$[Z_0]=diag[z_1,z_2,..z_n], \text{ and}$$

$$[R]=diag\,[R_1,R_2,...R_n]$$

and *diag[]* represents a diagonal matrix.

The matrix pencil is defined as follows.

$$[Y_2]-\lambda[Y_1]=[Z_1][R]\{[Z_0]-\lambda[I]\}[Z_2] \tag{14}$$

where [*I*] is identity matrix.

When $n \le L \le N-n$, the rank of $\{[Y_2]-\lambda[Y_1]\}$ is *n* if $\lambda \neq z_i$ [15]. However, if $\lambda = z_i$, then the *i*-th row of $\{[Z_0]-\lambda[I]\}$ becomes zero, and the rank of $\{[Y_2]-\lambda[Y_1]\}$ is reduced by one. Hence, the parameters z_i s are the generalized eigenvalues of the matrix pair $\{[Y_2];[Y_1]\}$. Or, equivalently, we can solve the ordinary eigenvalues of $\{[Y_1]^+[Y_2]-\lambda[I]\}$ to get the parameters z_i, where $[Y_1]^+$ is pseudo-inverse of $[Y_1]$. After solving for parameters z_i, we solve (5) for residues.

For the actual measured data, define a new matrix $[Y]$ containing the noisy data as follows.

$$[Y]=\begin{bmatrix} y(0) & y(1) & \dots & y(L) \\ y(1) & y(2) & \dots & y(L+1) \\ \dots & \dots & \dots & \dots \\ y(N-L-1) & y(N-L) & \dots & y(N-1) \end{bmatrix} \tag{15}$$

Comparing to (10) and (11), we can see that $[Y_1]$ is obtained by deleting the last column of $[Y]$, and $[Y_2]$ is obtained by deleting the first column of $[Y]$.

Next, apply SVD to $[Y]$ as follows.

$$[Y] = U\Sigma V^H \tag{16}$$

where *U* and *V* are unitary matrices. Σ is a diagonal matrix containing the singular values of $[Y]$ with descending order. The superscript *H* denotes conjugate transpose.

If the data were noise free, the matrix $[Y]$ has n nonzero singular values. However, when noise is present, the zero singular values are perturbed and become nonzero. Now, the Singular Value Decomposition provides an effective way of noise filtering. The singular values below some specified threshold are considered to be caused by noise and need to be set as zero.

Then, we use the n significant singular values to reconstruct the original data matrix. Now, we have

$$[V']=[v_1,v_2,..v_n] \tag{17}$$

$$[Y_1] = U\Sigma'[V_1']^H \tag{18}$$

$$[Y_2] = U\Sigma'[V_2']^H \tag{19}$$

where $v_i's$ are column vectors of V corresponding to the n dominant singular values. Σ' is the first n columns of Σ. $[V_1']$ is obtained from $[V']$ with the last row of $[V']$ deleted. $[V_2']$ is obtained from $[V']$ with the first row of $[V']$ deleted.

Now, we have

$$[Y_1]^+[Y_2] = [V_1' * V_1'^H]^{-1} * V_1' * V_2'^H = [V_1'^H]^+ V_2'^H$$

The nonzero eigenvalues of $[V_1'^H]^+ V_2'^H$ are the same as the eigenvalues of $V_2'^H[V_1'^H]^+$, where $V_2'^H[V_1'^H]^+$ is an $n \times n$ matrix. Calculating the eigenvalues of an $n \times n$ matrix is computationally inexpensive since n is usually a small number. After the eigenvalues are obtained, solve (5) for the residues.

3.3 Hankel Total Least Square (HTLS) Method

HTLS method is a more recent method and it also fits an exponential decay model onto a waveform. It is proposed in papers [19], [20], and the main steps are summarized next.

First, form the Hankel matrix as follows.

$$H = \begin{bmatrix} y_0 & y_1 & \cdots & y_{M-1} \\ y_1 & y_2 & \cdots & y_M \\ \cdots & \cdots & \cdots & \cdots \\ y_{L-1} & y_L & \cdots & y_N \end{bmatrix} \tag{20}$$

where L is a parameter chosen to be larger than n, $M = N + 1 - L$, N is the number of measurements.

If there is no noise, i.e $y(k) = \sum_{i=1}^{n} R_i z_i^k$, then H can be factorized as follows.

$$H = \begin{bmatrix} 1 & \cdots & 1 \\ z_1^1 & \cdots & z_n^1 \\ \cdots & \cdots & \cdots \\ z_1^L & \cdots & z_n^L \end{bmatrix} \begin{bmatrix} R_1 & & \\ & \ddots & \\ & & R_n \end{bmatrix} \begin{bmatrix} 1 & z_1^1 & \cdots & z_1^{M-1} \\ \cdots & \cdots & \cdots & \cdots \\ \cdots & \cdots & \cdots & \cdots \\ 1 & z_n^1 & \cdots & z_n^{M-1} \end{bmatrix} = SRT^T \tag{21}$$

where both *S* and *T* are Vandermonde matrices.

The matrix *S* is shift-invariant, that is

$$S_{\downarrow} Z = S_{\uparrow} \tag{22}$$

where the up (down) arrow placed behind a matrix stands for deleting the top (bottom) row of the matrix and *Z* is the $n \times n$ diagonal matrix whose diagonal entries are $z_1,\ldots,z_n$.

The Hankel matrix can also be decomposed by SVD as follows.

$$H = U\Sigma V^H = \begin{bmatrix} \hat{U} & U_0 \end{bmatrix} \begin{bmatrix} \hat{\Sigma} & \\ & \Sigma_0 \end{bmatrix} \begin{bmatrix} \hat{V} \\ V_0 \end{bmatrix}^H \tag{23}$$

where *U* and *V* and unitary matrix, i.e $UU^H = I$, $VV^H = I$, *I* is identity matrix, *H* denotes complex conjugate transpose. Σ is a diagonal matrix with singular values on the diagonal in decreasing order. $\hat{\Sigma}$ is the sub-matrix containing first *n* singular values. If there is no noise in the signal, the sub-matrix Σ_0 is null. Otherwise, Σ_0 is a full matrix with small singular values on the diagonal. When noise is present, the usual procedure is to set a threshold and those singular values below the threshold are considered to be generated by noise and can be discarded.

In the noise-free case, $H = \hat{U}\hat{\Sigma}\hat{V}^H$. Compare this equation with (21), we have the following relationship.

$$\hat{U} = SQ \tag{24}$$

where *Q* is a n by n nonsingular matrix. Deleting the first row in the above equation gives $\hat{U}_{\downarrow} = S_{\downarrow} Q$, while deleting the last row gives $\hat{U}_{\uparrow} = S_{\uparrow} Q$.

Thus $\hat{U}_{\downarrow}$ and $\hat{U}_{\uparrow}$ are related by the following equation.

$$\hat{U}_{\uparrow} = S_{\downarrow} ZQ = \hat{U}_{\downarrow} Q^{-1} ZQ = \hat{U}_{\downarrow} \tilde{Z} \tag{25}$$

where $\tilde{Z} = Q^{-1} ZQ$, which has the same eigenvalues as *Z*, ie. $z_1,\ldots,z_n$.

In the noisy case, equation (25) does not hold exactly. In this case, we solve $\tilde{Z}$ by

total lease square method. After calculating $\tilde{Z}$, the signal poles are calculated as the eigenvalues of $\tilde{Z}$.

When we need to analyze multiple signals simultaneously, simply replace *H* in (20) by the horizontally stacked Hankel matrices as follows.

$$H_{series}=\begin{bmatrix} H_1 & H_2 & \dots & H_m \end{bmatrix} \tag{26}$$

where *m* is the number of signals.

The last step to calculate residues R_i 's is the same as that of Prony's method.

3.4 Comparison of Three Methods

Given three analysis methods described above, we are now interested in comparing their performances. The accuracy of the estimated frequency and damping ratio under noisy measurement is of special interest to our problem. In the following, we add different levels of noise to the data, and then calculate the mean value and standard deviation of the estimated frequencies and damping ratios from 100 independent runs. The test signal used for comparison is shown below.

$$y(t) = e^{-0.05t}\cos(2\pi * 0.2t) + e^{-0.1t}\cos(2\pi * 0.3t) + n(t)$$

where *n(t)* denotes noise component. *y(t)* is sampled at 30 Hz and a total of 10 seconds data is used for analysis.

The signal contains two modes at 0.2 and 0.3 Hz with damping ratio of 3.98% and 5.30% respectively. Hundred simulation runs for each Signal-Noise-Ratio (SNR) level and each method are carried out and the results are shown in Table I and II. For Matrix Pencil method and HTLS method, the SVD threshold is set to 10% of the largest singular value.

From Tables I and II, we can see that all of the three methods can estimate the frequencies of both modes quite accurately. However, damping ratio estimation, which is more important in Oscillation Monitoring System, has larger variance, especially under higher noise level. For example, at the 20 dB SNR level, the standard deviations of the estimated damping ratio of the first mode are 1.41%, 0.99% and 0.92% for Prony's Method, Matrix Pencil and HTLS respectively. These standard deviations are comparable to the mean values, and this indicates we get less reliable estimation results when the noise is high. Among the three methods, Matrix Pencil Method and HTLS method have similar noise performance, and they are better than Prony's Method as shown by their standard deviations. In other words, Prony's Method is more sensitive to noise.

Table I. Comparison of Three Methods under Noisy Measurements (30 dB noise)

	Frequency (Hz)	Damping Ratio (%)	Frequency (Hz)	Damping Ratio (%)
True Value	0.2000	3.98	0.3000	5.30
Mean Value (Prony's Method)	0.1999	4.12	0.2999	5.20
Standard Deviation (Prony's Method)	0.0008	0.74	0.0013	0.38
Mean Value (Matrix Pencil)	0.1990	4.05	0.3031	4.93
Standard Deviation (Matrix Pencil)	0.0004	0.26	0.0005	0.16
Mean Value (HTLS)	0.1990	4.07	0.3032	4.89
Standard Deviation (HTLS)	0.0004	0.26	0.0005	0.18

Table II. Comparison of Three Methods with Noisy Measurements (20 DB noise)

	Frequency (Hz)	Damping Ratio (%)	Frequency (Hz)	Damping Ratio (%)
True Value	0.2000	3.98	0.3000	5.30
Mean Value (Prony's Method)	0.1991	3.97	0.3010	4.84
Standard Deviation (Prony's Method)	0.0017	1.41	0.0021	1.15
Mean Value (Matrix Pencil)	0.1990	4.11	0.3031	4.91
Standard Deviation (Matrix Pencil)	0.0012	0.99	0.0017	0.68
Mean Value (HTLS)	0.1988	3.86	0.3036	5.01
Standard Deviation (HTLS)	0.0011	0.92	0.0015	0.65

Next, a comparison of the speeds of three methods is performed and the average time needed for one simulation run is shown in Table III. For Prony's method, the speed depends on how we solve the least squares problem (section IIIA). The SVD based least square procedure is numerically more robust than the QR based procedure, but it is much more time-consuming since SVD is an $O(n^3)$ procedure. For Matrix Pencil and HTLS method, they have similar procedure of SVD for the Hankel matrix. The result in Table III shows that the HTLS method is relatively the fastest among the three methods.

Table III. Average Time Needed for One Simulation Run

Methods	Average Time (sec)
Prony (SVD)	0.44983
Prony (QR)	0.12250
Matrix Pencil	0.17046
HTLS	0.11625

The average computational times reported in Table III were computed using Matlab code running in a "typical" three-year old laptop. The times are meant for relative comparison among the three methods. In actual field implementation with efficient C code, the algorithms are quite fast as reported in [9].

4 Oscillation Monitoring System Framework

The complete Oscillation Monitoring System being developed at WSU includes both ambient type methods and post-disturbance type methods. A simplified flowchart of Oscillation Monitoring System is shown in Fig. 1. The program reads data from the PDC typically located in the control center. Depending on whether any event is detected in the system, the Oscillation Monitoring System will choose the ambient type or post-disturbance type methods accordingly. If the results from moving window analysis are consistent, the Oscillation Monitoring System can send an alarm to the system operator or trigger damping controllers directly. The content in this report corresponds to the blocks with emphasized border and light blue background in the flowchart of Fig. 1, and these algorithms have been developed under PSERC funding.

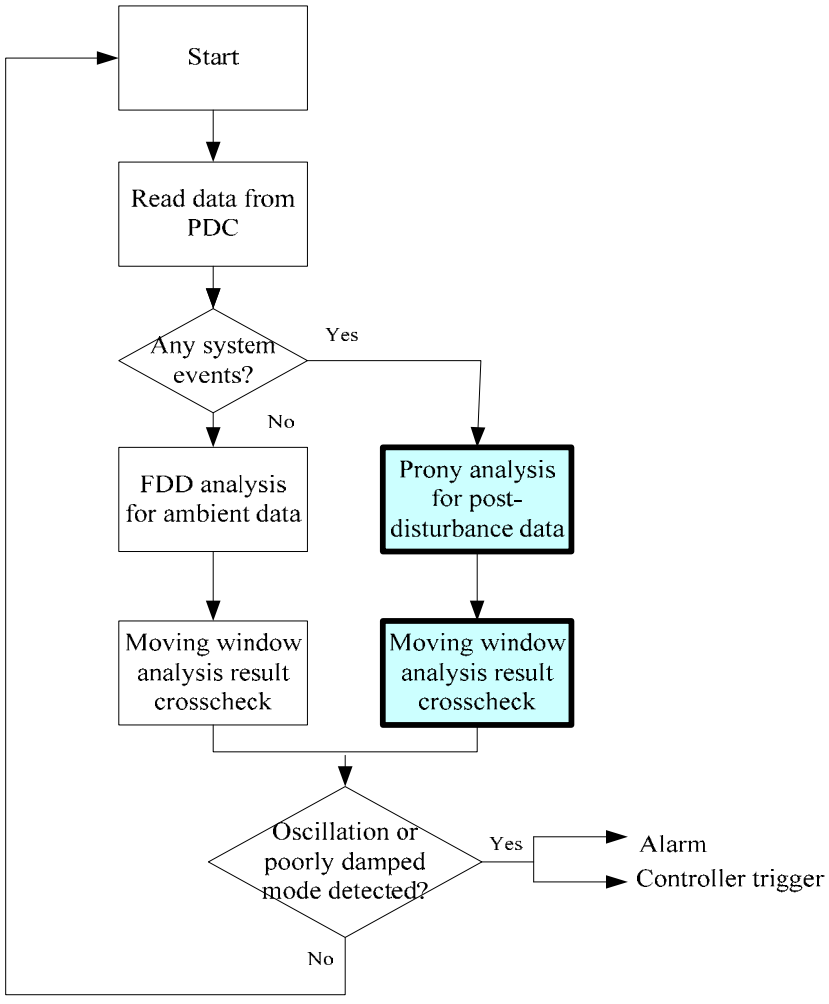

Figure 1. Simplified flowchart for Oscillation Monitoring System

The reason to use moving window analysis or other types of crosscheck rules is to avoid false alarms from the Oscillation Monitoring System. In practice, the power system

responses contain both linear and nonlinear phenomena. Moreover, presence of noise in the measurements can upset the accuracy of results. Typically, there are also many discrete switching events that occur during a routine disturbance event, and these damping of the modes can change after each of these switching events. Therefore, it is not uncommon to get different results from different methods, different signal groups or different time windows for the actual signals measured from power systems. Crosscheck is a crucial step to ensure the consistency of the online modal analysis.

In the proposed Oscillation Monitoring System, rules have been developed to crosscheck results from a) moving time-window analysis, b) multiple signal groups that contain modal responses, and c) different types of signal processing engines. Only when all the results are considered to be consistent will the system trigger an alarming signal, and here 'consistent' means the identified dominant modes from all the results fall into a pre-specified frequency range and damping ratio range. The choice of parameters in crosschecking is a trade-off between the speed of detection and accuracy.

The proposed Oscillation Monitoring System provides two levels of oscillation detection. That is, OMS is able to detect local modes as well as inter-area modes. For the local oscillation detection, we use the signals from the same PMU. The signal groups used for local analysis are pre-specified. However, the pre-specified signal groups for inter-area mode may be not enough to capture some unexpected inter-area oscillations. For this reason, we form the inter-area mode signal groups automatically from the subset of the PMUs that participate in the oscillations. All these tasks of local oscillation detection are executed in parallel by multi-threading in a powerful computer exclusively for oscillation monitoring in the control center.

After the local mode analysis, the next step is to determine the dominant mode in each PMU for each method, and then the crosscheck for all methods is performed in each PMU. The results are considered to be consistent if the dominant modes from different methods fall in a specified frequency range and damping ratio range. The above crosscheck is called local mode crosscheck. If more than two PMUs have consistent local crosschecks, then the inter-area mode detection tasks are activated. Inter-area mode crosscheck is performed from the subset of PMUs showing oscillations of the same frequency. Moving window crosscheck is to compare results along the sliding data windows. If several moving window crosschecks give consistent estimates, for example, four consecutive consistent moving windows crosschecks, then the resulting damping ratios are compared to a threshold to determine whether an alert is triggered. For instance, the damping ratio threshold for detecting poorly damped oscillations could be set to be say +3% for reliable operation of power systems.

5 Oscillation Monitoring Following Large Disturbances

Power system is basically a high-order nonlinear system. These nonlinearities are caused by many factors such as the fundamentally nonlinear nature of power balance equations, the limiting functions in exciters, Power System Stabilizers (PSS), etc., the nonlinearities of generator saturation curves as well as nonlinear load responses in the system [21]. The power system responses following large disturbances usually show strong nonlinearities, especially immediately following a line outage when the field currents in the exciters may hit the upper limits trying to boost generator terminal voltages. If the system is transient stable, the system should move to the previous or a new operating point in the form of a damped oscillatory response which is also sometimes referred to as the “ring-down”.

In [22], the authors apply the Hilbert spectral analysis to the responses following the fault and obtain the instantaneous frequency and damping. The resulting instantaneous damping ratios are comparable to the damping ratio from Prony analysis. However, the instantaneous damping varies much after fault, and it has to be averaged over time to provide useful information.

In the following paragraph, we will show that the proposed Oscillation Monitoring System is able to give good estimate for the ring-down case following a large disturbance. The test system is a two-area four-generator system from [1]. The one-line diagram of the system is shown as follows.

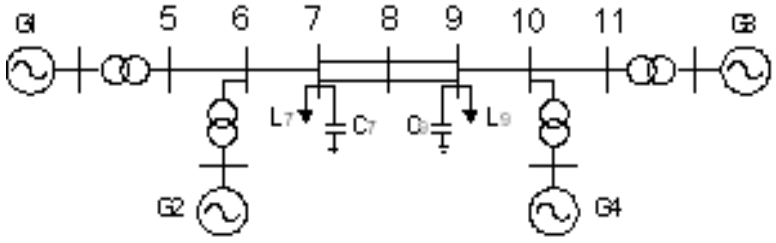

Figure 2. One line diagram of two-area system

The operating condition and system parameters are the same as those in [1]. Note that only two PSSs are installed on G1 and G3 respectively. The complete eigenvalue analysis is done using SSAT [23] for the system. The original system has an inter-area mode with 0.6176 Hz and 5.35% damping ratio. When line 7-8 circuit #1 is out of service, the inter-area mode will change to 0.4589 Hz and 4.70% damping ratio. Now, for the original system, we apply a three-phase fault using TSAT [24] in the middle of the line 7-8 circuit #1, and clear the fault after 0.1 sec. by tripping the faulted line. No reclosing action is performed and the active power of the parallel line 7-8 circuit #2 is shown below.

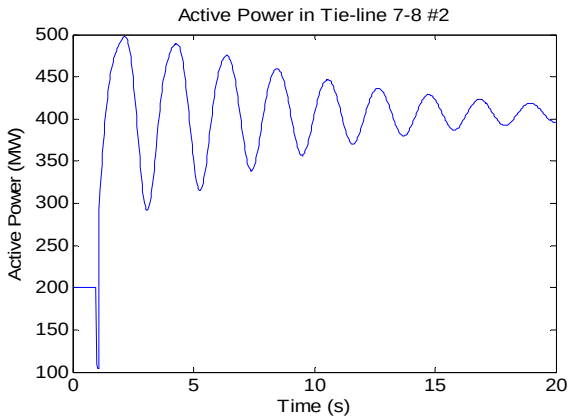

Figure 3. Active powers of line 7-8 circuit #2 following a 0.1 sec three phase line fault

The three methods are applied to the above tie-line active powers using a 5 second sliding window after the fault and the resulting frequency and damping ratio are plotted at the end of each analysis window in Fig. 4. The upper part of the plot shows the frequency estimates and the lower part shows the damping ratio estimates.

From Fig. 4, we clearly see the nonlinear effects on the analysis results. In the first few swings after the fault, the damping ratios from three methods are different from each other and they also differ a lot from the result from eigenanalysis. The nonlinearities in the first few swings from factors such as saturations and exciter limiters can result in an underestimate (or overestimate) of damping ratio for the inter-area mode. From linear system theory, we note that the concepts of eignevalues and modal analysis are only applicable for small disturbances away from an equilibrium point. It is imperative that we ignore the results of modal analysis when the system responses are large in being away from the equilibrium point. However, after the first few swings, the three methods give consistent and accurate damping ratio estimates. This test shows the importance of avoiding the adverse effect of nonlinearities. In the proposed Oscillation Monitoring System, the first one or two swings are ignored immediately after the fault by our consistency crosscheck rules in order not to trigger false warning signals.

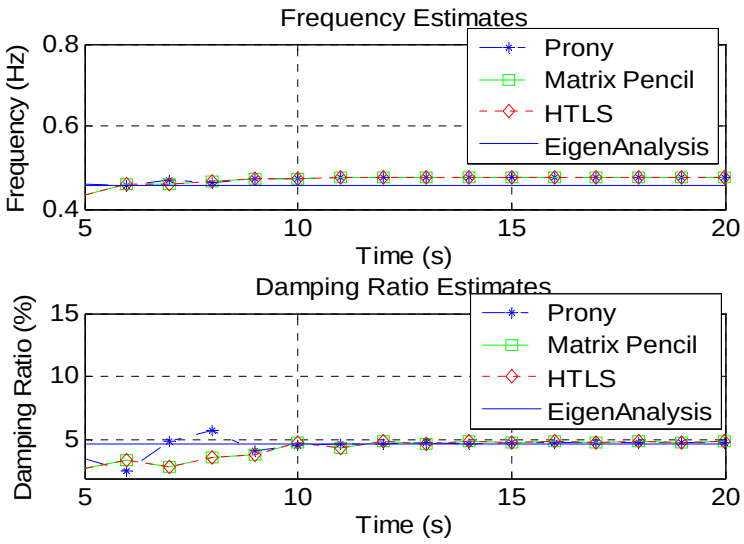

Figure 4. Frequency and damping ratio estimates following a 0.1 sec three phase line fault

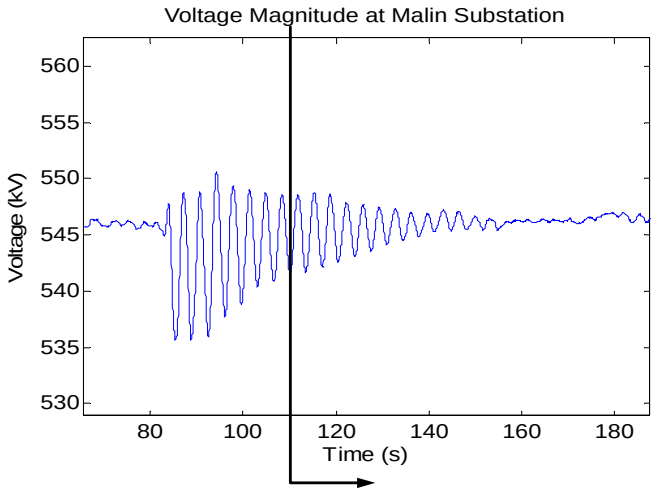

Figure 5. The voltage magnitude at Malin in Aug. 4, 2000

6 Case Studies for Oscillation Monitoring

6.1 Case I

In this test case, we will apply three methods to PMU measurements recorded in WSCC system on August 4th, 2000. At about 19:56 GMT Standard Time, the Alberta system separated from the rest of the system, resulting in poorly damped oscillations [25]. The voltage magnitude at Malin Substation is shown in Fig. 5. The 0.27 Hz inter-area mode involved in this event appears to be the same inter-area mode that led to the August 10, 1996 WSCC blackout. The solid black vertical line in the middle of the figure shows the time instant when the Oscillation Monitoring System issues an alarm. This is explained in more detail in the following paragraphs.

The recorded data contains measurements from a total of ten PMUs, eight of which are located at 500kV substations, including Grand Coulee, Malin, Colstrip, Devers etc. In the following analysis, we only use the measurements from these eight PMUs. First, we form signal groups in each PMU and cross-check their results for all methods. The signals used for analysis are voltage and current magnitudes in each PMU, while the frequency measurements are avoided because of lesser accuracy. A series of analyses using a 5-second sliding window are applied to the data segment from 60 sec. to 130 sec., where the time at 0 sec corresponds to 19:55:00 GMT Standard Time. The results are plotted at the end point of the sliding widow for each analysis. The frequency and damping ratio estimates shown in Figs. 6, 7 and 8 correspond to the results at Grand Coulee, Malin and Devers substation respectively. Again, the upper part of the plot shows the frequency estimates and the lower part shows the damping ratio estimates.

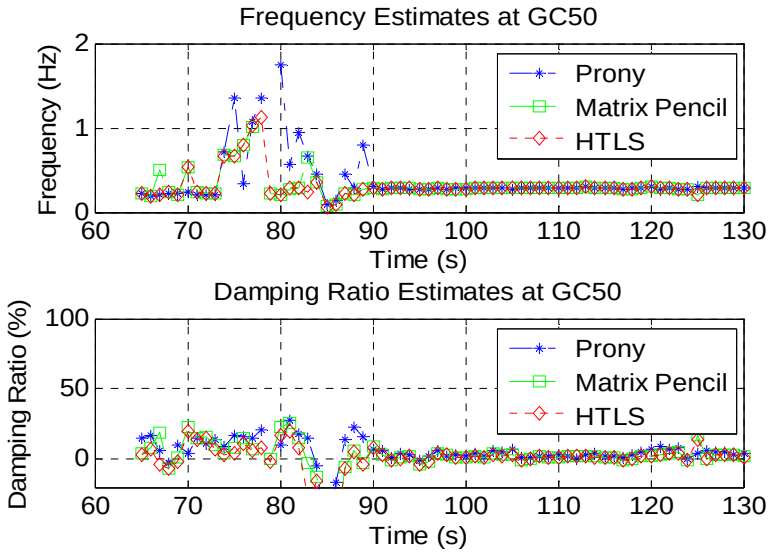

Figure 6. Frequency and damping ratio estimates at Grand Coulee for Case I

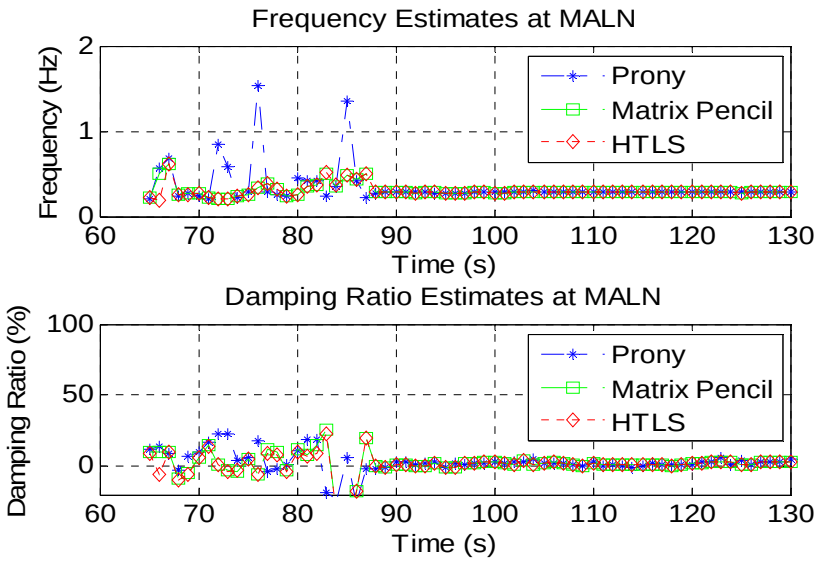

Figure 7. Frequency and damping ratio estimates at Malin Substation for case I

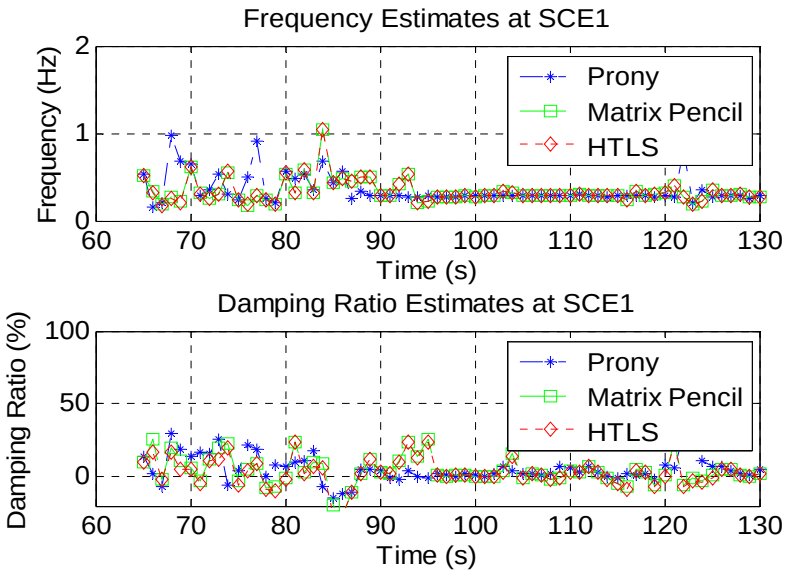

Figure 8. Frequency and damping ratio estimates at Devers (SCE1) for case I

From the figures above, we see that the estimates become consistent for all three methods when the analysis window begins to cover the oscillation segment. Fig. 9 shows consistent estimates in all the PMUs, where each dot stands for a consistent estimate in the corresponding PMU. It is seen that the measurements at John Day, Malin and Keeler substations have more consistent estimates than others during this event. This is because these PMUs are located along main transmission corridors for the inter-area oscillation.

All three methods, Prony's Method, Matrix Pencil, and HTLS can compute for the mode shape associated with an inter-area mode when we use consistent measurements from each PMU in the inter-area mode detection stage above. That is, if we use all bus voltage measurements or bus voltage phase angles from different PMUs, the related residues and phase angles in the inter-area detection shape can give us valuable insight into the mode shape of that oscillatory mode. Owing to space limitations, the mode shape computation and discussion are postponed to a future publication.

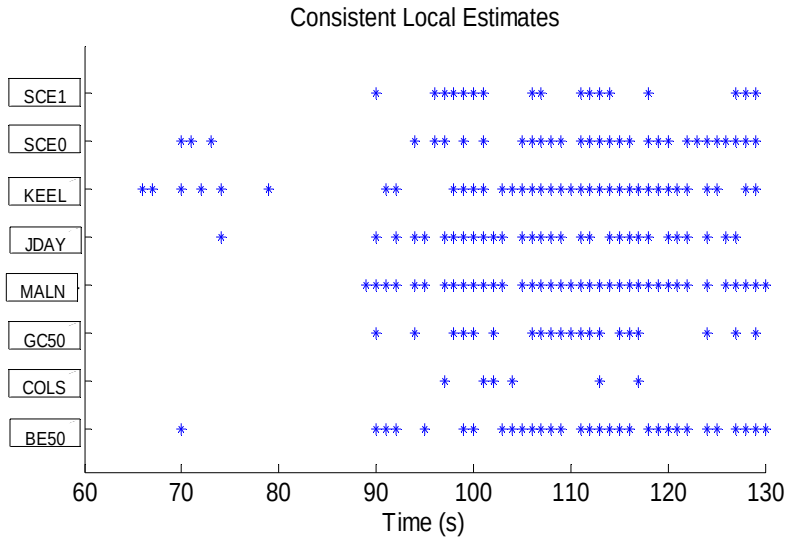

Figure 9. Consistent local estimates in all PMU's for case I

When more than two consistent local crosschecks are found at a specific time, the inter-area mode detection is activated automatically. The signals used here for inter-area mode detection are voltage magnitudes at the PMUs showing consistent local crosschecks. The results for inter-area mode detection are shown in Fig. 10. An acceptable result of a predefined number (say 4) of consecutive moving window consistent inter-area crosschecks occur at 109 sec., with the mean frequency at 0.2871 Hz and the mean damping ratio is +0.96%. Therefore, the Oscillation Monitoring System is able to trigger an alert to system operator with a reliable estimation at the early stage of the oscillation, showing a good compromise between the speed of detection and accuracy.

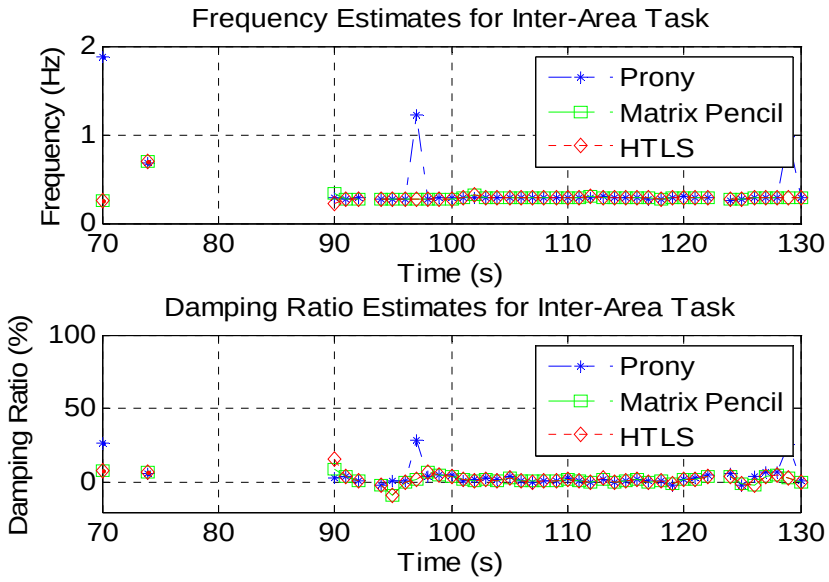

Figure 10. Frequency and damping ratio estimates of inter-area mode detection for Case I

6.2 Case II

The second case is recorded recently in eight PMUs located in TVA system [9]. After a 500kV line tripping, we can see an oscillation in the system. The voltage magnitude at one 500kV substation PMU 3 is plotted below for the initial stage of the oscillation. The bold black vertical line again shows the time instant when the Oscillation Monitoring System issues an alarm.

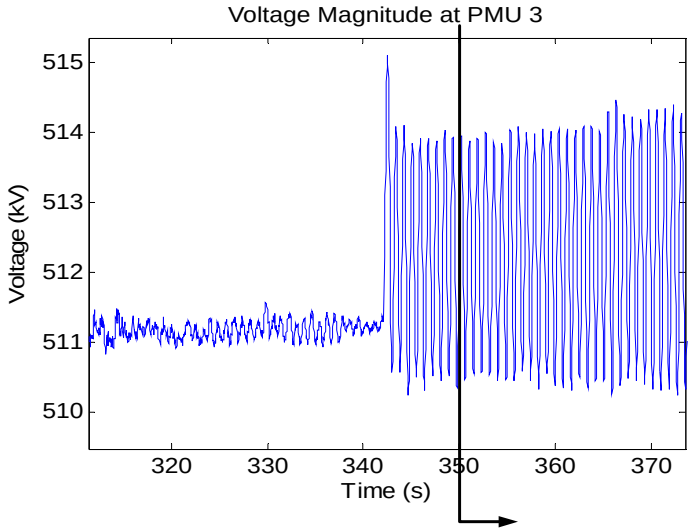

Figure 11. The voltage magnitude at PMU 3 for Case II

The measurements from each PMU form a signal group. A series of analyses using 5-second sliding window are applied to the data segment from 330 sec. to 360 sec. The consistent estimates for all PMUs are shown in Fig. 12. The results show that this event is either a local oscillation or an intra-area oscillation, and the problematic area is somewhere between PMU 2 and PMU 3. This information is also quite useful to choose appropriate damping controls.

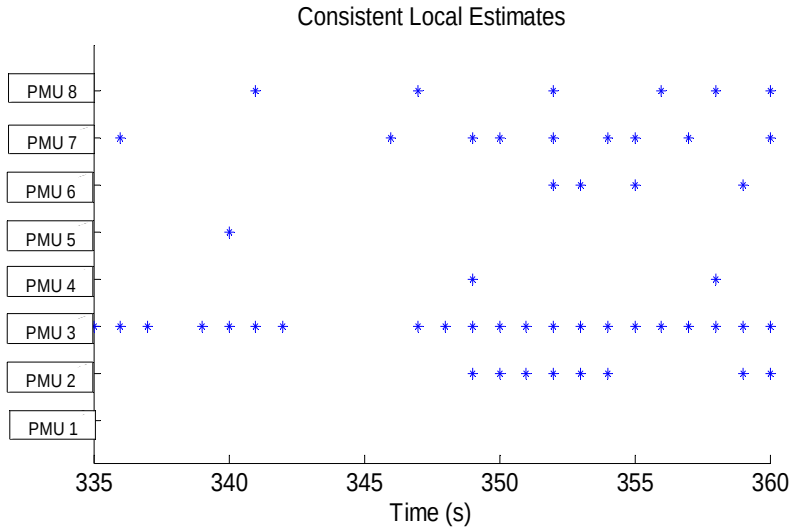

Figure 12. Consistent local estimates in all PMU's for Case II

The local crosscheck at PMU 3 is shown in Fig. 13. The inter-area crosscheck is activated automatically and the results are shown in Fig. 14. The Oscillation Monitoring System will trigger an alert at 350s, when the number of moving window consistent inter-area estimates reaches a predefined number say 4. The mean frequency is 1.1754 Hz and the mean damping ratio is +0.39% for the inter-area crosscheck. The local crosscheck at PMU 3 also gives a consistent estimate at 350s with the mean frequency at 1.1777 Hz and the damping ratio at 0.14%, The Oscillation Monitoring System will therefore issue an alarm or a control trigger thus indicating the need for some operator intervention or control action.

6.3 Case III

This case is also from the eastern interconnection. Here we only have measurements from three PMUs, so the OMS will trigger an alarm when local moving window crosscheck reaches a consistent estimate. Again, the signal groups are formed in each PMU. The voltage magnitude at PMU 1 is shown in Fig. 15. The bold black vertical line shows the time instant when the Oscillation Monitoring System issues an alarm.

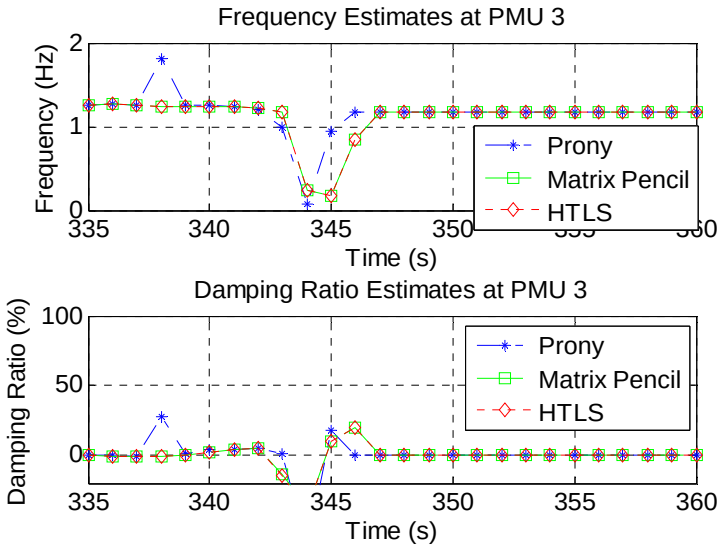

Figure 13. Frequency and damping ratio estimates at PMU 3 for Case II

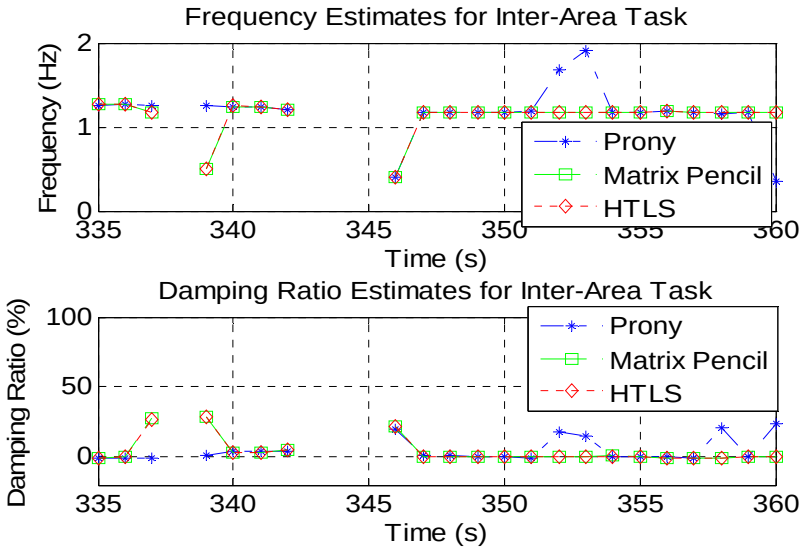

Figure 14. Frequency and damping ratio estimates of inter-area mode detection for Case II

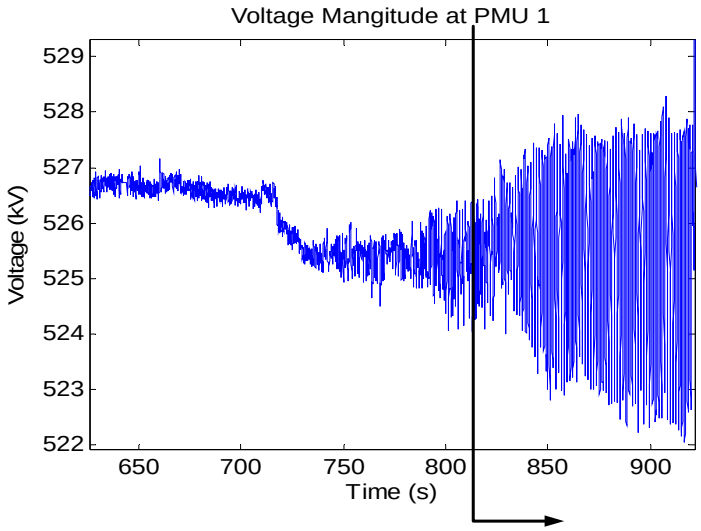

Figure 15. The voltage magnitude at PMU 1 for Case III

Sliding 5 second time-windows are applied to the data segment form 740 sec. to 820 sec. The results for the signal group from PMU 1 are shown in Fig. 16. Consecutive 4 moving window consistency crosschecks occur at 811 sec., with the mean frequency at 0.6892 Hz and the mean damping ratio of -0.59%. This shows that system operator may have seen an alert at the beginning stage of the oscillation if OMS had been installed. The signal groups in other PMUs do not have consistent estimates, so they are not shown here. Had any damping control been applied in the early stage, the system may have avoided the eight minutes of sustained oscillation.

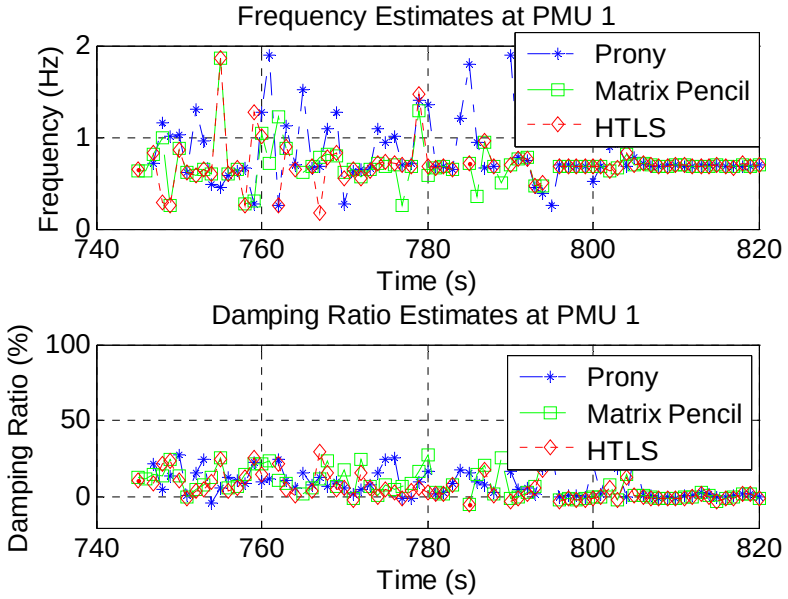

Figure 16. Frequency and damping ratio estimates of PMU 1 for Case III

7 Oscillation Damping Control by HVDC Modulation

The Oscillation Monitoring System can be extended to initiate triggers for damping controllers [10], so that it can provide aggressive damping control actions to damp out poorly damped or growing oscillations. For instance, the oscillations can possibly be reduced or eliminated by reducing appropriate tie-line power flows or by the use of Flexible Alternating Current Transmission System (FACTS). Tie-line power flow reduction can be achieved through specific generation tripping in the sending area and/or load shedding in the receiving area. Alternately, if there are many FACTS devices available in the system, the use of damping controllers in these devices is more desirable. The candidate damping controllers include Static Var Compensation (SVC) modulation [10], Thyristor Controlled Series Compensator (TCSC) modulation and High Voltage Direct Current (HVDC) modulation.

Our previous work in [10] shows that SVC modulation is an effective way to add system damping in case of poorly damped oscillation. Here, we will study the impact of HVDC modulation on system damping. The system in Figure 2 is now modified by adding a HVDC link between the two areas. In the base case, the HVDC link transfers 200MW of power and the parallel AC tie-lines also transfer 200MW of power. Only one PSS is installed in Gen #1. Other parameters are as described in [1]. The test system without HVDC modulation has an inter-area mode at 0.6226 Hz and the damping ratio is 1.48%. A block diagram of a HVDC modulation system from [1] is shown in Figure 17. The modulation block diagram is shown in more detail in Figure 18. In the following paragraphs, we will study the effects of different parameters on the damping ratio of the inter-area mode.

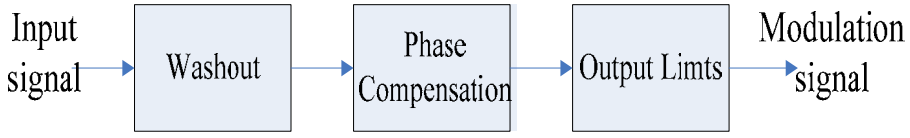

Figure 17. Functional diagram of HVDC modulation system

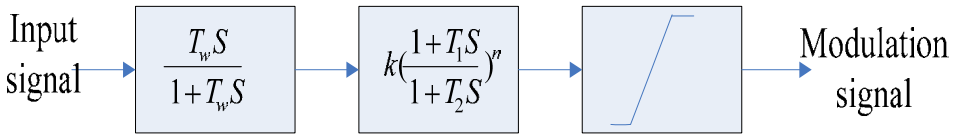

Figure 18. Block diagram of HVDC modulation system

First, we will use the AC tie-line active power as the input signal for the HVDC modulation as in [1]. First, we study the effect of phase lead and phase lag compensation. The results from different gain and phase compensation are calculated using SSAT and shown in Table IV. From Table IV, it is seen that the two-area system has the largest damping ratio with 90 degree phase lead compensation and k = 0.25. Phase lag compensation is not recommended for HVDC modulation because it is shown that phase lag compensation has little positive impact on the damping ratio of the inter-area mode.

When k is large, phase lag compensation even leads to undamped oscillation, which is worse than without any HVDC modulation control at all.

Table IV. Damping Ratios with Different Gains and Phase Compensations

(Tw=10 s and 0.1 p.u. output limits, tieline MW input)

	k = 0.1		k = 0.25		k = 0.5	
Phase Lead	Freq (Hz)	Damping Ratio (%)	Freq (Hz)	Damping Ratio (%)	Freq (Hz)	Damping Ratio (%)
30	0.6399	1.84	0.6638	2.11	0.6981	2.14
60	0.6505	4.51	0.6942	7.18	0.7577	7.95
90	0.656	11.48	0.7686	17.28	0.871	11.34
120	N/A	N/A	0.9366	13.9	0.9678	6.35
Phase Lag	Freq (Hz)	Damping Ratio (%)	Freq (Hz)	Damping Ratio (%)	Freq (Hz)	Damping Ratio (%)
30	0.6257	0.89	0.6304	0.07	0.6381	-1.16
60	0.6231	1.08	0.6239	0.5	0.6254	-0.45
90	0.6222	1.28	0.6216	0.98	0.6206	0.48
120	0.6221	1.41	0.6213	1.3	0.62	1.12

Next, different constants for washout block are tested and shown in Table V. We can see that the system damping changes slightly with different washout time constant. It means the washout time constant is not a significant parameter to the system damping for HVDC modulation.

Table V. Effect of Washout Time Constants on the System Damping

(90 degree phase lead compensation and k=0.25)

T_w	Frequency (Hz)	Damping Ratio (%)
3	0.7704	18.32
5	0.7694	17.72
10	0.7686	17.28
15	0.7684	17.13
20	0.7682	17.06

In the large system, it is difficult to identify the parallel AC path for measuring the tie-line MW power input signal that was used in the design of Table IV. With the development of WAMS, the phase angle difference of bus voltage angles at the two terminals of a HVDC installation can now be used as the remote input signal for HVDC modulation. For the above two-area system, the phase angle difference between bus 7 and bus 9 is used and the resulting table is shown below to show the effect of different phase compensation and gains. This table also recommends phase-lead compensation, with the

largest system damping ratio at 120 degree phase-lead compensation and k = 1. Compared to the modulation effect when the active tie-line power-flow is used, the HVDC with phase difference as input signal has even higher damping ratio for the inter-area mode in the two-area system.

Table VI. Damping Ratios with Different Gains and Phase Compensations

(TW=10 S AND 0.1 P.U. OUTPUT LIMITS, PHASE DIFFERENCE INPUT)

	k = 0.5		k = 1		k = 2	
Phase Lead	Freq (Hz)	Damping Ratio (%)	Freq (Hz)	Damping Ratio (%)	Freq (Hz)	Damping Ratio (%)
30	0.6344	1.70	0.6486	1.86	0.6667	2.01
60	0.6414	3.57	0.6609	5.23	0.7004	7.25
90	0.6428	8.19	0.6757	14.47	0.7846	17.05
120	0.5940	18.41	0.8770	25.68	0.9533	12.95
Phase Lag	Freq (Hz)	Damping Ratio (%)	Freq (Hz)	Damping Ratio (%)	Freq (Hz)	Damping Ratio (%)
30	0.6246	1.08	0.6267	0.69	0.6308	-0.05
60	0.6229	1.21	0.6232	0.95	0.6238	0.43
90	0.6223	1.35	0.6220	1.22	0.6214	0.95
120	0.6223	1.43	0.6219	1.39	0.6212	0.6208

Now, we compare the effects of different damping controllers to the original case without HVDC modulation. A three phase fault is applied at bus 8 and cleared after 0.1 sec. The active powers in Line 7-8 #1 are shown in Figure 19 for comparison. As we can see from Figure 19, the original case shows an undamped oscillation. With HVDC modulation, the oscillation is damped out in three swings for both damping controllers. The difference between the two modulation schemes is not significant in the simulation.

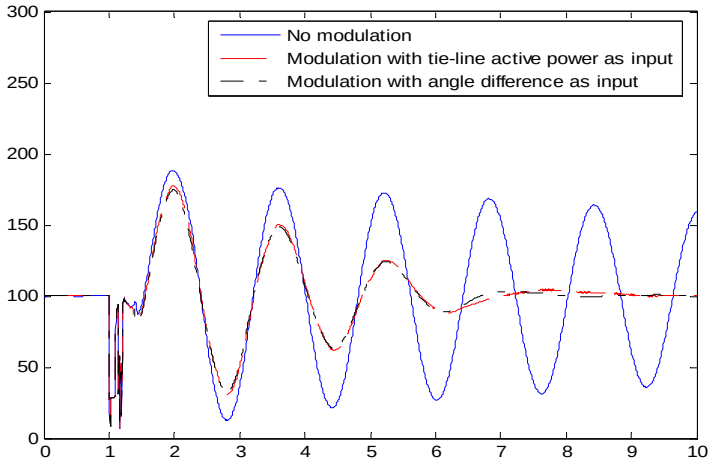

Figure 19. Comparison of different HVDC modulation controllers

Finally, we test the modulation controller for drastic variations in AC tie-line power transfers. The results in Table VII show that HVDC modulation provides satisfactory damping under very different operating conditions, which shows that the same phase lead design of the HVDC modulation can be used under wide variations in AC power transfers. It is interesting that the damping of the inter-area mode remains strong even under reversed direction of AC power transfers. Therefore, the HVDC modulation design using the phase angle difference input signal appears to be a strong candidate for a real-time damping control action.

Table VII. System Damping in Different Power-Flow Cases with Phase Lead Compensation

	Tie-line MW as HVDC modulation input (k = 0.25, 90° lead)		Angle difference as HVDC modulation input (k=1 and 120° lead)	
Tie-line Powerflow (MW)	Frequency (Hz)	Damping Ratio (%)	Frequency (Hz)	Damping Ratio (%)
400	0.7039	17.94	0.8656	27.34
200	0.7686	17.28	0.8770	25.68
100	0.7816	17.18	0.8814	25.28
0	0.7854	17.39	0.8852	25.13
-200	0.7661	19.32	0.8920	25.35
-400	0.6783	25.66	0.8975	26.25

8 Conclusions

This report presents a methodology for automatic real-time modal analysis of wide area PMU measurements. The framework can detect poorly damped or negatively damped oscillations caused by local, intra-area as well as inter-area oscillatory modes. The report discusses crosscheck rules that have been developed to avoid inconsistent estimations that can be caused by noise, nonlinearities or switching events. The rules and results have been illustrated on actual PMU recordings. Results from field implementation of the WSU Oscillation Monitoring System at Tennessee Valley Authority will be reported in a future publication. We plan to continue testing, tuning and enhancing the capabilities of OMS from field implementation results. Future research is also needed for determining correct mitigating actions by either operators or automatic control devices that can improve the damping of problematic oscillatory modes whenever poorly damped oscillations are detected by OMS.

9 References

1) P. Kundur, *Power System Stability and Control*. McGraw-Hill, Inc., New York, 1994
2) M. Klein, G. J. Rogers, and P. Kundur, "A fundamental study of inter-area oscillations in power systems," *IEEE Trans. Power Systems,* vol. 6, pp. 914-921, Aug. 1991.
3) D.N.Kosterev, C.W.Taylor, W.A.Mittelstadt, "Model validation for the August 10, 1996 WSCC system outage," *IEEE Trans. Power Systems*, vol.14, no.3, pp.967-979, Aug. 1999.
4) V. Venkatasubramanian and Y. Li, "Analysis of 1996 western American electric blackouts," in *Proc. Bulk Power System Phenomena-Stability and Control*, Venice, Italy, 2004.
5) J. Y. Cai, Z. Huang, J. Hauer, and K. Martin. "Current status and experience of WAMS implementation in north america," in *Proc. Transmission and Distribution Conference and Exhibition: Asia and Pacific*, pp. 1-7, 2005.
6) G. Liu and V. Venkatasubramanian, "Oscillation monitoring from ambient PMU measurements by Frequency Domain Decomposition," *Proc. IEEE International Symposium on Circuits and Systems*, Seattle, WA, May 2008, pp. 2821-2824.
7) J. W. Pierre, D. J. Trudnowski, and M. K. Donnelly, "Initial results in electromechanical mode identification from ambient data," *IEEE Trans. Power Systems*, vol. 12, pp. 1245-1251, Aug. 1997.
8) N. Zhou, J. W. Pierre, and R. W. Wies. "Estimation of low-frequency electromechanical modes of power systems from ambient measurements using a subspace method," in *Proc. 35th North American Power Symposium*, Rolla, Missouri, Oct 2003.
9) V. Venkatasubramanian and J. R. Carroll, "Oscillation Monitoring System at TVA", presentation at NASPI meeting, New Orleans, LA, Mar. 2008.http://www.naspi.org/meetings/workgroup/2008_march/session_one/tva_oscillation_monitoring_venkatasubramanian.pdf
10) J. Quintero, "A real-time wide-area control for mitigating small-signal instability in large electric power systems," Ph.D. dissertation, School of EECS, Washington State University, Pullman, WA, May 2005.
11) G. R. B. Prony, "Essai experimental et analytique sur les lois de la dilatalrlite de fluids elastiques et sur cells de la vapeur de l'alcool, à différents tempoeratures," *Journal de l'Ecole Polytechnique (París),* vol. 1, pp. 24-76, 1795.
12) J. F. Hauer, C. J. Demeure, and L. L. Scharf, "Initial results in Prony analysis of power system response signals," *IEEE Trans. Power Systems,* vol. 5, pp. 80-89, Feb. 1990.
13) D. J. Trudnowski, J. R. Smith, T. A. Short, and D. A. Pierre, "An application of Prony methods in PSS design for multi-machine systems," *IEEE Trans. Power Systems*, vol. 6, pp. 118-126, Feb. 1991.
14) D. J. Trudnowski., J. M. Johnson, and J. F. Hauer, "Making prony analysis more accurate using multiple signals," *IEEE Trans. Power Systems*, vol. 14, pp. 226-231, Feb. 1999.

15) T. K. Sarkar and O. Pereira, "Using the matrix pencil method to estimate the parameters of a sum of complex exponentials," *IEEE Antennas and Propagation Magazine*, vol. 37, pp. 48-55, Feb. 1995.
16) Y. Hua and T. K. Sarkar, "On SVD for estimating generalized eigenvalues of singular matrix pencil in noise," *IEEE Trans. Signal Processing*, vol. 39, pp. 892-900, Apr. 1991.
17) Y. Hua and T. K. Sarkar, "Matrix pencil method for estimating parameters of exponentially damped/undamped sinusoids in noise," *IEEE Trans. Acoustics, Speech, and Signal Processing*, vol. 38, pp. 814-824, May 1990.
18) M. L. Crow and A. Singh, "The matrix pencil for power system modal extraction," *IEEE Trans. Power Systems*, vol. 20, pp. 501-502, Feb. 2005.
19) J. M. Papy, L. D. Lathauwer, and S. V. Huffel, "Common pole estimation in multi-channel exponential data modeling," *Signal Processing*, vol. 86, pp. 846-858, 2006.
20) L. Vanhamme and S. V. Huffel, "Multichannel quantification of biomedical magnetic resonance spectroscopy signals," *Advanced Signal Processing Algorithms, Architectures and Implementations VIII, Proceedings of SPIE*, vol. 3461, pp. 237-245, 1998.
21) D. J. Trudnowski, and J. E. Dagle, "Effects of generator and static-load nonlinearities on electromechanical oscillations," *IEEE Trans. Power Systems*, vol. 12, pp. 1283-1289, Aug. 1997.
22) A. R. Messina and V. Vittal, "Nonlinear, non-stationary analysis of interarea oscillations via Hilbert spectral analysis," *IEEE Trans. Power Systems*, pp. 1234-1241, Aug. 2006.
23) *Small Signal Analysis Tool (SSAT), User's Manual*, Powertech Labs Inc., Surrey, BC, Canada, 2002.
24) *Transient Security Assessment Tool (TSAT), User's Manual*, Powertech. Labs Inc., Surrey, BC, Canada, 2002.
25) J. F. Hauer, M. J. Beshir, and W. Mittelstadt, "Dynamic performance validation in the western power system," Presented on behalf of the WSCC Performance Validation Task Force at the APEx 2000 in Kananaskis, Alberta, Oct. 2000.

Detection, Prevention and Mitigation of Cascading Events:

Adaptive Islanding with Selective Under-Frequency Load Shedding

Final Project Report
Part III

Part III Project Team

Vijay Vittal
Ruisheng Diao
Siddharth Likhate
Kai Sun
Guangyue Xu
Arizona State University

Information about Part III of the final project report

For information contact:

Vijay Vittal
Ira A. Fulton Chair Professor
Department of Electrical Engineering
Arizona State University
PO Box 875706
Tempe, AZ 85287-5706
Tel: 480-965-1879
Fax: 480-965-0745
Email: vijay.vittal@asu.edu

Power Systems Engineering Research Center

The Power Systems Engineering Research Center (PSERC) is a multi-university Center conducting research on challenges facing the electric power industry and educating the next generation of power engineers. More information about PSERC can be found at the Center's website: http://www.pserc.org.

For additional information, contact:

Power Systems Engineering Research Center
Arizona State University
577 Engineering Research Center
Box 878606
Tempe, AZ 85287-8606
Phone: 480-965-1643
FAX: 480-965-0745

Notice Concerning Copyright Material

Acknowledgements

This is Part III of the final report for the Power Systems Engineering Research Center (PSERC) research project S-29, titled "Detection, Prevention and Mitigation of Cascading Events." We express our appreciation for the support provided by PSERC's industrial members and by the National Science Foundation under grants received through the Industry/University Cooperative Research Center program. We also thank Entergy Corporation for its additional support.

We recognize the postdoctoral researchers and graduate students that contributed to the research and creation of the reports: Ruisheng Diao (Arizona State University), Dr. Kai Sun (Arizona State University, now at EPRI), Siddharth Likhate (Arizona State University, now at AREVA T&D) and Guangyue Xu (Arizona State University).

The authors thank all PSERC members for their technical advice on the project, especially the industry advisors for the project:

Sharma Kolluri – Entergy Corporation
Sujit Mandal – Entergy Corporation
Dan Glaser – Entergy Corporation
Lei Wang – Powertech Labs
Frederic Howell – Powertech Labs

Table of Contents

List of Figures

List of Tables

1 Introduction

This research effort demonstrates the application of the tools developed in PSERC project S-19 to the Entergy system for the purpose of controlled islanding following a large disturbance which could lead to cascading outages and eventual blackout. In order to perform controlled islanding, two important questions need to be answered; 1) Where to island? and 2) When to island? The topic of the first question was addressed in detail in project S-19 where a slow coherency based group approach was used in conjunction with a graph-theoretic tool to develop a minimal cutest which created the necessary islands. In this work, the solution to the second question is addressed using PMU measurements and a decision tree (DT) approach to determine whether an initiating disturbance could result in cascading outages and eventual blackout. The DT identifies the critical attributes and determines the thresholds for these attributes together with the associated initiating disturbance. It is envisioned that the critical attributes will be monitored using PMUs. If a critical attribute measurement violates a threshold as the operating scenario unfolds, the controlled islanding scheme will be armed. If the associated initiating contingency occurs, then the controlled islanding scheme will be initiated. If the associated contingency does not occur then the system operated normally and would be continually monitored. This report is organized as follows:

Section 1 introduces the background of this project. Literature reviews dealing with the transient stability problems in modern power systems and the main causes of cascading events are discussed. In addition, principles of synchronized phasor measurements and decision trees are explored. Section 2 details the controlled separation strategy including slow coherent generator grouping, optimal cut set identification and DT training techniques. Section 3 tests the scheme on the Entergy system operational models and takes a critical contingency case to examine the DT performance and benefits of the controlled separation strategy.

1.1 Background

It has been over a century since electricity was first invented and commercialized. In the very beginning, only a few customers were supported by a single generator with very simple connections. Due to the development of innovative manufacturing and control techniques, power systems all over the world were continuously expanded by constructing larger power plants and installing new transmission lines to transport large amounts of electric power over thousands of miles to meet increasing demands. Thus, the existing power networks have experienced an evolution to a highly interconnected topology for both reliability and economical reasons.

As a result of globalization, countries with highly developed economies have seen the consumption of electric power in industrial, commercial and residential areas rise at a rapid rate during the past few decades. Figure 1-1 shows the growth in the world electric power consumption in different regions from the year 1980 to 2005 and Figure 1-2 provides the total electricity installed capacity for the same time period [1]. In 2005, the world's total electricity power consumption increased to 15,746.54 million Kilowatts,

which is approximately double the consumption in 1980. This load growth has brought a corresponding increase in total electricity installed capacity, but it has not resulted in a concomitant increase in the transmission capability due to the difficulty of siting and approving new transmission lines. Hence, existing power networks are likely to be operated under greater stress with transmission lines carrying electric power near their limits, especially during peak load periods. In such situations, certain severe disturbance with low probability may initiate system wide unstable power swings that will lead to cascading outages of transmission lines and finally a large scale blackout. It is therefore of vital importance to identify these critical contingencies for a given system, analyze the causes of cascading events and develop an effective control strategy to quickly and accurately predict loss of synchronism in the system in order to take proper control actions and prevent a large scale blackout.

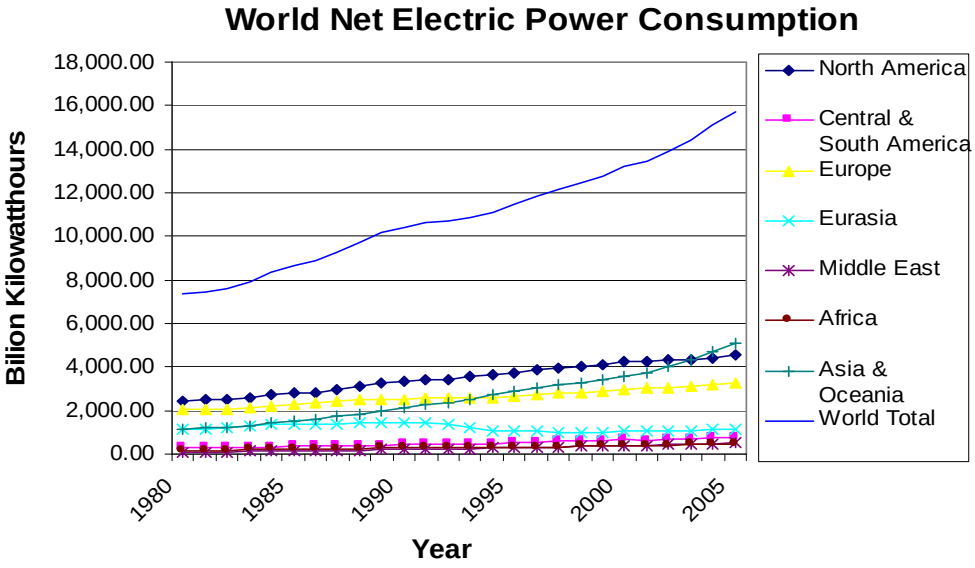

Figure 1-1: World Power Consumption Growth (1980-2005)

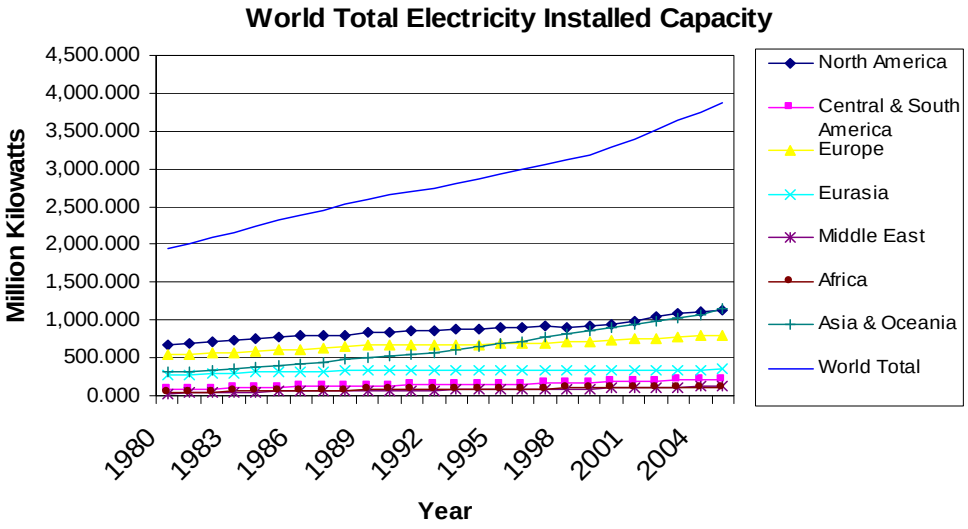

Figure 1-2: World Total Electricity Installed Capacity (1980-2005)

1.2 Cascading Events and Controlled Separation

At steady state, the operating power system should have the capability of tolerating the loss of any one element in the system (N-1) according to NERC standards, such as a generator, transmission line, transformer or critical load. When a disturbance occurs, the electric torque output in the generator suddenly changes and is no longer equal to the mechanical torque input. Therefore, the machines move away from equilibrium governed by the swing equation of the generators that is described by:

$$\frac{2H}{\omega_0}\frac{d^2\delta}{dt^2} = T_m - T_e$$

where H is the inertia constant, ω_0 is the rated value of angular velocity of the rotor, δ is the angular position of the rotor in electrical radians, T_m is the mechanical torque input and T_e is the electric torque output [2]. The modeling of T_m and T_e depends on the detail to which the whole system is represented. If the disturbance is small, the oscillations could be eliminated by the action of controls such as exciters, governors and power system stabilizers. However, synchronism of generators may be lost due to severe disturbances like loss of two or more critical system elements at the same time. Take the sample system shown in Figure 1-3 as an example, if an important path of power transfer is damaged, severe power imbalances will occur at both of the sending and receiving ends. Thus, the generators at the sending area will speed up while the ones at the receiving area will slow down. The transients tend to separate the two groups of generators away from each other in terms of the power angles. Such a phenomenon is depicted in Figure 1-4. Since voltage magnitudes at buses and active power flows on transmission lines are closely related to power angles, out of step swings will occur without timely control actions.

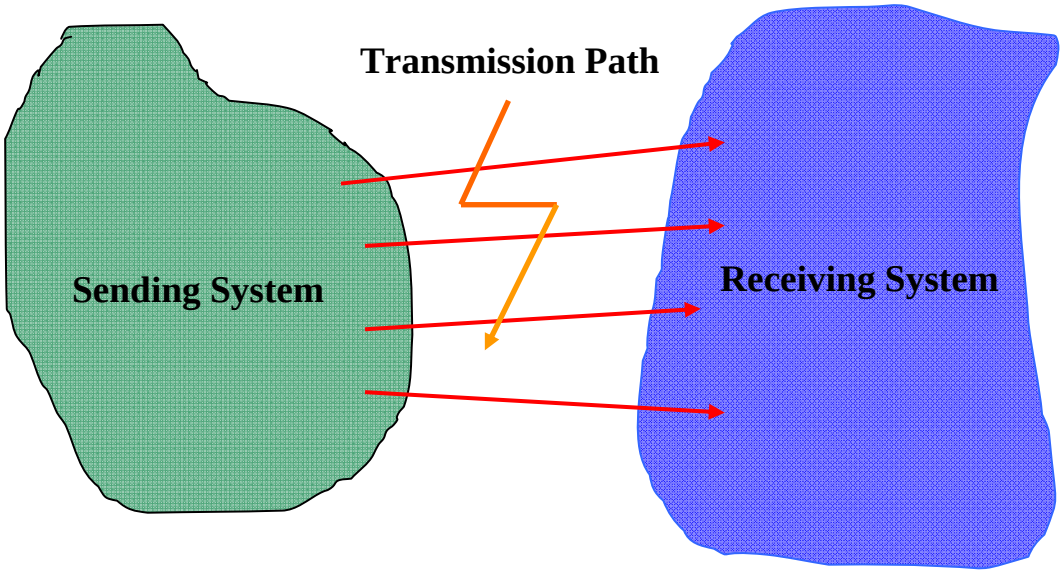

Figure 1-3: A Sample of Power System with a Critical Transmission Path

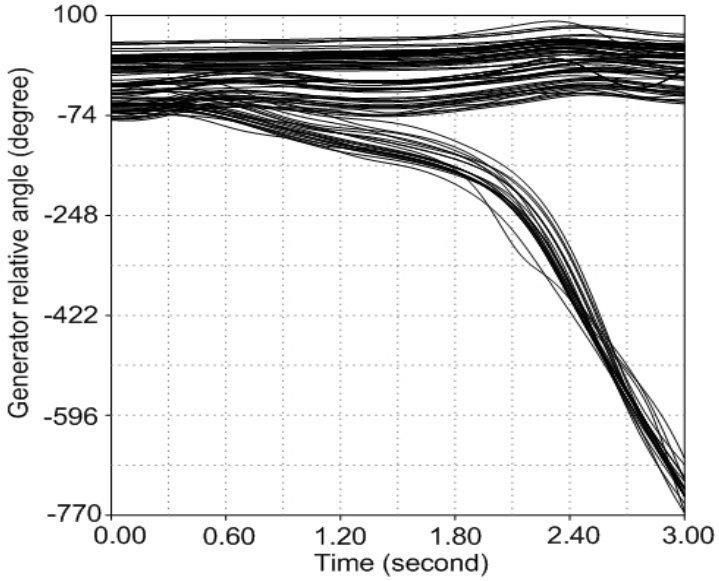

Figure 1-4: Generator Angles after Line Outages

Different protective relay devices are installed across the system to protect generators, transmission lines and transformers from damage during fault conditions. For high voltage transmission line protection, impedance or distance relays are usually used to detect faults and trip the branches by comparing the monitored impedance locus with the relay zone settings. The principle of the impedance relay is depicted in Figure 1-5. The three impedance loci monitored on line A-B represent the impedance behavior under fault, stable swing and unstable swing conditions respectively. For case 1, a fault occurs on the branch from bus A to bus B and the impedance locus enters zone 1 almost instantaneously. Thus, the relay detects this situation and trips the line for protection. For case 2, a small disturbance in the system occurs and causes the monitored impedance

locus to move towards zone 2, but the locus does not enter zone 2 or zone 1 due to proper control actions. In this case, this branch will not be tripped.

It is important to note that an out of step swing can also cause the tripping of a line since the impedance locus such as the one in case 3 may travel through zone 2 and zone 1 at a relatively slow velocity. In this case, the traditional impedance relay logic does not have the capability of differentiating an unstable swing from a fault and therefore trips the branch as if a fault is seen by the relay monitoring system. Once a severe swing is initiated, cascading outages are likely to occur because tripping the first branch gives the system another jolts and deteriorates the unstable swing, which makes it extremely difficult to bring the whole system back to a normal state using existing control devices. As the swings continue, whenever a line sees a violation of relay settings, this line is tripped and this is how the cascading events progresses. It has been reported that false tripping of protective relays during transient periods is the main problem leading to cascading outages [3].

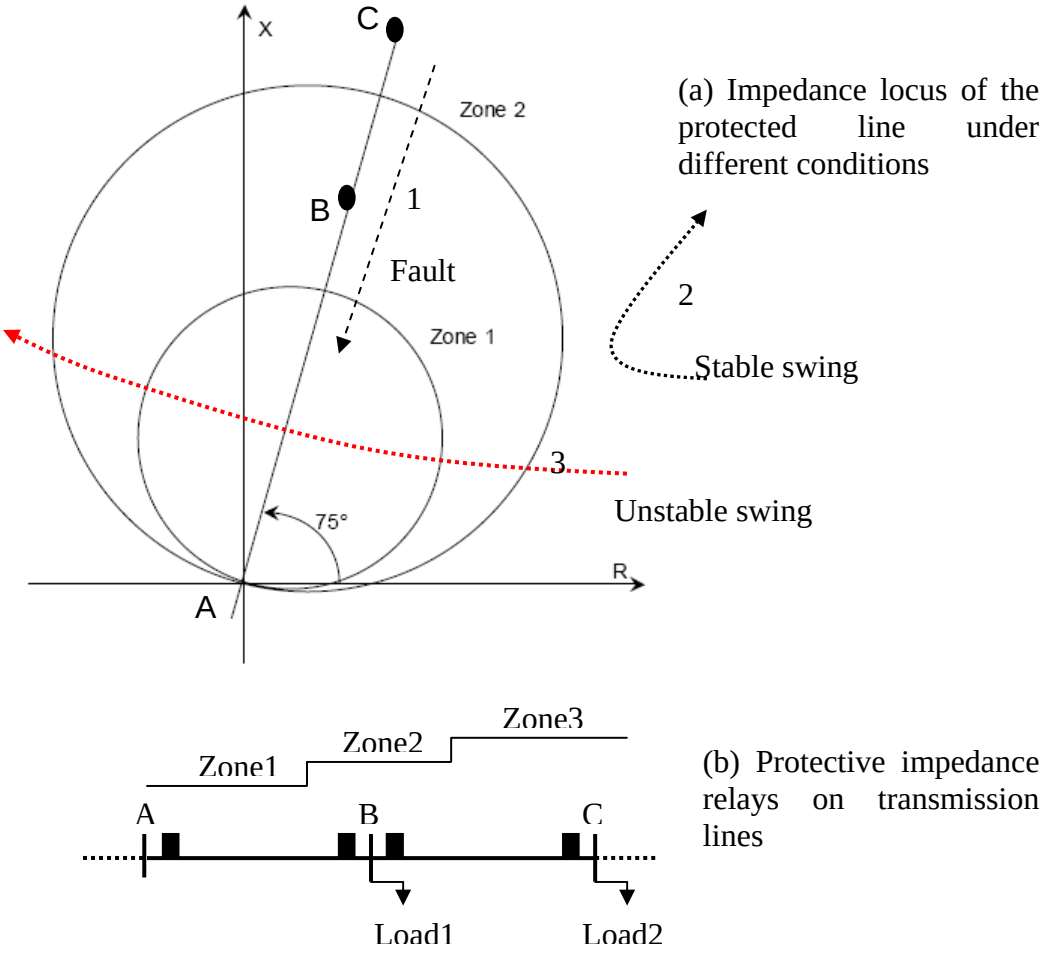

Figure 1-5: Principle of Protective Impedance Relay

In order to detect unstable swings, out of step (OOS) relays have been developed that utilize regular impedance relays by properly setting the timing logic. The basic principle is that the time for an unstable swing to travel from zone 2 to zone 1 is much longer than a fault condition, which is recorded by a timer. If this time exceeds a set threshold, an unstable swing is determined and further action can be taken [4]-[6]. Such a relay can effectively detect impending loss of synchronism and trip the line for protection. However, without centralized control, OOS relay may function similar to traditional impedance relays during cascading events. As a result, it is necessary to design a timely and effective control scheme for the purpose of overall system stability after a power system experiences a large disturbance.

Among different special stability control schemes, power system controlled islanding (or separation) is considered as the last line of defense. It provides an effective approach to stop cascading outages by separating the whole system into several predefined islands, which are simple to restore. This control strategy confines the disturbance to a local area instead of allowing the disturbance to spread throughout the whole system. After the islands are created, subsequent control actions are required to keep the voltage and frequency profiles in each island at normal levels. Thereafter, different islands can be connected together again by proper restoration procedures. Controlled islanding schemes must be carefully designed and implemented due to the severe impact on power systems caused by a false trip or failure to trip. In this control strategy there are two major issues to be addressed: (1) Where to island? (2) When to island? Many of the previous research efforts on controlled separation were focused on answering the question “where to island?” That is, to find the best cut set in the power system based on slowly coherent generator groups under certain constraints. The separation strategy is usually defined offline since the grouping of slowly coherent generators is relatively insensitive to disturbance locations and the search space is relatively large [7]-[8]. The details of identifying where to island will be further discussed in Section 2.

This research project mainly focuses on addressing the second issue “when to island?” That is to accurately and rapidly determine the timing to form the islands. From our simulations in the following sections and the conclusions in [9], the progress of cascading outages usually occurs within a few seconds after a severe disturbance is initiated. In order to analyze the detailed system transient behaviors, a variety of dynamic models representing all of the generators, exciters, governors, PSSs and protective relays across the whole system need to be included in the transient stability simulation. As the size of the system grows, the computation time increases significantly because of the high nonlinear and dimensional characteristics. Therefore, using the traditional time-domain simulation methods to evaluate system transient behavior in real time may not be suitable for determining when to perform the controlled islanding action. It is desirable to develop an online monitoring mechanism which can provide a fast and accurate prediction result as to whether the initiating disturbance will cause cascading events in the system. If so, the controlled separation scheme should be triggered before the outages really occur.

Based on previous methods of online transient stability prediction developed in [10]-[12], an event-triggered online transient stability assessment tool is developed in this

research project by using offline trained decision trees and real time phasor measurements. The main idea is to identify critical system attributes as transient stability indicators, train efficient decision trees for accurate predictions using these critical system attributes and compare measurements from PMUs with the thresholds in the DTs to obtain a fast stability assessment. Before discussing the details of this proposed method, principles of PMUs and decision trees are first introduced together with a discussion of their advantages in the following sections.

1.3 Phasor Measurement Unit

State monitoring in power systems plays an important role in system operation and online decision making. Traditionally system states were monitored using analog devices such as current transformers and potential transformers and communicated to the energy management system (EMS) through the supervisory control and data acquisition (SCADA) system. This approach served the industry well but lacks the ability of observing measurements across the whole system because the data was not time synchronized. The advent of phasor measurement units has revolutionized the field of power system state monitoring. PMUs have significant advantages over the traditional measurements in terms of both accuracy and frequency of sampling. A typical PMU configuration consists of a global positioning system (GPS) receiver, a filter, an analog/digital converter and a microprocessor. The GPS receiver provides one pulse per second (PPS) signal with a time stamp containing the year, day, hour, minute and second, which is divided into a number of pulses for the sampling of the analog signals derived from conventional measurement devices. The number of pulses can be defined by the users, which is usually 12 times per cycle in a 60 Hz system [13]. With these synchronized time stamps, analog signals are converted to digital signals and sent to the microprocessor for further calculation. Thus, generator angles, bus voltages, bus angles, power flows, frequencies, currents, power factors and other system information can be calculated in the microprocessor. The time-stamped phasors calculated in the PMUs are synchronized to a common time frame by satellites and then assembled into a series of data streams for communication to remote control centers [14]. Therefore, a PMU has the ability to observe different system states across the whole system in real time, especially during transient periods. Phasor measurement units have been commercialized, an example of which is given in Figure 1-6 and Figure 1-7 [15]. Applications using phasor measurements in power systems have been developed for loss of synchronism detection, multi-area state estimation, oscillation mode identification, voltage stability protection and system dynamics monitoring [16]-[19].

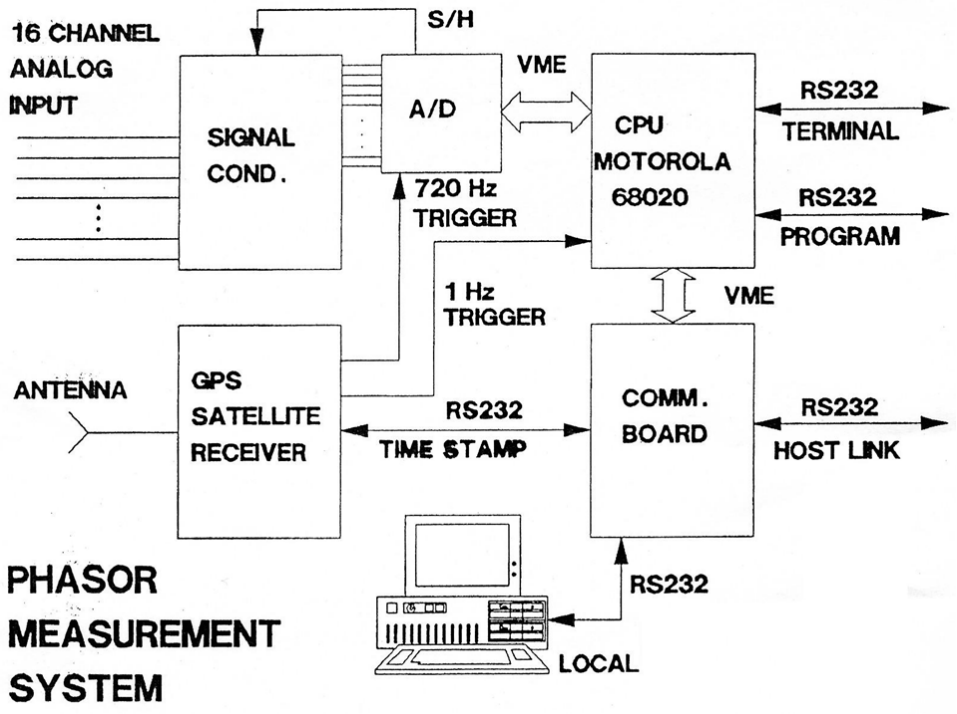

Figure 1-6: Block Diagram of Arun Phadke's PMS (taken from [15])

(Characteristics: (a) analog antialiasing input filter with a cutoff frequency of 360 Hz, (b) 12 bit sample and hold A/D technology 720 samples per second with analog multiplexing)

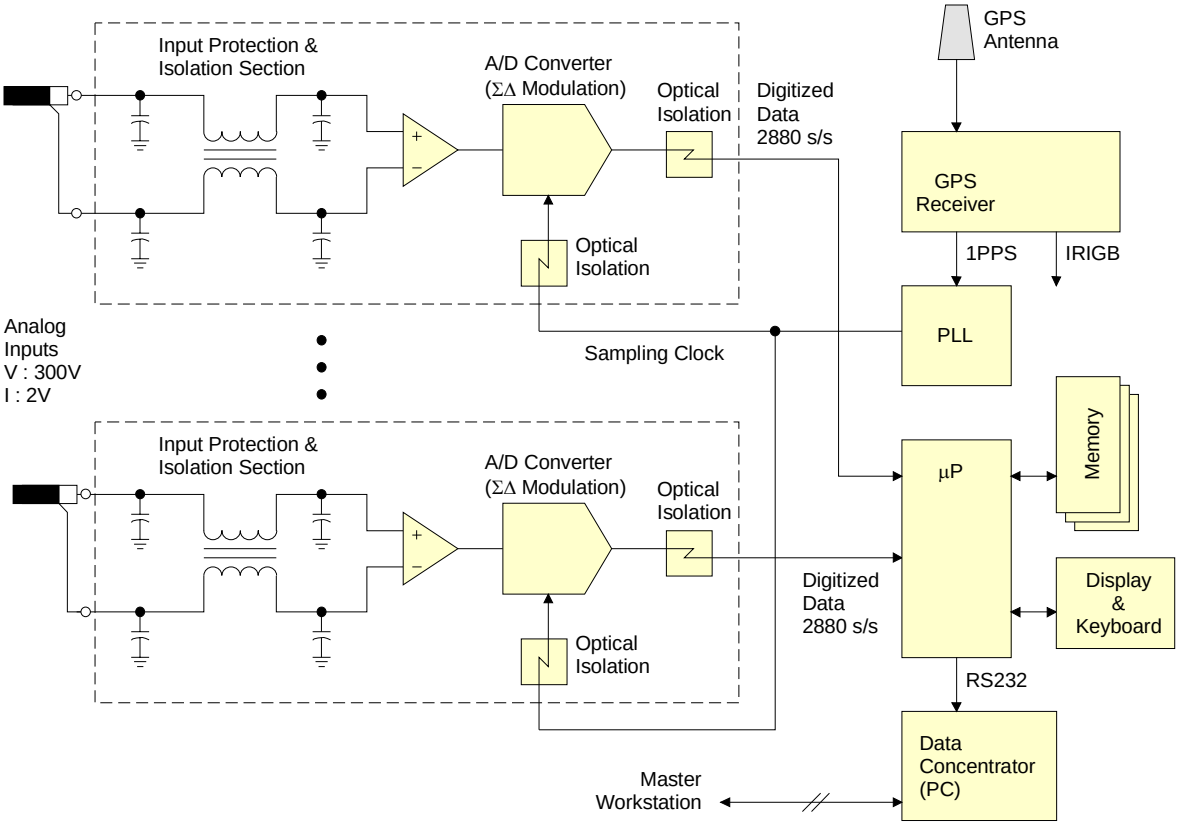

(a)

(b)

Figure 1-7: The Macrodyne 1620 PMU (January 1992) (taken from [15])
(a) Block Diagram, (b) Photograph

1.4 Decision Tree Principle

The decision tree technique is an effective supervised data mining tool to solve the classification problems in high data dimensions. It was first developed by Leo Breiman in 1980's, which is now widely used in many fields including medical diagnosis, financial analysis, statistical analysis and decision making in power systems [20]. A decision tree represents a classification or predictive model for an objective by identifying critical attributes that affect this objective most effectively and directly. Different applications of DTs depend on the approaches to describe the problem in terms of creating a **database** that consists of a sufficiently large number of **cases.** Each case is represented by a vector of **predictors** (or variables) along with an objective. The DT is designed for successful classifications of this objective by using only a small number of these predictors.

The decision tree structure is usually dimidiate and there are two types of nodes in a DT, the "internal node" with two successors and the "terminal node" without successors. For each internal node, a question or critical splitting rule (CSR) is asked to decide which successor the classification process should drop into. The splitting rule could be numerical or categorical, by comparing the variable value with a threshold or checking whether the current value belongs to a specific data set, respectively. For each terminal node, a classification will be assigned in terms of the majority classes of the objective, e.g., "secure" or "insecure". The classification process is very simple and fast, which is to drop the associated predictors down the tree model by comparing the CSRs in different levels. The whole process starts from the root node until a terminal node is reached. Figure 1-8 shows a decision tree example with 5 internal nodes and 6 terminal nodes, which is trained from a database that contains 680 cases.

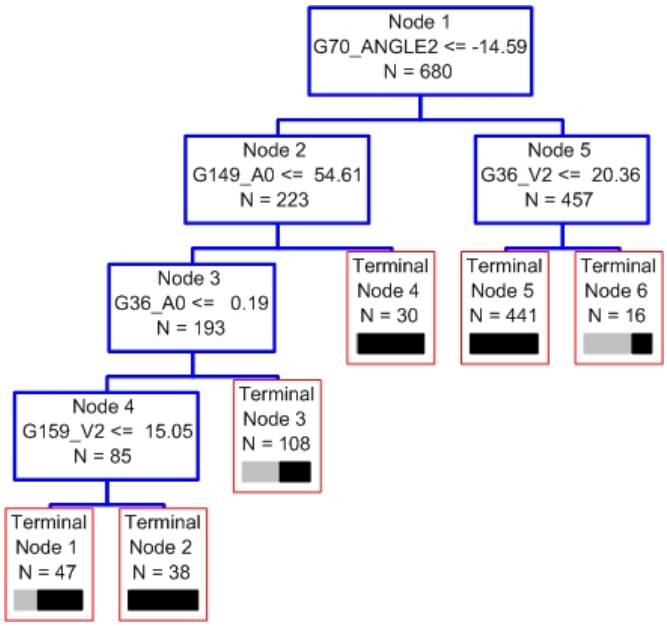

Figure 1-8: A DT with 5 Non-terminal Nodes and 6 Terminal Nodes

The classifications in this tree are “stable”, represented by the black bars at the terminal nodes and “unstable”, represented by the gray bars. The splitting variables in the DT are all numerical rules. For each internal node, the node description includes the node name, the critical splitting rule (CSR) with its threshold and the number of cases that go to this node. For each of the terminal nodes, the node name and the number of cases that fall into this classification are shown. The length of the bars at the bottom demonstrates the percentage of different classifications. A sample of the classification progress is as follows. Starting from the root node, if the measured variable G70_ANGLE2 obtained from PMU measurements is larger than -14.59 degree, the classification goes to the right branch of the tree. If the measured value of G36_V2 is smaller than 20.36 degree/second, a classification of “stable” will be obtained. This is the “decision” of the tree.

Training a DT not only uncovers important system parameters that contribute to the final objective for the known cases, but also optimizes the prediction ability on the unknown cases. Therefore, a learning set (LS) and a test set (TS) with the same data format are required before a DT is trained. In the beginning, a maximum DT is first trained from the LS by recursively splitting a parent node into two purer child nodes. The splitting process starts from the root of the tree and continues until further splitting of a node cannot improve the overall DT performance or when a predefined threshold is reached. In order to obtain the CSRs in the DT, all the available predictors in the LS are scored in terms of the impurity reduction performance by using the equation below.

$$\Delta I(\alpha, t) = I(t) - I(t_L) - I(t_R)$$

Where t represents the current node in the tree, t_L is the left child node, t_R is the right child node, α is the splitting rule and $I(t)$ is the tree impurity function. Each predictor has its own splitting rule, α, and the one with the highest score is selected to be the critical splitting rule for this node. The remaining splitting rules with equal or less scores are called “competitors”, which could provide good alternate candidates. Details of identifying CSRs and split stopping rules are discussed in [20]. By definition, this maximal tree possesses the highest accuracy for the LS involved. It is then pruned using the TS to generate a series of smaller DTs in terms of the misclassification cost on the TS, which is defined as

$$MC^{TS} = \frac{1}{N^{TS}} \sum_{i,j} c(i,j) N_{ij}^{TS}$$

where MC^{TS} is the misclassification cost of the whole tree, N^{TS} is the total number of cases in the TS, $c(i, j)$ represents the cost of misclassifying the i class as a j class and N_{ij}^{TS} is the number of j-class cases misclassified as i-class cases in the TS. The optimal tree is then defined as the one with the lowest misclassification cost. It always has a medium size, because a small tree does not contain enough useful information and a large DT usually has the over-fitting problem.

Two important advantages of DTs over the other data mining tools like neural networks and support vector machines are the simple structure and readability of the model, which makes it very convenient to input the PMU measurements directly and

compare with the threshold on the CSRs to obtain a security assessment. This process is very fast since only a few comparisons are required. Once a final DT is trained with satisfactory performance for online applications, the CSRs in the tree provide a "nomogram" in the space of critical attributes in the system, which defines a secure operating region. It is imperative that these critical attributes be measured simultaneously to determine whether the current OC falls inside the nomogram or outside it. This requirement can be satisfied by the synchronized measurements obtained from the PMUs across the system. From the perspective of speed, the DT training process from scratch usually takes one or two minutes on a PC with a Intel Core2 CPU 6700 (2.66 GHz) and 2.0 GB of RAM once the database is created. Therefore, properly trained DTs are quite suitable for identifying critical system attributes from various system states that are related to power system security problems and feasible for real time transient stability assessment. Several applications involving decision trees have been addressed in real-time transient stability prediction and assessment, voltage security monitoring and estimation, and loss of synchronism detection and timing of controlled separation in power systems [10],[21]-[28]. A recent effort combines DTs with the other data mining tools for prediction performance improvement in the field of dynamic security controls [29].

Robustness and a high level of accuracy are two aspects of great importance to be considered before a final DT is obtained for online application. One problem of training DTs is the need to conduct a large number of offline simulations to obtain sufficient large database. However, this problem can be easily solved by parallel computations because all the cases in the database are independent of each other.

2 Design of Controlled Islanding Scheme

2.1 Introduction

As discussed above, a controlled separation scheme should be able to detect unstable swings in a timely manner in order to prevent the occurrence of cascading outages that are mainly caused by protective relay actions. There are two important problems to be solved, including “where to island?” and “when to island?” This section first provides the main procedures of the controlled separation scheme and then discusses the methods to address these two issues separately.

2.2 Main Steps of the Proposed Scheme

The main steps of the proposed method include several aspects depicted in Figure 2-1. Each of the seven major steps is discussed below:

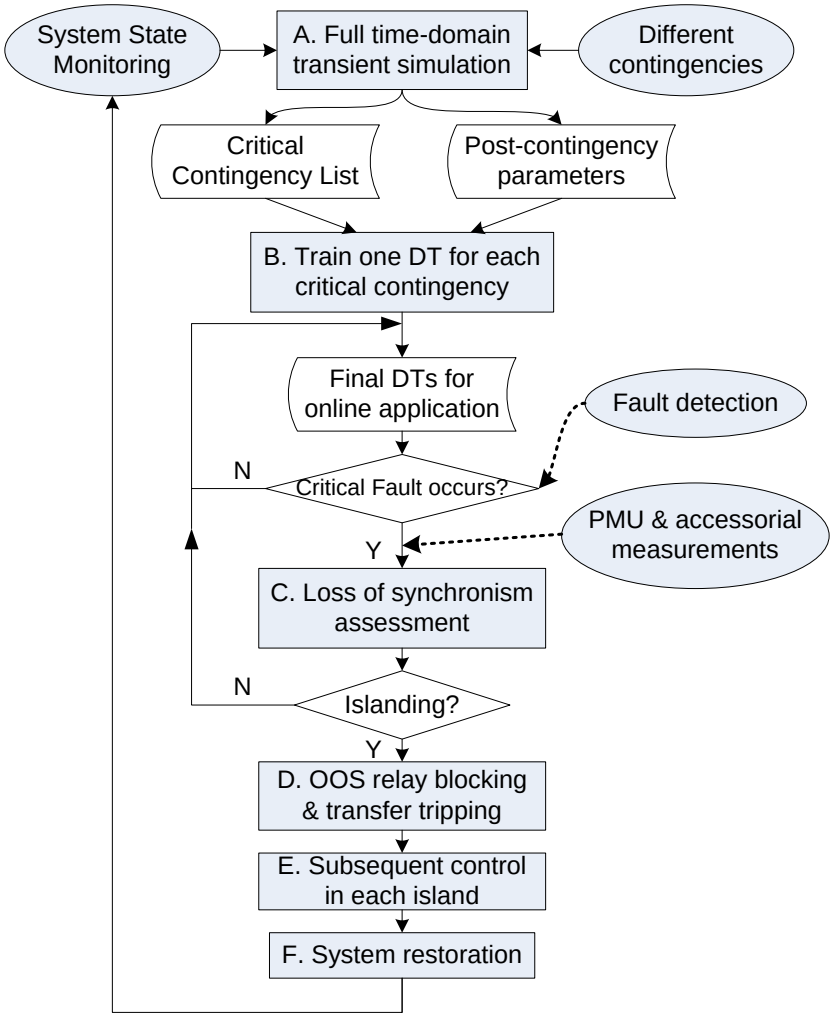

Figure 2-9: Flowchart of the Proposed Controlled Separation Scheme

(A) Different system operating conditions representing all the details of system states including load levels, generation patterns, power flows and equipment status are first collected. These OCs should be able to accurately reflect the system states for a specific time period, which could be a year, a season, a month, a day or even an hour. A list of important contingencies including N-1, N-2 and even N-k are used to conduct full time-domain transient simulations for the purpose of identifying the critical contingencies that may lead to loss of synchronism or cascading outages. Since the number of all the combinations of these contingencies is extremely huge for a large power system, only the contingencies that occur on high voltage kV buses and transmission lines (e.g. 200 kV and above) are used for the transient stability study. The severe contingencies from historical operational experiences can also be included. Besides the detailed steady state data, transient simulations need to consider modeling of all the available control devices including generators, excitation systems, governors and power system stabilizers (PSSs) to obtain an accurate representation of system behavior during transients. More importantly, the effects of protective relay actions like impedance relays and load shedding relays are also included since they play a very important role during cascading events. This step identifies a list of critical contingencies. In addition, the controlled islanding cut sets can also be determined offline for these OCs.

(B) With the availability of the post-disturbance system transient time evolution and the critical contingency list, decision trees are trained offline to obtain the desired prediction performance. Based on various simulations conducted in the Entergy system, most of the contingencies will not cause loss of synchronism and there are only a few contingencies that may cause severe transient stability problems. Therefore, it is quite reasonable to train a separate DT for each of these critical contingencies. This design improves the prediction accuracy of DTs and correctly implements the controlled islanding scheme, because different critical contingencies may cause different patterns of system instability. The details of selecting predictors and training DTs for online transient stability assessment will be discussed in Section 3.

(C) During real time operation, a fault detection system is required to identify whether a critical contingency in the list occurs. If so, the corresponding DT is used for online security assessment by using the measurements from PMUs to check whether the thresholds on the critical attributes identified by the DT are violated. In the meantime, accessorial measurements can be used to assist the DT to obtain a final security assessment, such as monitoring whether a cascading event has already been initiated or whether the separation of power angles among different generators has reached a threshold, e.g. 120 degrees.

(D) Once an insecure assessment is obtained which indicates controlled separation needs to be triggered, the existing out of step (OOS) relays (if there are any) need to be blocked for preventing their actions towards the local swings. Transfer

tripping schemes can be carried out at the pre-designed locations that are obtained by the optimal cut set identification program.

(E) Immediately after the islands are formed, subsequent control actions are required to maintain the frequency and voltage profiles in each island, including load shedding in load rich islands or generator tripping in generator rich islands. Other control actions like capacitor switching may also be required to provide sufficient reactive power support to avoid low voltage problems, especially near the cut set. The formation of pre-defined islands can effectively stop the unstable swings instead of allowing the initial disturbance to spread throughout the other parts of the system.

(F) After the impact of the disturbance has diminished and each island has entered into steady state operation, the tripped transmission lines can be reconnected to restore the whole power system following a pre-designed restoration procedure.

2.3 Where to Island?

To obtain the optimal cut sets, several important requirements should be satisfied, the most important of which is the slow coherent generator grouping. In a severely disturbed power system, the balance between mechanical torque and electrical torque is upset and some generators tend to swing together against other groups of generators. Determining potential generator groups is a critical step in searching for the optimal cut set to form the islands because the generators with similar swing patterns must stay in one island. Otherwise, the separating power angles between different generator groups in a single island will affect transient stability recovery. This would then reduce the efficacy of the controlled islanding scheme.

In [30], a two time scale method to determine the slowly coherent generator groups was developed. The system state variables are assumed to be divided into a number of slow states and fast states. Slow coherency corresponds to the slow modes of these state variables. Generators in the same group have strong connections with each other and different groups of generators are connected through weak tie lines. When a severe disturbance occurs, it propagates very fast within one generator group, but slowly between different generator groups. During unstable swings, voltage magnitudes at buses and power flows on branches also oscillate severely, and electrical centers between groups of generators may appear on weak tie lines, which may violate protective relay settings and cause “false” tripping of the branch. Therefore, if the weak tie lines connecting the other slowly coherent generator groups can be tripped in a timely manner, the disturbance can be effectively controlled inside one island. Overall system stability can also be maintained with proper subsequent control actions after the formation of islands. From the observations in [7]-[8], the slowly coherent generator grouping is relatively insensitive to the location of disturbances. The generator grouping method has become one of the most important requirements in finding the optimal cut set to separate the system.

Another important requirement is to minimize the overall power imbalance of the created islands for the purpose of minimizing the impact of tripping multiple transmission lines on the system. A graph theory based approach to search for the optimal cut set has been presented in [31] by using a graph analysis tool, METIS. This method takes advantage of the slowly coherent generator grouping information and system equivalence technique for cut set identification. The objective of this approach is to find a cutting path with the lowest summation of power flows on the branches and it is equivalent to the objective of minimized power imbalance of each island. The third requirement is that the number of lines to be tripped should be as few as possible, for the purpose of easy restoration. A software program which automatically identifies the cut set has been developed in other work done at Arizona State University and used in this project.

2.4 When to Island?

This section details the decision tree based method to determine when to perform controlled separation in real time. This is a post-disturbance prediction approach, which collects transient system state variables as predictors after the disturbance. It can provide a prediction result within a few cycles after fault clearance and provide enough time for arming the controlled islanding scheme. The details of the objective, predictor selection and database generation in this method are as follows:

(1) **Prediction Objective**: For each critical contingency in the list, create a database by collecting the cases that are represented by transient simulation results and system dynamic behavior during the first few cycles. Each case represents one full time-domain simulation for this contingency at a certain OC. The objective is then defined as “secure” or “insecure”.

(2) **Predictor Selection**: The predictors selected in this research project are all from transient voltage phase angles at high voltage buses (200 kV and above). For every state variable, six data points are defined. The first data point is the phase angle at the fault clearance time (Angle1). The second data point is the angle value 4 cycles later (Angle2) and the third is the one 8 cycles after the fault clearance (Angle3). The fourth data point is calculated as the angular velocity between the first two data points (V1). Similarly, the fifth variable is the angular velocity between the second and third voltage phase angles (V2). Finally, the last variable is defined to be the acceleration from the first three angle values (a0). Therefore, the unstable swings are predicted using the transient behaviors within 8 cycles after the fault clearance. Figure 2-2 shows how the transient phase angles are collected using an example. Some of the pre-fault state variables may also be collected as predictors to ensure high prediction accuracy, such as the power flows on critical tie lines. However, from the test studies in the Entergy system, transient phase angle values are sufficient to build DTs with high prediction accuracy. A sample of the created databases for DT training is shown in Table 2-1.

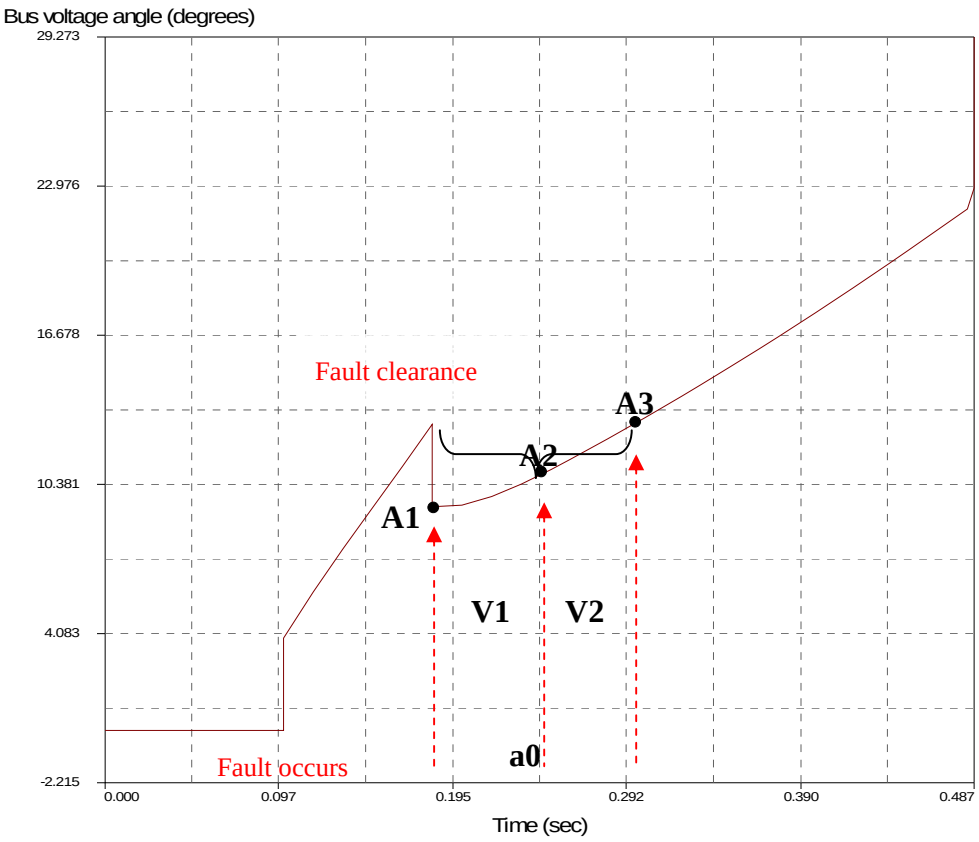

Figure 2-10: Method to Collect Transient Phase Angle Values as Predictors

Table 2-1: An Example of the Database for DT Training

Stable$	B36_Angle1	B36_Angle2	B36_Angle3	B36_V1	B36_V2	B36_a0	B30_Angle1	…
I	24.7731	24.7184	24.5086	-0.5475	-2.0977	-3.1003	10.9272	…
S	26.074	28.1432	29.6199	20.6925	14.7662	-11.8525	10.8821	…
I	24.8313	24.9733	25.2217	1.4203	2.4836	2.1267	10.922	…
S	24.8959	25.0661	25.1057	1.702	0.3964	-2.6112	10.8291	…
…	…	…	…	…	…	…	…	…

This idea of predictor selection arises from the approach developed in [10], which collect post-contingency power angles of all of the generators as predictors. However, the approach used in this project includes more innovative and practical considerations. Firstly, it could be very costly to install one PMU for every generator especially when the size of the power system grows too large. Secondly, installation of PMUs on high voltage buses can monitor more system information such as critical power flows, voltage levels and line currents compared to the ones installed only on generators. Thirdly, collecting generator variables is largely affected by the operating status of generators, but phase angles of high voltage buses are more reliable under different system topologies and OCs. Lastly, voltage phase angles can also effectively reflect the generator swinging patterns at the beginning of unstable swings, especially for the buses near a group of large generators.

Once the properly trained DTs are built from the created databases for the given OCs, they can be periodically updated at a certain time interval for improving prediction performance on the unknown or unforeseen cases. If there is a major change in system status and the newly predicted OCs are not in the existing database, new cases from transient stability analysis can be generated and new test sets based on these new OCs can be built. Once the existing DTs perform poorly on these new test sets, new DTs with good performance to obtain the final DTs for real time application can be built. The method using periodic DT updating for online dynamic security assessment in power systems has been proposed in [21]. The final DTs will pick critical system states as CSRs, which can be recommended PMU locations. The updated DTs are then used for determining real time controlled separation by checking the PMU measurements against these thresholds. The tests conducted in this research project show that voltage angle differences on high voltage buses are good transient stability indicators to determine the timing of controlled islanding scheme.

3 Case Study

3.1 Introduction

The proposed controlled separation scheme to prevent cascading events is tested on the Entergy system. This section explains all the details of modeling the Entergy power system, identifying critical contingencies, selecting transient stability predictors and training good decision trees. A critical case consisting of the loss of two 500 kV transmission lines, is analyzed to illustrate the effects and benefits of the controlled islanding scheme. In this case study, a software platform involving a variety of simulation tools has been developed to test this scheme. Operating conditions are all generated using the Powerflow & Short-circuit Analysis Tool (PSAT) and transient stability studies are performed using the Transient Security Assessment Tool (TSAT), both of which are components of the Dynamic Security Analysis Tool (DSA^{Tools}) package. DSA^{Tools} is an advanced package for power system security evaluation and is developed by the Powertech Labs, Canada [32]. The decision trees are trained and tested using a commercial data mining package, Classification and Regression Trees (CART), which is developed by Salford System, CA [33]. The slowly coherent generator grouping is identified using the dynamic reduction program (DYNRED) in the power system analysis package (PSAPAC) developed by Electric Power Research Institute (EPRI) [34]. The database generation, data conversion and analysis work are conducted using MATLAB and Microsoft Visual Studio VC++ codes.

3.2 Entergy System Model

The Entergy Corporation covers a wide area including Arkansas, Louisiana, Mississippi, and Texas in the United States, which serves more than 2.6 million customers. The power system consists of more than 2100 buses, 240 generators and 2600 transmission lines with the voltage level ranging from 1 kV to 500 kV. The total electricity generation capacity is around 30,000 MW with about 1450 substations and 15,000 miles of lines. There are five major operating areas defined in this system: WOTAB, AMITE SOUTH, CENTRAL, SHERIDAN NORTH and DELL, which are shown in Figure 3-1. This system model is also interconnected with the surrounding areas representing the eastern interconnected power system in North America. Therefore, a total number of 16100 buses, 3260 generators, and 20200 lines are all included for full time-domain transient simulations.

The Entergy system is involved in the Eastern Interconnection Phasor Project (EIPP) and there are 9 phasor measurement units currently installed in the system, which are shown in Table 3-1. One PMU is installed on a 138 kV bus, 3 PMUs are installed on 230kV buses and the remaining PMUs are all located on 500 kV buses. These PMUs are installed to monitor the states of the key buses and stations including bus voltage magnitudes, voltage phase angles, MW and MVAr flows, and current magnitudes of the associated branches.

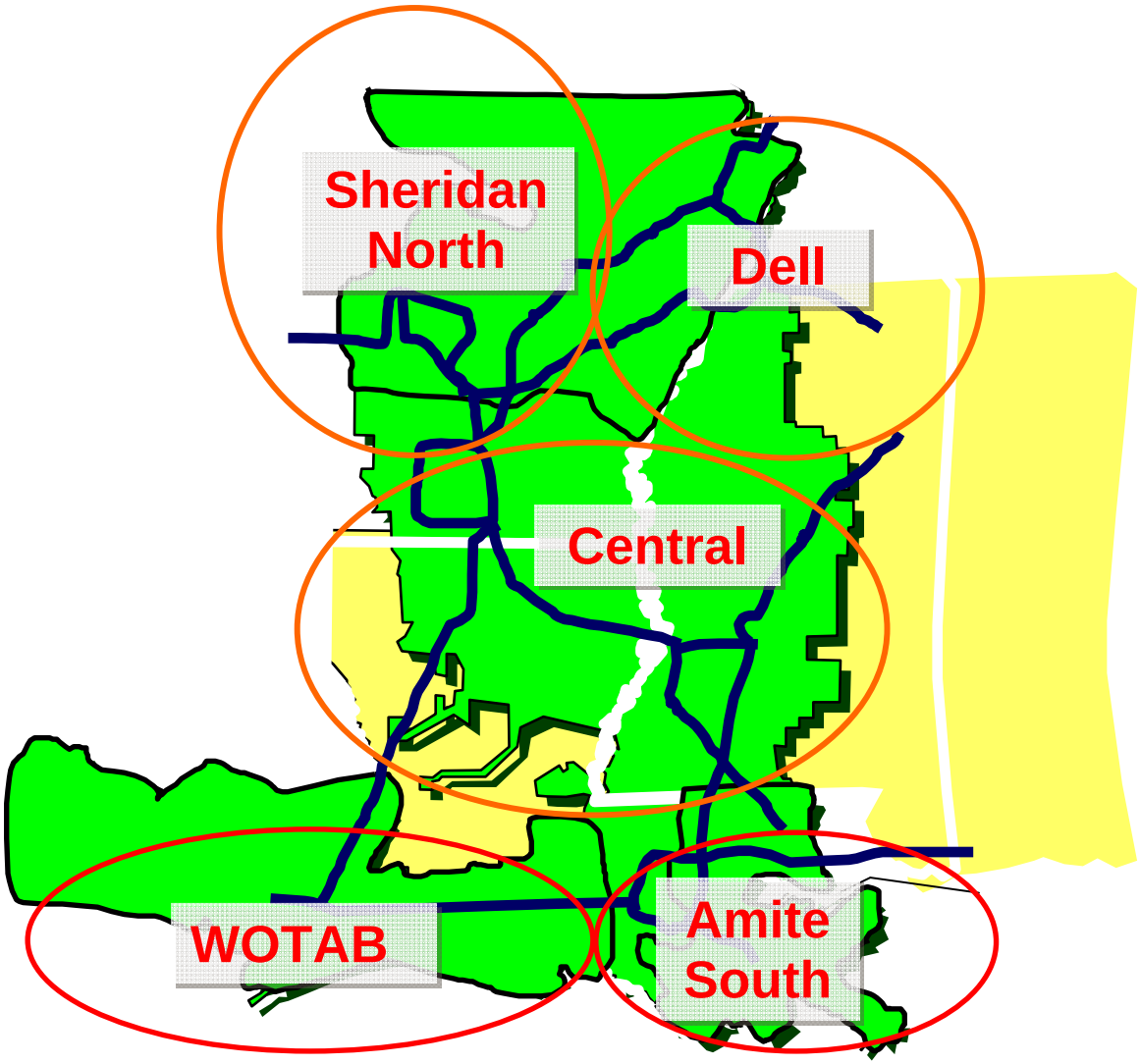

Figure 3-11: Five Operating Areas in the Entergy System

Table 3-1: PMU Locations in the Entergy System

No.	Bus No.	Bus Name	Looking at line to
1	97468	Goslin 138kV bus	Metro (bus # 97455)
2	98234	Fancy Point 230kV bus	Auto (bus # 98233)
3	98537	Waterford 230kV bus	Ninemile (bus # 98606)
4	98537	Waterford 230kV bus	Waterford auto (bus # 98539)
5	98952	Grand Gulf 500kV bus	Baxter Wilson (bus # 98937)
6	99295	ElDorado 500kV bus	Mt. Olive (bus # 99162)
7	99295	ElDorado 500kV bus	Sheridan (bus # 99333)
8	99565	Mabelvale 500kV bus	Sheridan (bus # 99333)
9	99565	Mabelvale 500kV bus	Mayflower (bus # 99572)

For the power flow data, 24 operating conditions are provided by the Entergy staffs to represent all of the system state variables for the year 2007. Each month has two OCs that represent the lowest and highest load levels respectively. These steady state files include details of network topology, load level, generation and power flows that comply with the changing load patterns and unit commitments in the system throughout the whole year. All the bus voltages in the Entergy area are within reasonable levels and no over loading problems exist on major transmission lines. For the dynamic data, a file that consists of the models for the available generators, excitation systems and power system stabilizers is provided and the details of these dynamic models are discussed in [35]. The models of protective relays were not included. These were created in conjunction with the Entergy relaying engineers and operations staff. The developed relay models are included in the dynamic data file. Under frequency load shedding relays are also represented across the Entergy system according to the settings shown in Table 3-2. This data was obtained from Entergy.

Table 3-2: Load Shedding Relay Blocks in the Entergy System

Block	Frequency setting	Time setting	Amount
1	59.3 Hz	6 cycles	10%
2	59 Hz	6 cycles	10%
3	58.7 Hz	6 cycles	10%

A user defined model for impedance relays with circuit breaker time settings is also designed in TSAT as shown in Appendix 1. This model considers the settings of Zone 1 (80% of the protected line) and Zone 2 (120% of the protected line) and does not model zone 3. The circuit breaker delay time is set to be 5 cycles for all of the high voltage transmission lines across the Entergy system.

3.3 Critical Contingency Identification

With all the power flow and dynamic data files that can accurately represent the full system behavior, transient simulations are conducted to identify critical contingencies. For all of the 24 OCs in the Entergy system, N-1 scan is first conducted to test the system performance following the loss of any single transmission line above 200 kV levels. The contingencies are set to be faults on high voltage buses, followed by a single line tripping. The simulation length is selected to be 3 seconds. From the simulation results, none of the N-1 cases for the 24 OCs causes out of step swings, except for a few single-machine-run-away cases that will not cause a large scale problem in the system. This shows that the provided operational models comply well with the NERC standards.

Therefore, N-2 contingencies were considered in order to uncover problematic contingencies, although such contingencies may have low probabilities of occurrence. In fact, there are altogether 2100 lines in the Entergy system. If all the combination of these lines is considered for transient simulation, more than 8 million simulations will have to be carried out. This would be impractical. Based on the analysis that is conducted on the

provided system data, high voltage branches usually carry more active power than low voltage lines and consequently they are more critical in affecting system transient stability. As a result, only the branches at 500 kV level are selected to perform the N-2 contingency scan. The number of different combination of all the 64 500-kV lines is about 8000, which is manageable.

Another important issue is the sequence of the double line outages. In modern power systems, it is rare that the outages of two branches occur exactly at the same time. The sequence is usually one after another, that is, one line has been out of service before another fault occurs in the system. During real time operations, once a fault occurs on one branch and this branch is cleared by protective relay devices, power flows need to be re-dispatched and actions need to be taken by system operators to withstand another N-1 fault. However, making such changes with changing system conditions takes time, which is in the range of a few or dozens of minutes due to the slow actions of governors and boiler controllers. During this specific time period, another severe contingency may jeopardize the transient stability of the system by significantly changing system topologies. This philosophy chosen for the N-2 contingency settings in this project reflects the reality in power systems.

N-2 Contingency Settings:

All the N-2 contingencies among the 64 500 kV lines are uniformly set as follows:

i. One 500-kV line is out of service before transient simulations start.
ii. Solve the power flow of the whole system to represent the re-dispatched system conditions without this faulted line.
iii. Add another fault to the other 500-kV line that is cleared 3 cycles after the occurrence of the fault.
iv. Start the full time-domain simulation and monitor generator angles and protective relay actions across the whole Entergy system for further study.

In TSAT, these settings can be achieved by applying the first fault at a **minus** time and the second fault at a positive time. The selection of this minus value is arbitrary and TSAT will solve the power flow of the system without the faulted line before simulation is initiated. A sample of such a contingency file with comments is shown below:

```
/
DESCRIPTION 1 98937 99203 99162 99295
SIMULATION 3.000000 Seconds
Integration RK4
Step Size 0.500000 Cycles
/
At Time -0.5 Seconds        / The first fault is applied at -0.5 seconds
Remove line ;98937 ;99203 ;1 / The first line is removed
At Time 0 Seconds  /The second fault is applied
Three Phase Fault On Line ;99162 ;99295 ;1  0.000000 / Fault details
After 5.000000 Cycles  / Time delay of fault clearance
Clear Three Phase Fault On Line At Near End  / Clear the second line
/
Clear Three Phase Fault On Line At Far End    / Clear the second line
Nomore
/
```

Simulation Results:

The transient simulations are then conducted for the 8000 N-2 contingencies by using calculations in parallel, which is a great advantage in TSAT. Therefore, with 16 PCs, all the simulations are finished within about 1 hour. The simulation results indicate the followings:

i. The loss of two lightly loaded 500-kV branches causes no stability problems.

ii. No problem occurs if the locations of the two faulted branches are far away, e.g. one is in WOTAB area and the other is in DELL area.

iii. Loss of two heavily loaded branches is more likely to cause out of step swings, especially when the two lines are close geographically. Most of the observed cases that lose synchronism are related to loss of a tie line connecting different areas, which carries a large amount of power. There are six critical cases that were observed and they are shown below individually.

1) Case 1: Line 97717 (HARTBRG) to 99162 (MT.OLIVE) is out of service, which is a tie line connecting the WOTAB area and CENTRAL area and carries 1057 MW from CENTRAL to WOTAB. The other fault is on line 98107 (RICHARD) to 98109 (WELLS), which is a part of the tie line connecting WOTAB area and AMITE SOUTH area and carries 287 MW active power from AMITE SOUTH to WOTAB. There are 19 generators in the WOTAB that form one group and swing against the other machines in the Entergy system.

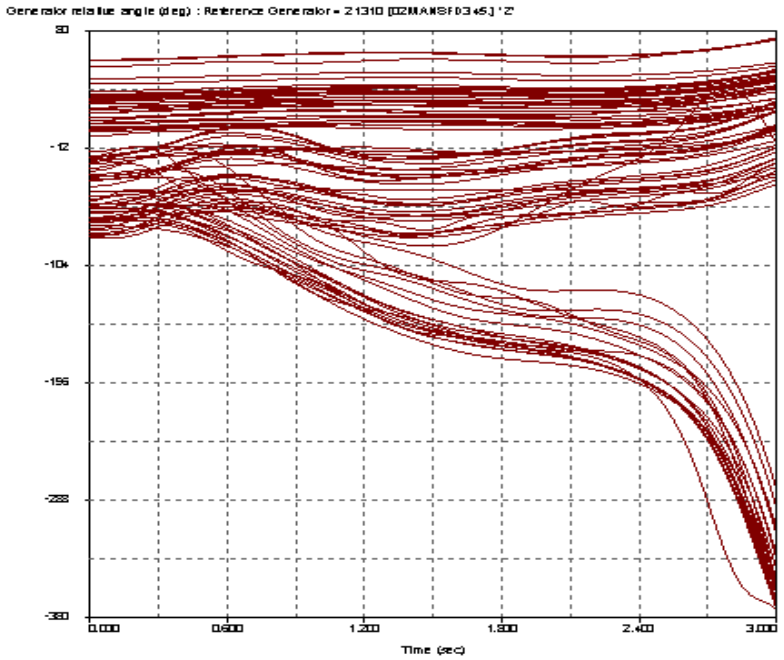

Figure 3-12: Relative Generator Angles for Case 1

2) Case 2: Line 97717 (HARTBRG) to 99162 (MT.OLIVE) is out of service before another fault on line 98109 (WELLS) to 98430 (WEBRE) occurs, which is the other part of the tie line connecting WOTAB area and AMITE SOUTH area and

carries 167 MW active power from AMITE SOUTH to WOTAB. Almost the same generator group is formed in the WOTAB area.

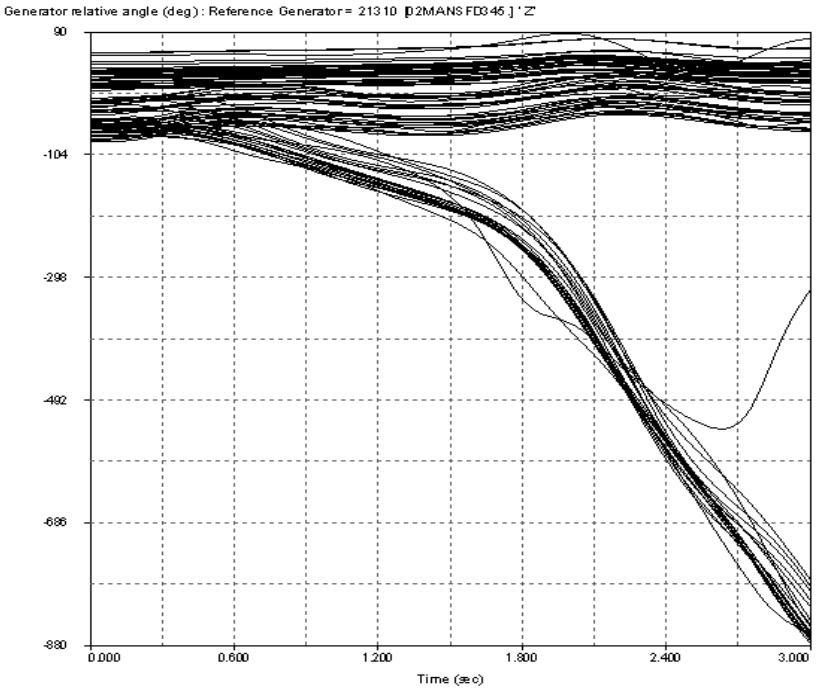

Figure 3-13: Relative Generator Angles for Case 2

3) Case 3: Line 99162 (MT.OLIVE) to 99295 (ELDORADO) is out of service, which is an important tie line in CENTRAL area and carries 1395 MW active power from the north to the south. The second fault is applied on line 98109 (WELLS) to 98430 (WEBRE), and there are 20 generators in WOTAB area that form one group.

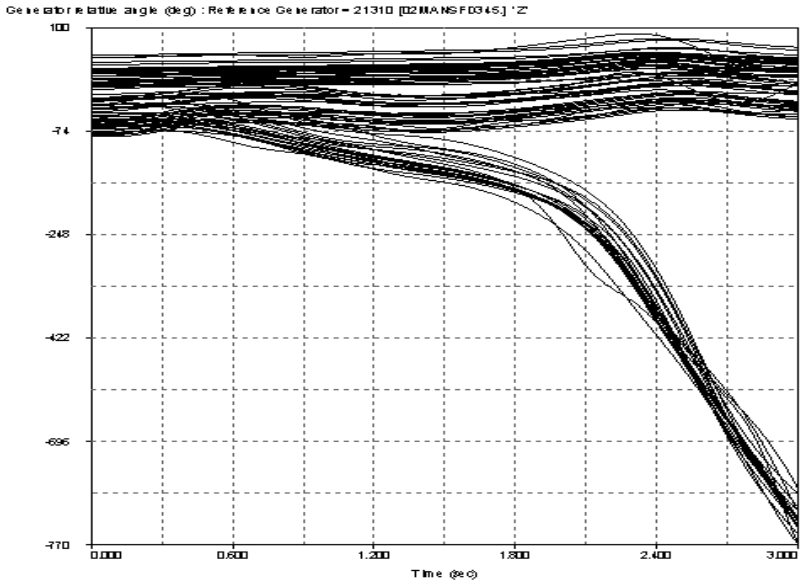

Figure 3-14: Relative Generator Angles for Case 3

4) Case 4: Line 98937 (B. WLSN) to 99203 (PERYVIL) is fist taken out of service, which carries 1788 MW active power in CENTRAL area. The second fault occurs on line 99162 (MT.OLIVE) to 99295 (ELDORADO). The system has seen 2 large generator groups that separate the Entergy system. The generators in the north part swing against the ones in the south part, with the swinging interface in CENTRAL area.

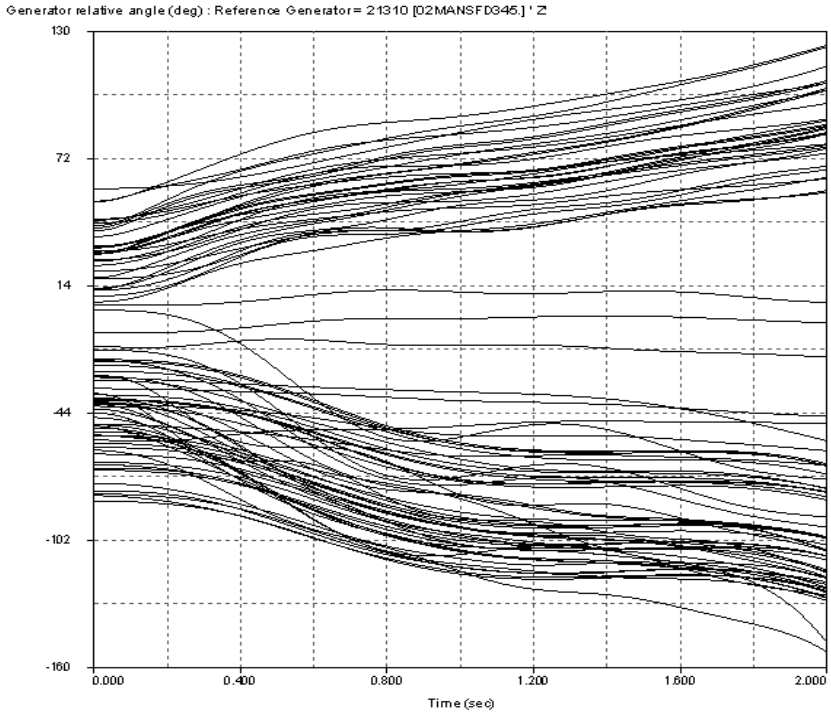

Figure 3-15: Relative Generator Angles for Case 4

5) Case 5: Line 97717 (HARTBRG) to 99162 (MT.OLIVE) is taken out of service, which is the tie line connecting WOTAB area and CENTRAL area and carries 1057 MW from CENTRAL to WOTAB. The second fault occurs on line 98235 (MCKNIGHT) to 99027 (FRANKLIN), which is tie line connecting CENTRAL area to AMITE SOUTH area, carrying 713 MW from CENTRAL to AMITE SOUTH. In this case, Generators in WOTAB and AMITE SOUTH areas swing against the machines in the rest of the Entergy system.

6) Case 6: Line 99309 (MCNEIL) to 99441 (ETTA) is taken out of service first, which is a tie line connecting NORTH area and CENTRAL area and carries 416 MW active power from NORTH to CENTRAL. The second fault is on line 99333 (SHERID) to 99450 (MAGCOVE), which is an important line in SHERIDAN NORTH area and carries 389 MW power from 99450 to 99333. In this situation, ten machines in SHERIDAN NORTH area form one group and swing against the rest of the Entergy system.

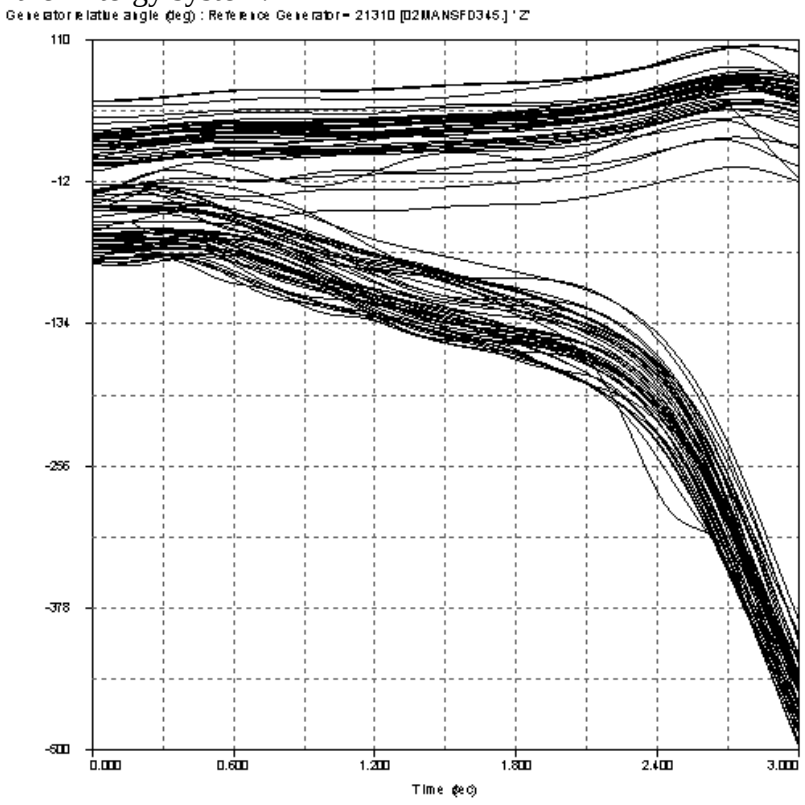

Figure 3-16: Relative Generator Angles for Case 5

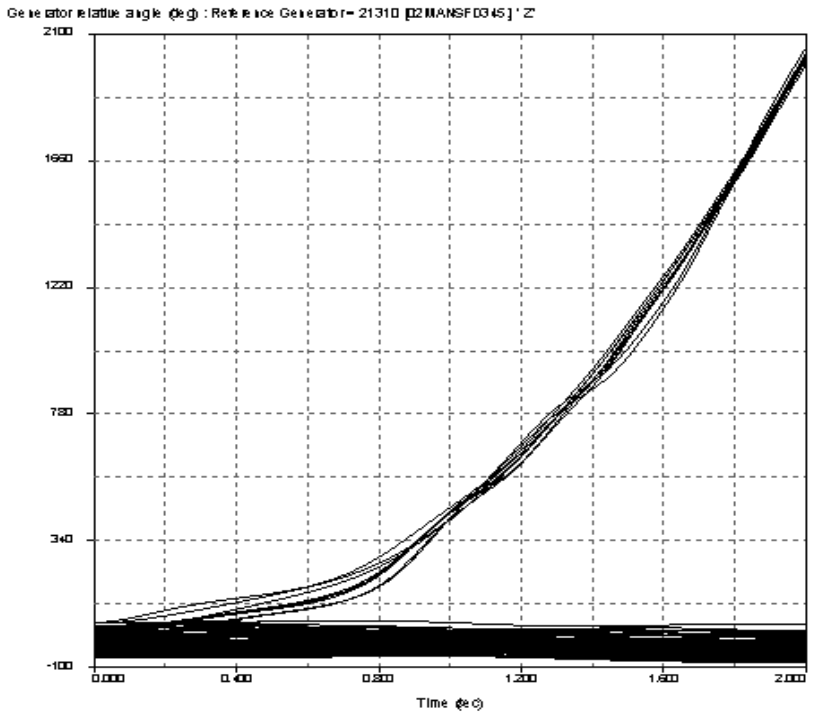

Figure 3-17: Relative Generator Angles for Case 6

Based on the observation that unstable swings may occur only when certain critical lines are out of service and the unstable patterns at different OCs are relatively fixed when the fault locations are specified, it is quite reasonable to build one DT for each critical contingency for determining when to island in real time.

3.4 Controlled Islanding Design for the Two-Line Outage in CENTRAL

This section uses the Case 4 as an example to demonstrate the controlled islanding scheme. The design of other critical cases follow similar procedures discussed below.

3.4.1 Detailed System Behavior

Following the loss of two important 500 kV lines in the CENTRAL operating area, a full time-domain simulation is conducted by extending the simulation length to 20 seconds for further investigation. Before conducting the transient simulation, line 98937-99203 (BAXTER WILSON SES 500-PERRYVILLE 500) is first removed and the power flow is solved to obtain the steady state conditions. This constitutes an (N-1) condition. At time 0 second, a three phase to ground fault occurs on the line, 99162-99295 (MOUNT OLIVE 500-ELDORADO EHV 500). The fault is cleared after 3 cycles and the line is removed (This is now a (N-2) condition). Following the loss of these two 500 kV lines, generators in the WOTAB and SOUTH areas begin to separate from the rest of the Entergy system. These swings cause impedance relays to trip other lines once the ZONE 1 or ZONE 2 settings are violated.

By monitoring different transient states, an uncontrolled system separation in the Entergy area is observed within 4 seconds after the fault clearance. There are 12 lines tripped due to the out of step relay actions, which significantly affects the transmission path in the CENTRAL area. The sequence of these tripping actions is shown in Table 3-3 below. This uncontrolled islanding path is shown in Figure 3-8.

Table 3-3: Sequence of Out of Step Line Tripping in the Central Area

No.	At Time	From Bus	To Bus	From Name	To Name	kV level
1	1.65	99161	99164	VIENNA	MTOLIV	115
2	1.65	99109	99110	COLMBIA	STAND	115
3	1.817	99168	99177	SAILES	TEXASE	115
4	2.083	97307	99120	GILBRT	WISNER	115
5	2.367	99154	99155	TALULA	DELHI	115
6	2.767	98930	99027	R.BRAS	FRKLIN	500
7	2.767	98952	99027	G.GULF	FRKLIN	500
8	2.767	99014	99015	LORMN*	FAYETE	115
9	2.783	98489	99066	BOGLSA	DEXTER*	115
10	2.867	15030	98497	HATBG S	ADMSCRK	230
11	3.65	99052	99054	JAYES*	TYLRTN	115
12	3.667	99011	99072	HZLHST	JAM RD*	115

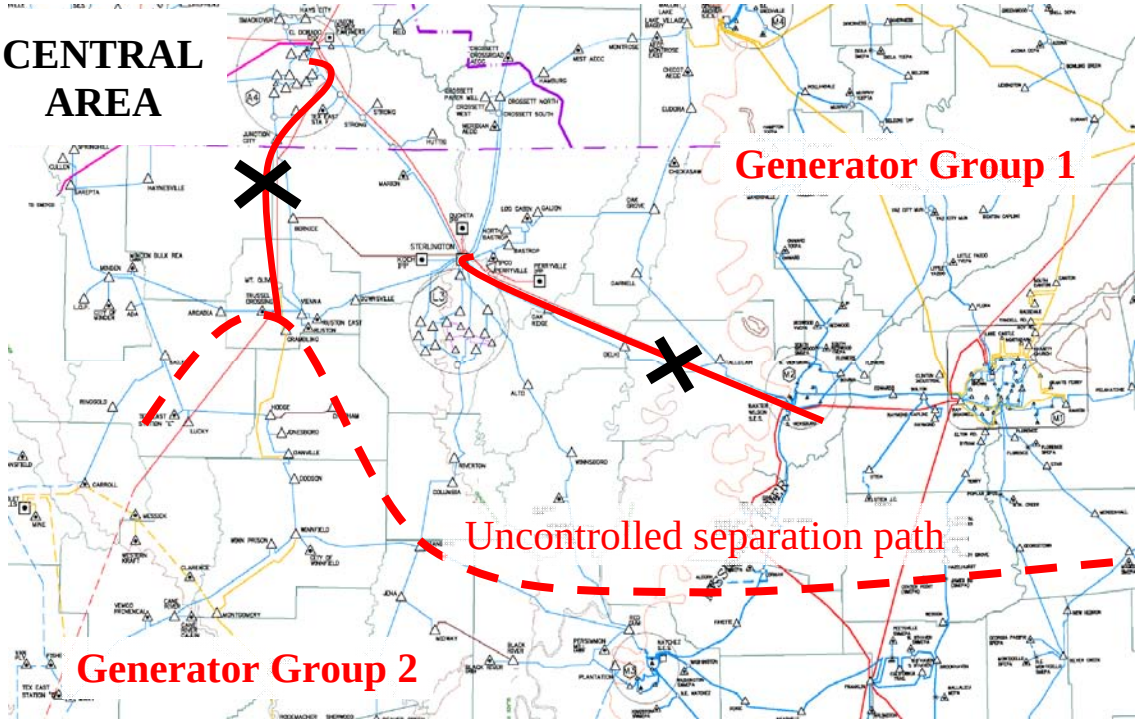

Figure 3-18: Uncontrolled Separation Path in CENTRAL Area

The details of the system transient behavior during the cascading events and the formation of uncontrolled separation are shown in Figure 3-9(a) to Figure 3-9(e).

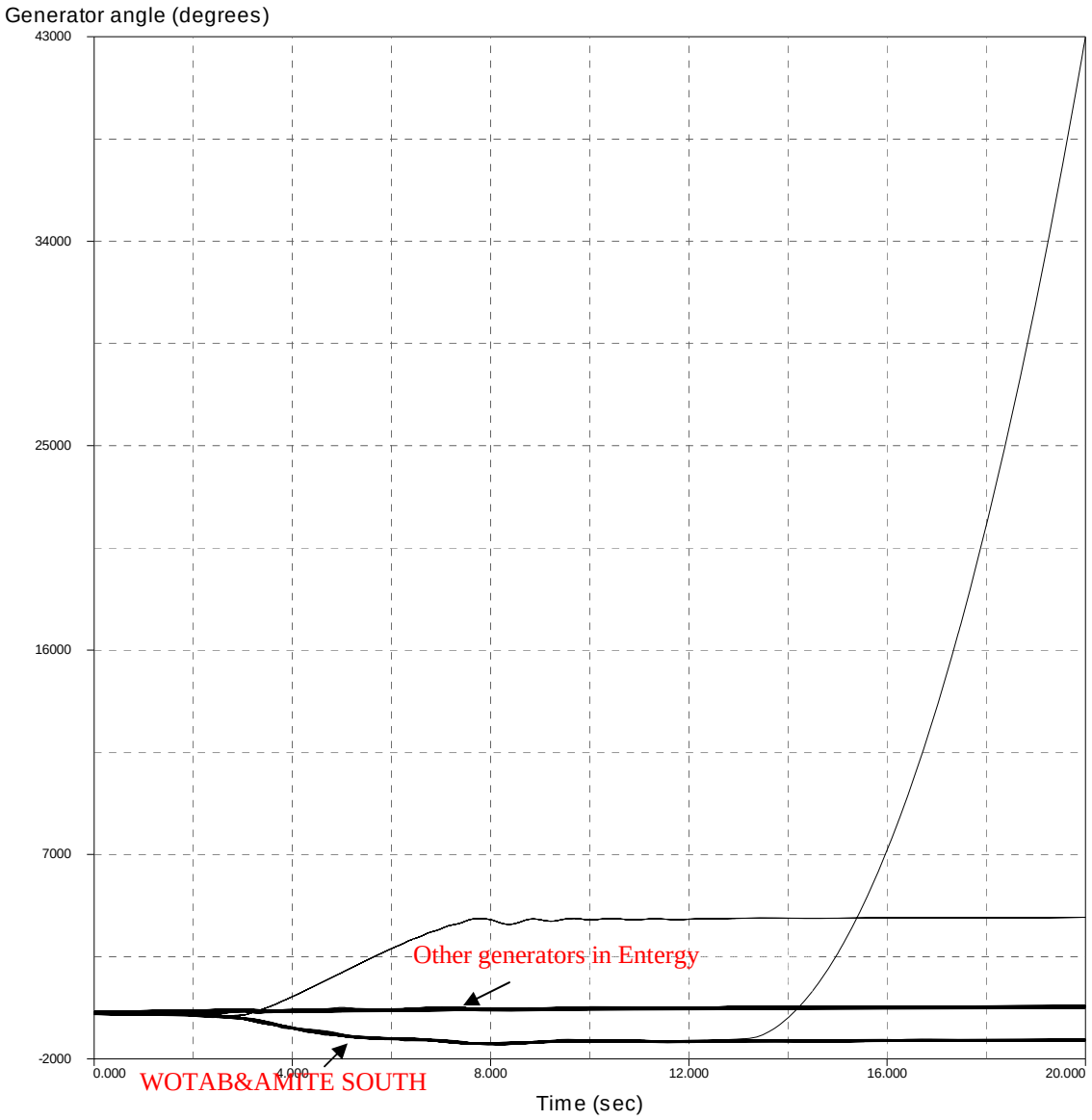

Figure 3-19: (a) Relative Generator Angles in the Entergy System

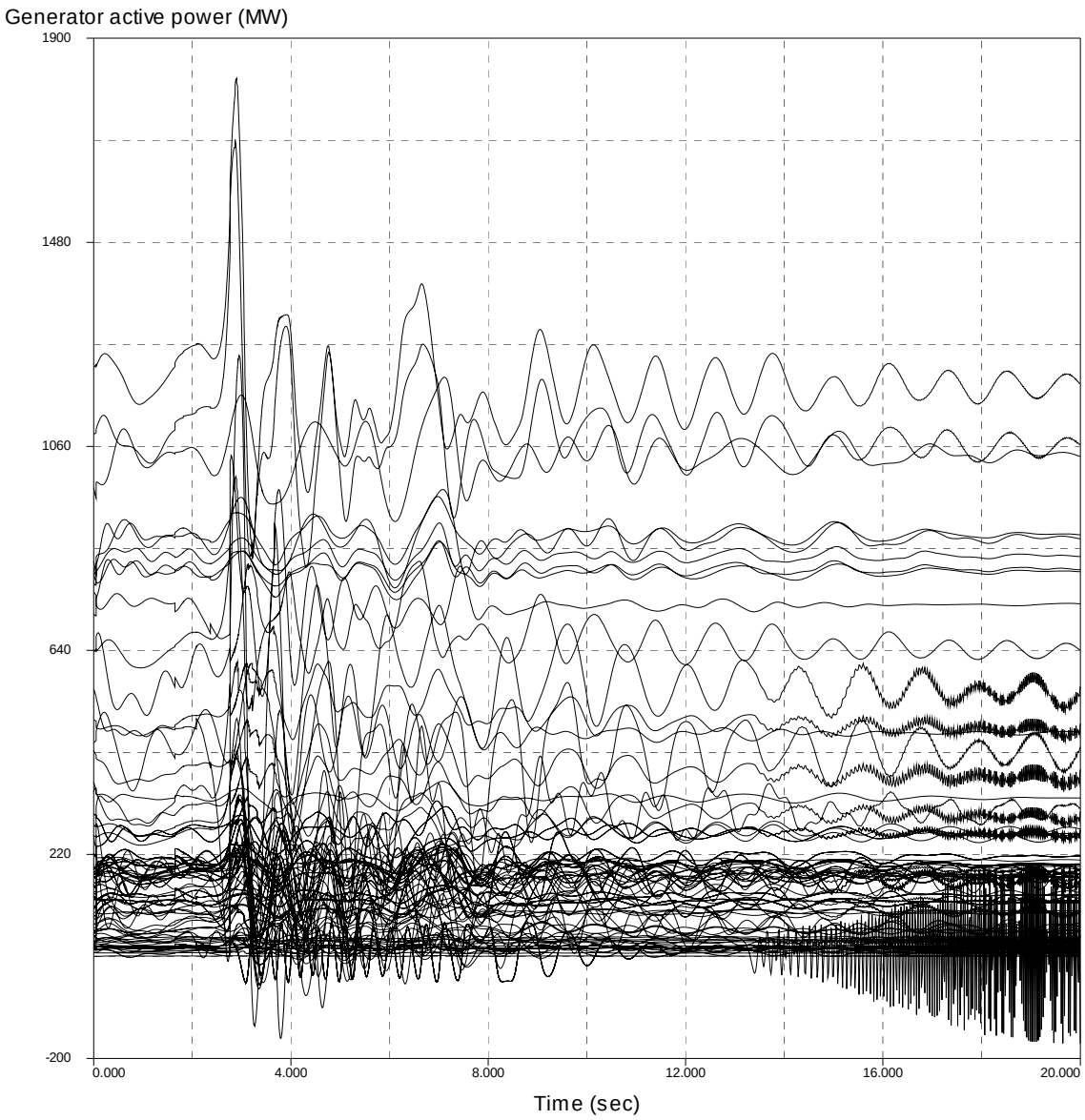

Figure 3-20: (b) Generator Active Power Outputs

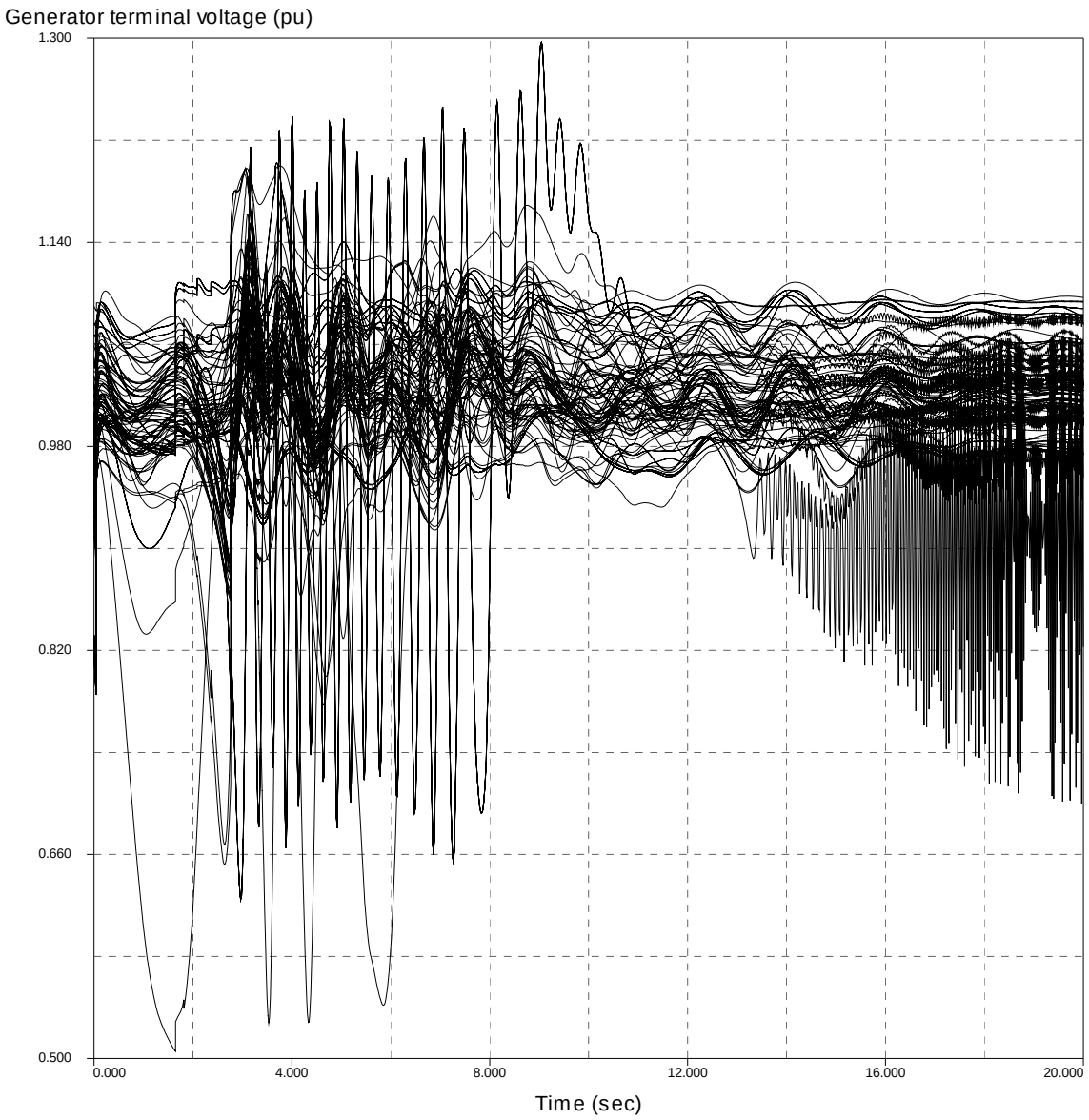

Figure 3-21: (c) Generator Terminal Voltages

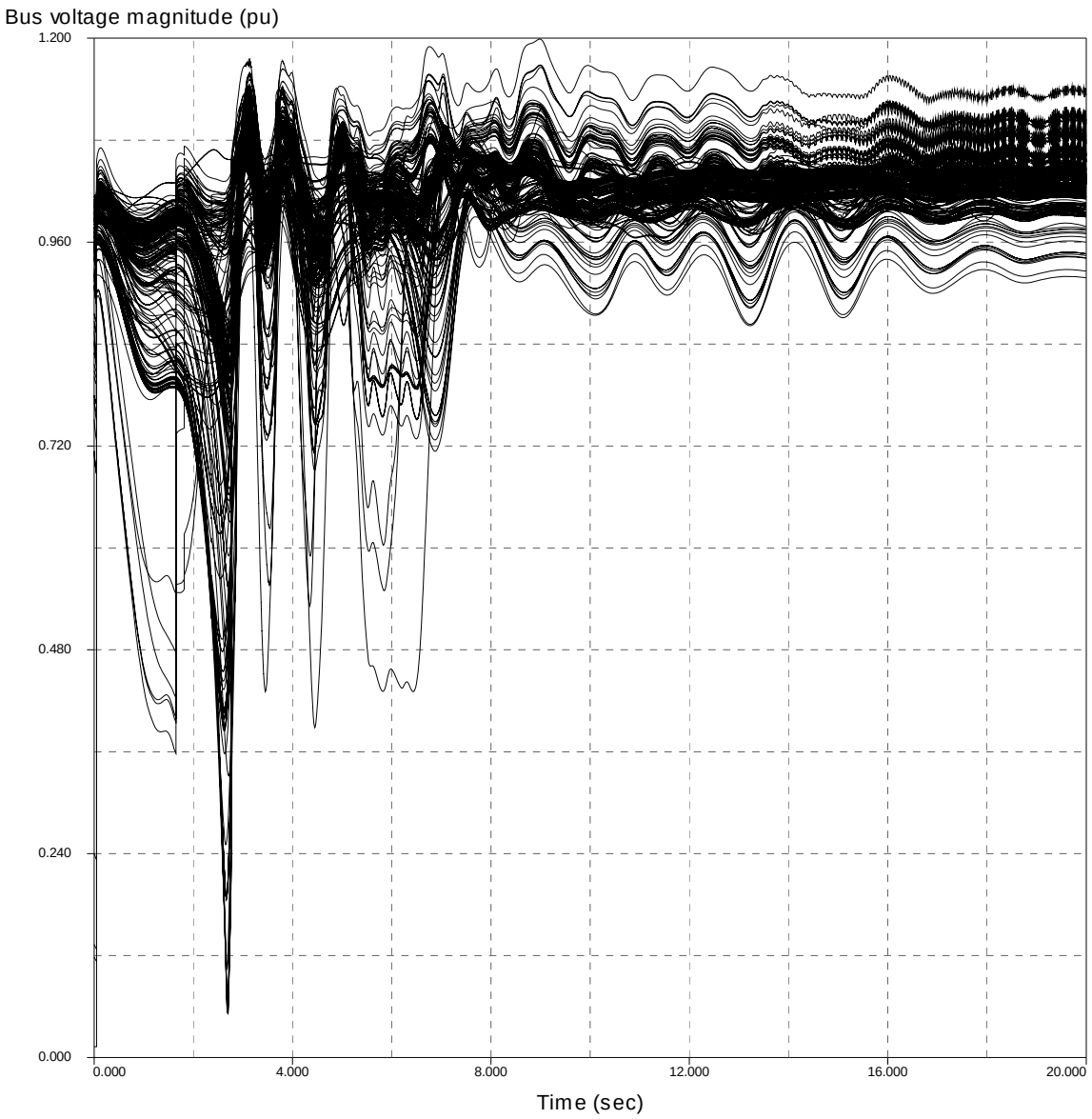

Figure 3-22: (d) Bus Voltage Magnitudes (200 kV and Above)

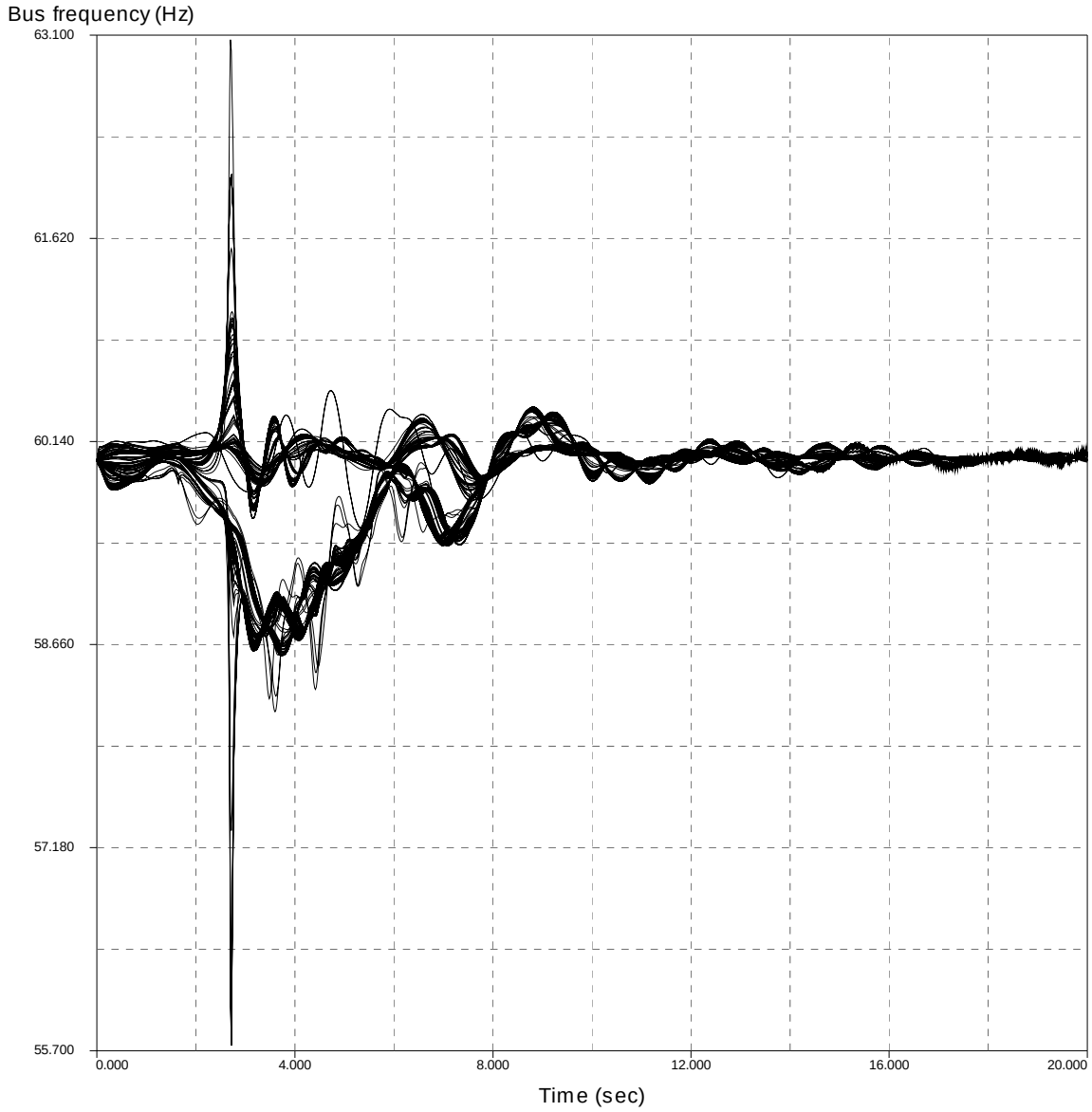

Figure 3-23: (e) Bus Frequencies (200 kV and Above)

The above plots show that two major generator groups have been formed in the Entergy system and two individual generators run away, 97704 (SAM RAYBURN 4) and 99183 (MURRAY12). Although the whole Entergy system is finally separated into two islands with relatively stable performance, severe oscillations still exist in the generator active power outputs and terminal voltages. Also, a large amount of load was shed during this uncontrolled separation phenomenon, which is **3970.52 MW+ 1238.57 MVAr** in the Entergy area. The load shedding effects in the other operational areas are not monitored. This critical contingency causes severe disturbance to the system and the following procedures are used to illustrate the proposed controlled separation scheme in terms of both of the two important issues, “when to island” and “where to island”.

3.4.2 Database Generation & DT Performance

Focusing on the above critical contingency, a database is generated to train DTs with good prediction performance. To improve robustness, 9 more OCs for each of the original 24 operating conditions are created based on the original ones. This OC creation step does not change system topology and equipment status for these OCs since the equipments that are not in service may be scheduled for maintenance and should not be turned on in such cases. Therefore, all the loads in the Entergy area are randomly changed within ±10 % range of their original values. Once all the load values in the Entergy area are modified, power flows are re-solved in PSAT and saved to a new data file and only the reasonable OCs are saved for further simulations. Therefore, 216 more OCs are generated.

In addition, fault locations on the branch and the sequence of the two faults are also changed for transient stability simulations at the 240 created OCs. For example, the outages of line A-B and line C-D may cause severe disturbances in the system. The first line is assumed to be out of service at time -0.5 seconds and power flow can converge successfully, which indicates the system has reached another operating point without this line. At time t = 0 seconds, a 3 phase fault is placed on line C-D by changing the fault locations, from 0%, 10%, 20%... to 100%. Also, the reverse sequence of the two line outages are simulated, which is to assume line C-D is out of service first and place the second fault on line A-B by changing the fault locations on line A-B. As a result, the two-line outage case in CENTRAL area contains a total number of 2*11*240 = 5280 transient simulations. The simulation length is set to be 5 seconds instead of 20 seconds to reduce computational burden. This length of simulation should be long enough to observe the formation of generator groups and to determine if the case was “secure” or “insecure”. The post-contingency phase angle values on the buses above 200 kV across the Entergy system are calculated and recorded as predictors using the method discussed in Section 2.4. There are altogether 232 buses above 200 kV that are in service for all of the 240 OCs, which yields a total of 232*6 =1392 predictors. From the simulation results, all the unstable cases have a unique unstable pattern with the same group of generators, which make the prediction objective quite clear. There are 220 out of 5280 cases that lead to unstable swings. With all of these predictors and the simulation results, a database is generated to train DTs for transient stability prediction.

A final decision tree is then trained for the above database, which is shown in Figure 3-10. The result shows that the prediction accuracy is 100% with only one critical splitting rule, B98606_V1, which represents the first relative phase angle velocity value on bus 98606 after fault clearance. In addition, the only CSR has several competitors with equal performance and they are shown in Table 3-4.

Table 3-4: Equivalent CSRs in DT1

CSRs	Bus name
98256_V1	6BELL HE 230.
98222_V1	6TP.GRAN 230.
98249_V2	6A.A.C. 230.
98472_V1	6G5EXXON 230.

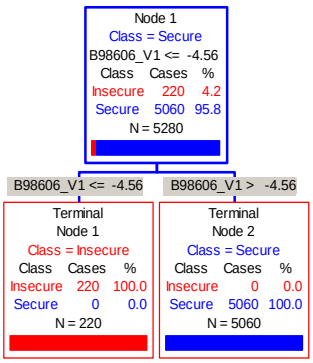

Figure 3-24: DT1 Trained for Two Line Outages in CENTRAL Area

After examining the locations of these buses, an important observation is that these buses are all very close to a group of large generators in the AMITE SOUTH area and they can effectively reflect the generator swing patterns under this critical contingency within the first few cycles following fault clearance. Therefore, they can serve as good candidates for new PMU locations for real time transient stability prediction.

Another test has been conducted on the critical contingency (loss of line 97717 to 99162 and line 98107 to 98109) that causes the generators in the WOTAB area to swing against the rest of the Entergy system. The same 240 OCs are used for transient simulation and a similar database has been constructed. There are 187 out of 5280 cases that lead to out of step swings. The final DT also shows excellent performance on the created database with 100% of accuracy, which is shown in Figure 3-11.

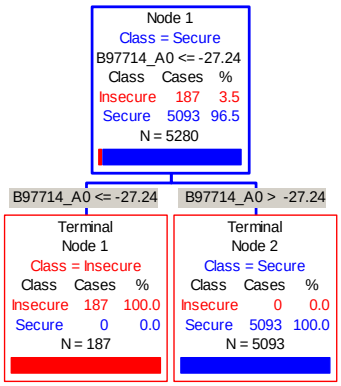

Figure 3-25: DT2 Trained for Two Line Outages in WOTAB Area

The bus locations for the CSR and its equivalent competitors (shown in Table 3-5) in DT2 are located near a large group of generators in the WOTAB area. Therefore, the two DTs have shown that phase angles on high voltage buses are good predictors of the impending loss of synchronism in the Entergy system if one decision tree is trained especially for each of the critical contingencies.

Table 3-5: Four Equivalent CSR Buses for DT2

Bus No.	Bus name
97714_A0	China 230 kV
97567_A0	PORTER 230 kV
97478_A0	JACINTO 230 kV
97744_A0	GEOTOWN 230 kV

3.4.3 Controlled Separation Scheme

Since the whole Entergy system is strongly coupled with the eastern interconnected power system in the U.S., an equivalent model that only covers the Entergy area is desired to search for the optimal islanding cut set using the automatic program. For the power flow files provided, all the inter-area branches that connect the Entergy area to other areas are identified first. For each of these lines, an equivalent load is inserted at the Entergy System boundary bus. The value of this equivalent load is exactly the same as the P and Q flows on the corresponding branch. After the loads are inserted, all these inter-area lines are disconnected. The equivalent model has shown good match in power flows when compared to the original power flow file.

With the equivalent system model, the slow coherent generator grouping information is then obtained using DYNRED, a function in PSAPAC that can identify coherent generators. Two groups of generators are defined for the Entergy system and the automatic islanding program identifies an optimal islanding path, which is listed below.

Table 3-6: Optimal Controlled Islanding Cut Set

No.	From Bus	To Bus	F.B. Name	T.B. Name
1	50024	99221	CARROLL4 138.	4RINGLD 138.
2	97717	99162	8HARTBRG 500.	8MTOLIV 500.
3	50070	98652	FRONTST6 230.	6MICHO 230.
4	50106	50171	MADISON6 230.	RAMSAY 6 230.
5	50106	50109	MADISON6 230.	MANDEV 6 230.
6	98235	99027	8MCKNT 500.	8FRKLIN 500.
7	98482	98484	3INDEPD 115.	3HAMMND 115.
8	99108	99110	3JENA 1 115.	3STAND 115.
9	99113	99116	6WINFLD 230.	6MONTGY 230.

Tripping these 9 lines will result in the desired two islands that separate the CENTRAL area and WOTAB&AMITE SOUTH area. The design and execution of the controlled separation scheme is to prevent the cascading events caused by conventional out of step impedance relays, therefore, the islanding scheme is triggered 0.5 second after the fault clearance, before the first line is tripped due to the first out of step impedance relay action at 1.65 seconds. These 9 lines are assumed to be tripped simultaneously using transfer trips. The system performance with this islanding scheme is shown below:

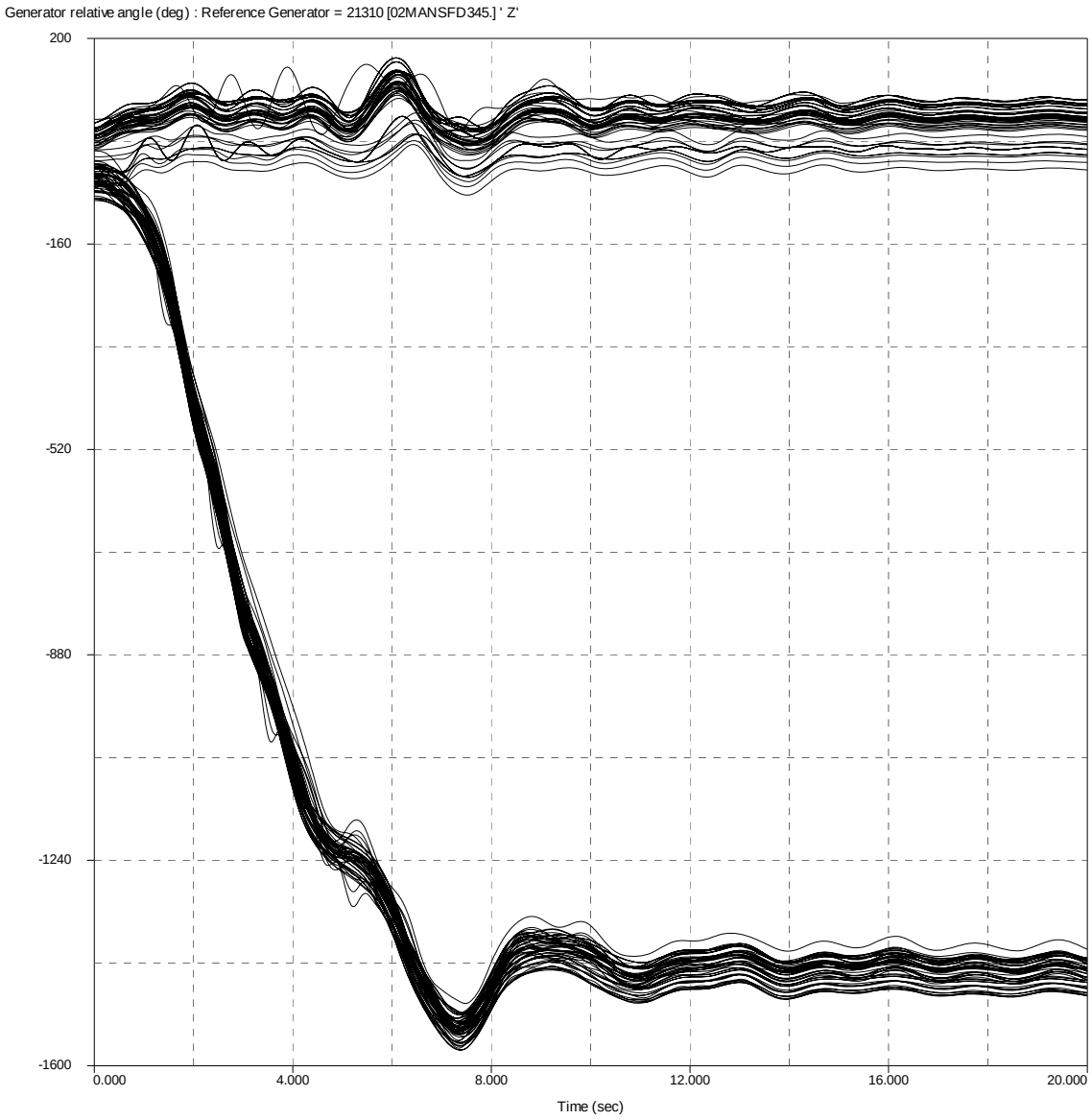

Figure 3-26: (a) Relative Generator Angles in the Entergy System

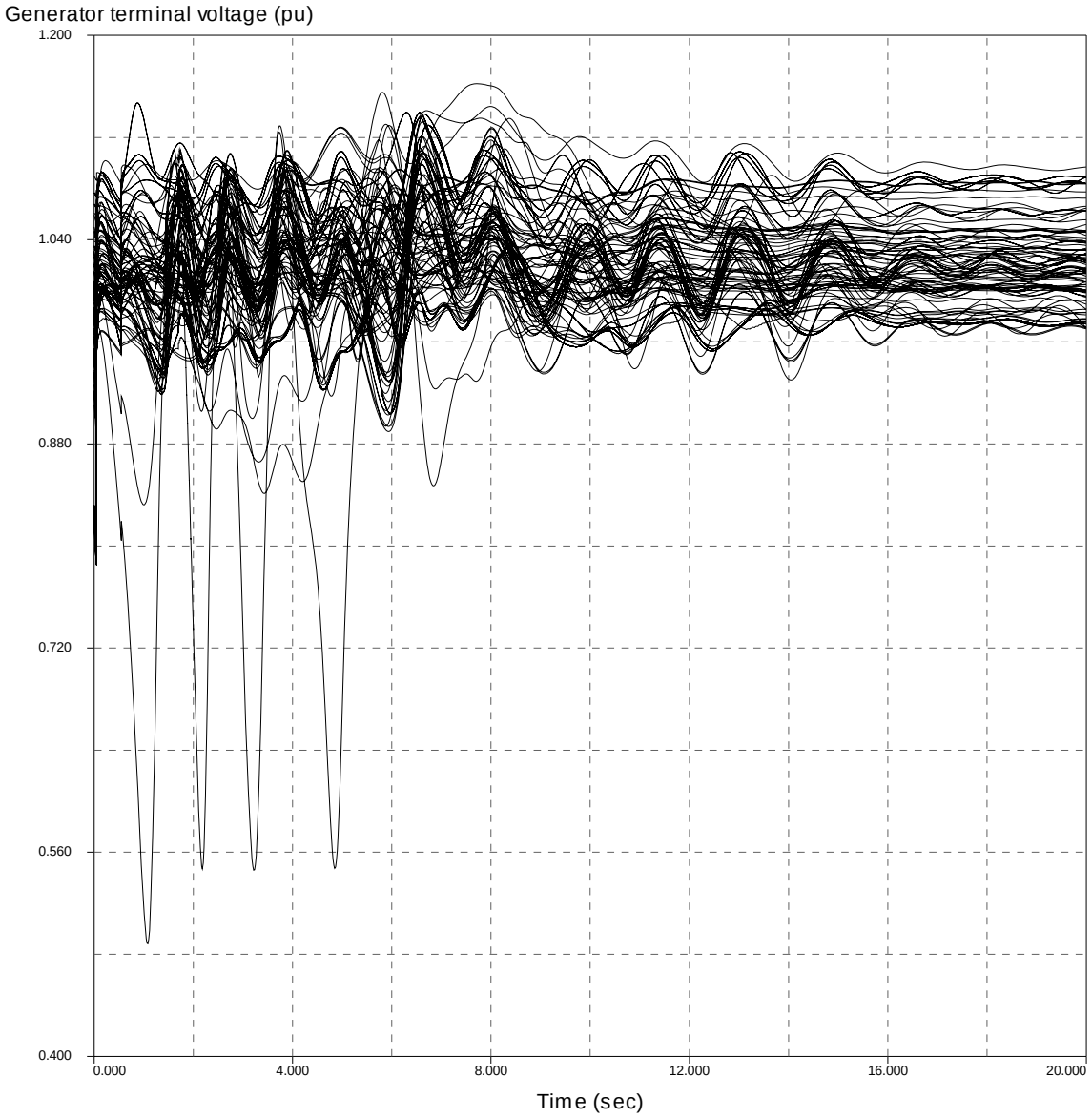

Figure 3-27: (b) Generator Terminal Voltages

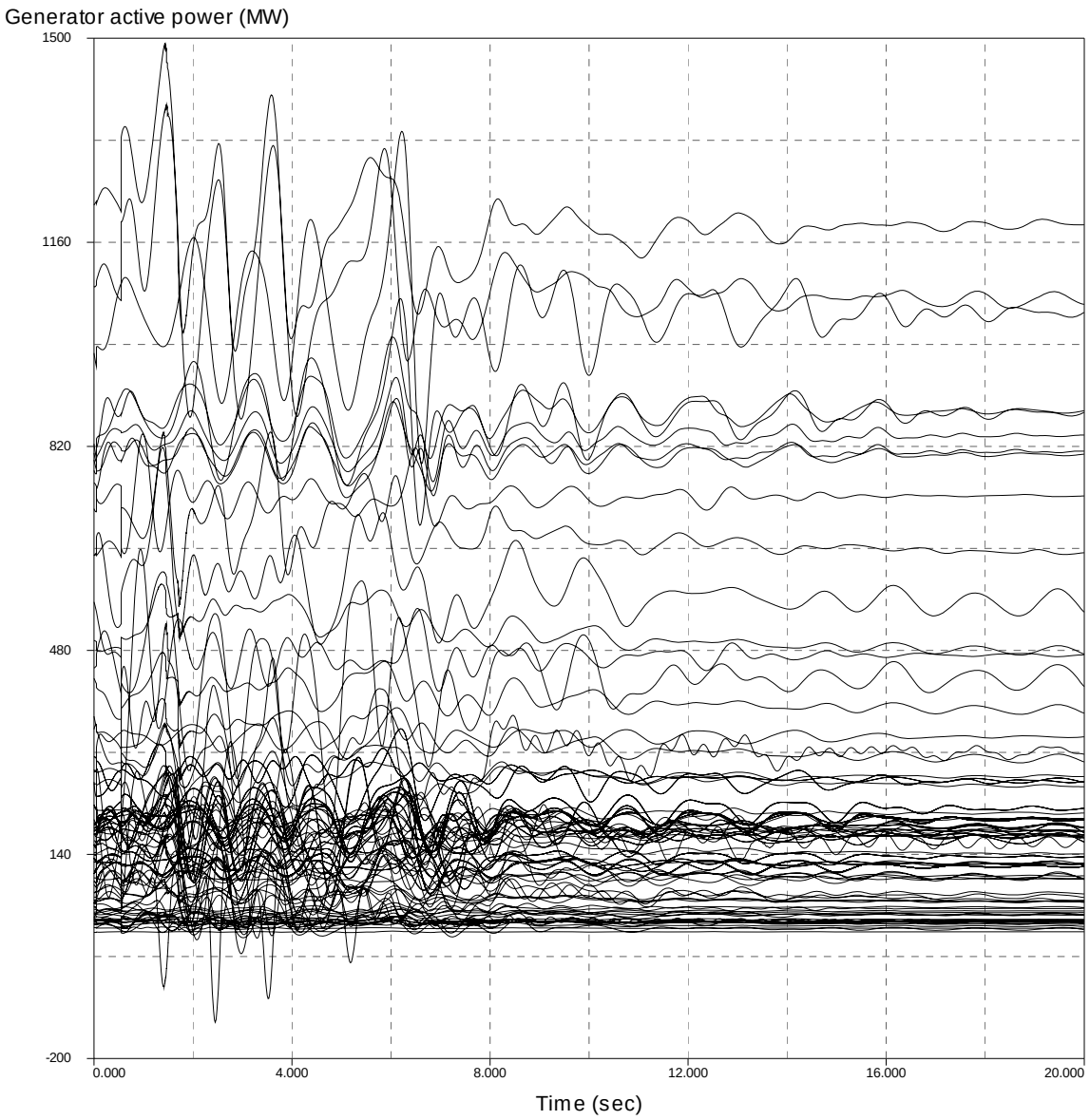

Figure 3-28: (c) Generator Active Power Outputs

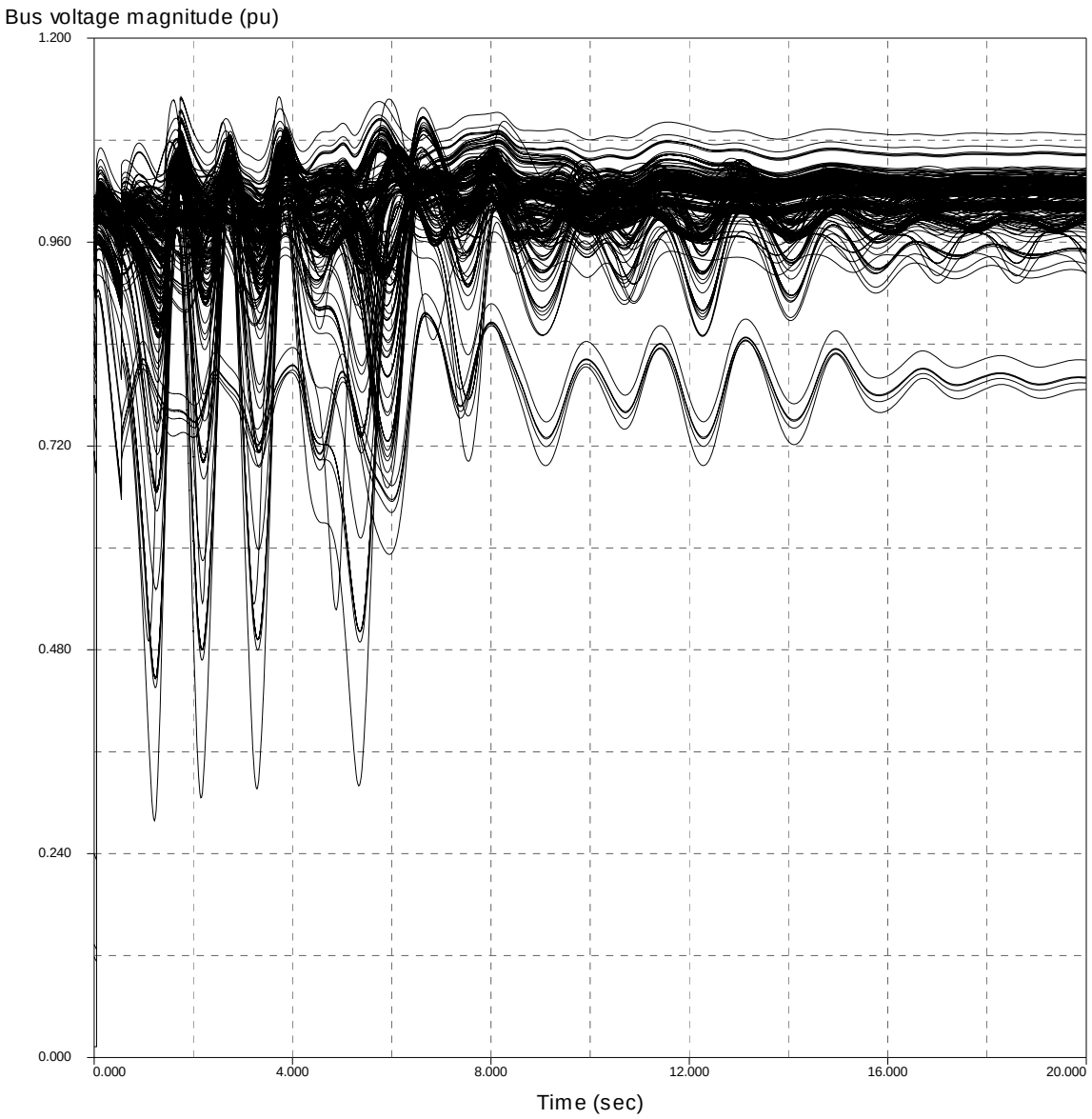

Figure 3-29: (d) Bus Voltage Magnitudes (200 kV and above)

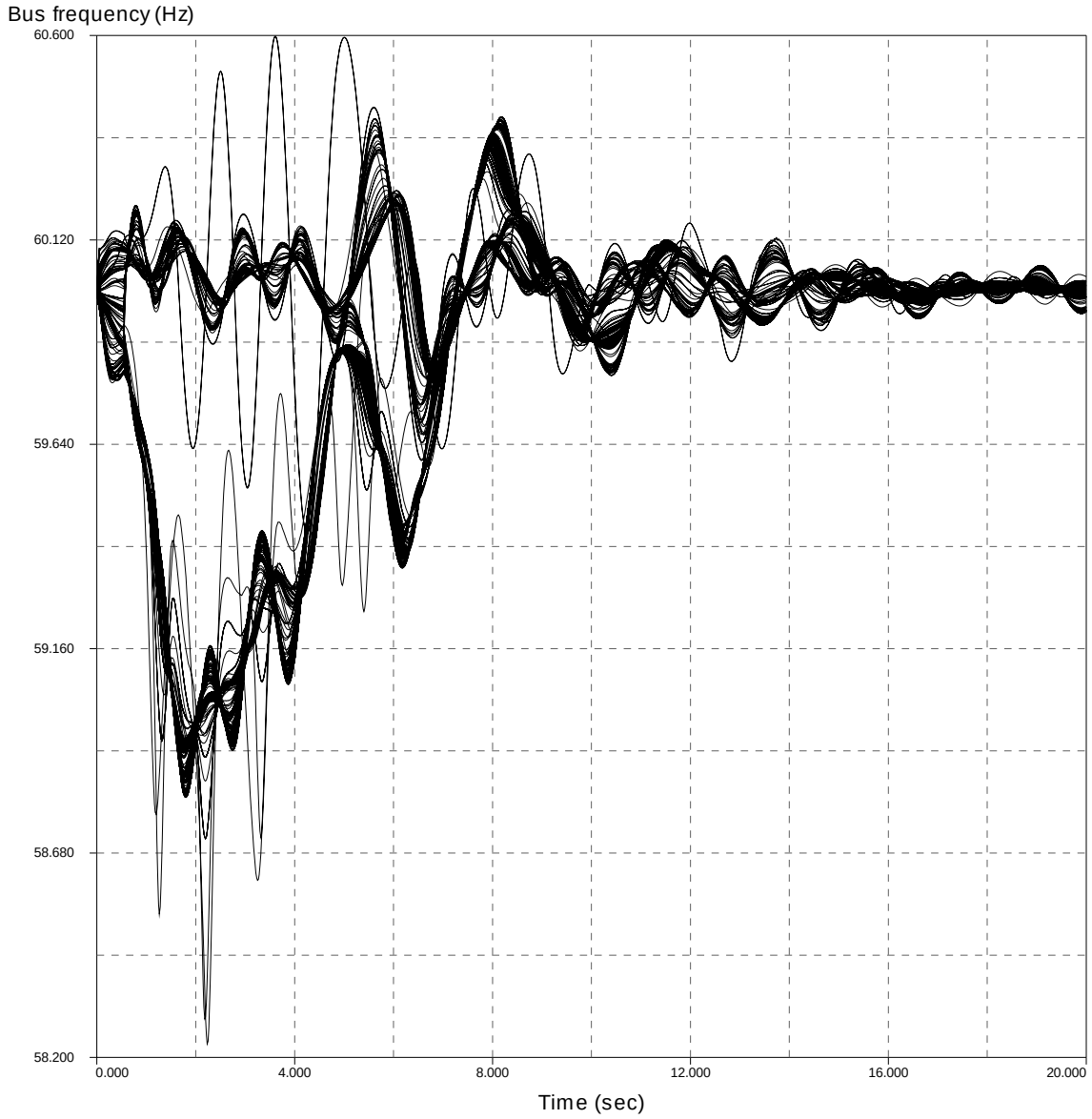

Figure 3-30: (e) Bus Frequency (200 kV and above)

With this controlled islanding scheme, the Entergy system can be successfully stabilized in a faster manner and with less oscillation. No impedance relay settings are violated in this simulation. The total amount of load shedd is 2561.18 MW+ 795.89 MVAr, which saves about 1500 MW and 300 MVAr over the uncontrolled islanding case discussed in Section 3.4.1. In addition, the generators in each group operate in synchronism without any system separation (Figure 3-12(a)) and the generator active power outputs damp out more quickly (Figure 3-12(c)). The only problem of concern is that four buses near the islanding cut set (**99113**-WINNFIELD 230, **99162**-MOUNT OLIVE 500, **99163**-MOUNT OLIVE 230 and **99169**-DANVILLE 230 (LPL)) have low voltage magnitudes after system separation (Figure 3-12(d)).

The main reason is that this islanding strategy does not avoid tripping the line from the bus 97717 to bus 99162, which carries about 1000 MW active power from the CENTRAL area to WOTAB area. However, the reactive power flows in the other direction and in the amount of about 300 MVAr. Following the outage of the two critical 500 kV lines, the loss of this 500 kV line will result in the loss of reactive power support to the MT. OLIVE area and cause the low voltages. Therefore, sufficient reactive power support is necessary immediately after system separation. This is an important factor in the design of the controlled separation scheme. A test has been conducted by switching on several shunt elements for reactive power support and the low voltage cases can be avoided.

From the above observations and analysis, the properly trained DTs are able to provide a fast and accurate prediction result to arm the controlled islanding strategy once the severe disturbance occurs. Controlled islanding is the last line of defense to stabilize the whole power system, which provides a promising control strategy for system operators under extreme system conditions. Once properly designed, it can save a large amount of load from being shed and effectively stop the cascading events.

4 References

[1] Energy Information Administration, "World Net Conventional Thermal Electricity Generation (Billion Kilowatthours), 1980-2005," [Online]. Available: http://www.eia.doe.gov/iea/elec.html.

[2] P. M. Anderson and A. A. Fouad, *Power System Control and Stability-Second Edition*, Piscataway, NJ: A JOHN WILEY & SONS, 2003.

[3] U.S. – Canada Power System Outage Task Force, "Final Report on the August 14th Blackout in the United States and Canada: Causes and Recommendations," [Online]. Available: https://reports.energy.gov/

[4] P. Kundur, *Power System Stability and Control*, New York: McGraw-Hill, 1994.

[5] Westinghouse Electric Corporation, *Applied Protective Relaying*, Coral Springs, Florida, 1982.

[6] J. Lewis Blackburn, *Protective Relaying – Principles and Applications*, Bothell, Washington: Marcel Dekker, 1987.

[7] Haibo You, Vijay Vittal and Xiaoming Wang, "Slow Coherency-Based Islanding," IEEE Trans. Power Syst., vol. 19, no. 1, February 2004.

[8] Haibo You and Vijay Vittal, "Self-Healing in Power Systems: An Approach Using Islanding and Rate of Frequency Decline-Based Load Shedding," IEEE Trans. Power Syst., vol. 18, no. 1, February 2003.

[9] M. M. Adibi, R. J. Kafka, Sandeep Maram and Lamine M. Mili, "On Power System Controlled Separation," IEEE Trans. Power Syst., vol. 21, no. 4, November 2006.

[10] Steven Rovnyak, Stein Kretsinger, James Thorp and Donald Brown, "Decision Tree for Real-Time Transient Stability Prediction," IEEE Trans. Power Syst., vol. 9, no. 3, August 1994.

[11] Nilanjan Senroy, "Emergency State Stability Control of Power Systems Through Intelligent Islanding," Ph.D. thesis, the Department of Electrical Engineering, Arizona State University, Tempe, AZ, 2006.

[12] Y. Morioka, K. Tomiyama, H. Arima, K. Sawai, K. Omata, T. Matsushima,K. Takagi, A. Ishibashi and H. Saito, "System Separation Equipment to Minimize Power System Instability Using Generator's Angular-Velocity Measurements," IEEE Trans. Power Delivery., vol. 8, no. 3, July 1993.

[13] A.G. Phadke, "Synchronized Phasor Measurements in Power Systems," IEEE Computer Applications in Power, vol. 6, no. 2, pp. 10-15, April 1993.

[14] R. O. Burnett, M. M. Butts and P. S. Sterlina, "Power system applications for phasor measurement units," IEEE Computer Applications in Power, vol. 7. no. 1, 1994.

[15] A.P. Sakis Meliopoulos, George J. Cokkinides, Floyd Galvan, Bruce Fardanesh and Paul Myrda, "Delivering Accurate and Timely Data to All – Model-Based Substation Automation Applications for Advanced Data Availability," IEEE Power & Energy Magazine, pp. 74-86, May/June 2007.

[16] Naoto Kakimoto, Masahiro Sugumi, Tohru Makino and Katsuyuki Tomiyama, "Monitoring of Interarea Oscillation Mode by Synchronized Phasor Measurement," IEEE Trans. Power Syst., vol. 21, no. 1, pp. 260-268, Feb. 2006.

[17] Liang Zhao and Ali Abur, "Multiarea State Estimation Using Synchronized Phasor Measurements," IEEE Trans. Power Syst., vol. 20, no. 2, pp. 611-617, May 2005.

[18] J. W. Ballance, B. Bhargava, G. D. Rodriguez, "Monitoring Power System Dynamics using Phasor Measurement Technology for Power System Dynamic Security Assessment," in Proc. IEEE Power Tech Conference, Bologna, Italy, Jun. 2003.

[19] B. Milosevic, M. Begovic, "Voltage-stability Protection and Control using a Wide-area Network of Phasor Measurements," IEEE Trans. Power Syst., vol. 18, no. 1, pp.121-127, Feb. 2003.

[20] L. Breiman, J. Friedman, R. A. Olshen and C. J. Stone, Classification and Regression Trees, Wadsworth International Group, 1984.

[21] K. Sun, S. Likhate, V. Vittal, V. Kolluri and S. Mandal, "An Online Dynamic Security Assessment Scheme Using Phasor Measurements and Decision Trees," IEEE Trans. Power Syst., vol. 22, no. 4, pp.1935-1943, Nov. 2007.

[22] A. R. Khatib, R. F. Nuqui, M. R. Ingram, A. G. Phadke, "Real-time Estimation of Security from Voltage Collapse using Synchronized Phasor Measurements," in Proc. IEEE Power Eng. Soc. General Meeting, 2004, vol. 1, pp.582-588.

[23] L. Wehenkel, M. Pavella, E. Euxibie, et al, "Decision Tree Based Transient Stability Method A Case Study," IEEE Trans. Power Syst., vol. 9, no. 1, pp.459-469, Feb. 1994.

[24] L. Wehenkel, M. Pavella, "Decision Trees and Transient Stability of Electric Power Systems," Automatica, vol. 27, no. 1, pp.115-134, Jan., 1991.

[25] T. Cutsem, L. Wehenkel, M. Pavella, B. Heilbronn, M. Goubin, "Decision Tree Approaches to Voltage Security Assessment," IEE Proceedings, vol. 140, no. 3, pp.189-198, May 1993.

[26] S. Rovnyak, C. Taylor, Y. Sheng, "Decision Trees Using Apparent Resistance to Detect Impending Loss of Synchronism," IEEE Trans. Power Syst., vol. 15, no. 4, pp 1157-11162, Oct. 2000.

[27] K. R. Padiyar and S. Krishna, "On-Line Detection of Loss of Synchronism Using Locally Measurable Quantities," Transmission and Distribution Conference and Exhibition 2001, Vol. 1, pp. 537-542.

[28] N. Senroy, G. T. Heydt and V. Vittal, "Decision Tree Assisted Controlled Islanding," IEEE Trans. Power Syst., vol. 21, no. 4, pp 1790-1797, Nov. 2006.

[29] E. M. Voumvoulakis and N. D. Hatziargyriou, "Decision Trees-Aided Self-Organized Maps for Corrective Dynamic Security," IEEE Trans. Power Syst., vol. 23, no. 2, pp 662-630, May 2008.

[30] J. H. Chow, Time-Scale Modeling of Dynamic Networks with Applications to Power Systems, Berlin Heidelberg, New York: Springer-Verlag, 1982.

[31] Bo Yang, “Slow Coherency Based Graph Theoretic Islanding Strategy,” Ph.D. Thesis, the Department of Electrical Engineering, Arizona State University, Tempe, AZ, 2007.

[32] DSATools Dynamic Security Assessment Software. [Online]. Available: http://www.dsatools.com/

[33] CART for Windows V5.0 – User’s Guide, Salford Systems, CA.

[34] P Plus Corporation, Release Notes for the Dynamic Reduction Program (DYNRED) V5.3, Electric Power Research Institute (EPRI), Palo Alto, CA.

[35] TSAT Transient Security Assessment Tool V7.0 Users Manual, Powertech, Canada.

Appendix A. Impedance Relay Models in TSAT

This appendix introduces the default impedance and distance relay models in TSAT and a user defined model for out of step impedance relay is constructed. They are discussed separately in the following two parts:

TSAT version 7.0 has the capability of modeling protective impedance and distance relays in a modern power system. These relay data need to be prepared in a separate dynamic data file that works in parallel with the provided dynamic file during transient simulation. The data format of impedance and distance relay models are explained below.

IBUS1, 'DIST', I, IBUS2, ITYPE, DT1, DT2, DT3, DT4, DT5, DT6, DT7, DT8, TRC /
Where
BUS1 – From bus number of the branch
BUS2 – To bus number of the branch
I - ID of the branch
ITYPE - Flag to indicate relay type:
= 0 or 1: impedance relay (default).
= 2: distance relay.

Depending on the relay type, parameters DTi (i = 1, . . ., 8) and TRC are interpreted differently:

For impedance relay (ITYPE = 0 or 1): referring to Figure A-1
DT1 - CT, center location of Circle T in per unit on system MVA base.
DT2 - Angle AT in degrees.
DT3 - ZT, diameter of Circle T in per unit on system MVA base.
DT4 - TT, Circle T tripping time in cycles.
DT5 - CB, center location of Circle B in per unit on system MVA base.
DT6 - Angle AB in degrees.
DT7 - ZB, diameter of Circle B in per unit on system MVA base.
DT8 - TB, Circle B tripping time in cycles.
TRC - Time delay for line reclosing in cycles. If TRC is nonzero, the tripped line will be reclosed after TRC cycles. There is no reclosing if TRC = 0.

For distance relay (ITYPE = 2): referring to Figure A-2
DT1 - R/X ratio.
DT2 - R1, ZONE 1 reach (default value = 0.8).
DT3 - R2, ZONE 2 reach (default value = 1.2).
DT4 - AMIN, minimum torque angle that activates the relay logic in degrees (default value = 60 degrees).
DT5 - AMAX, maximum torque angle in degrees (default value = 70 degrees).
DT6 - Not used for this relay.
DT7 - Not used for this relay.
DT8 - T, relay time delay in cycles.
TRC - Time delay for line reclosing in cycles. If TRC is nonzero, the tripped line will be reclosed after TRC cycles. There is no reclosing if TRC = 0.

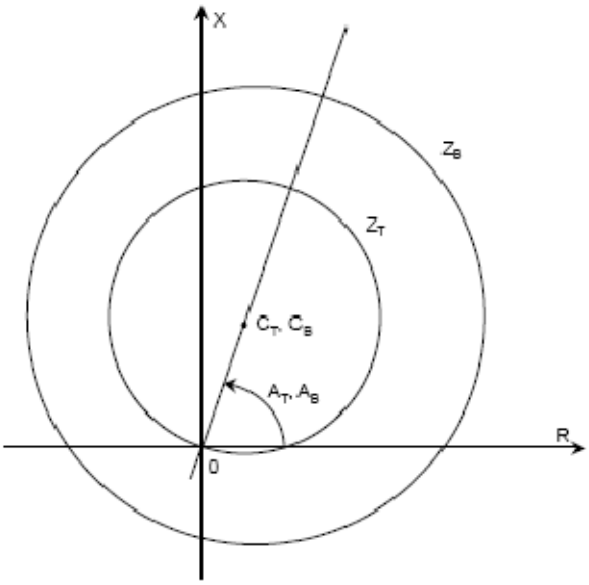

Figure A. 1 Impedance Relay Diagram

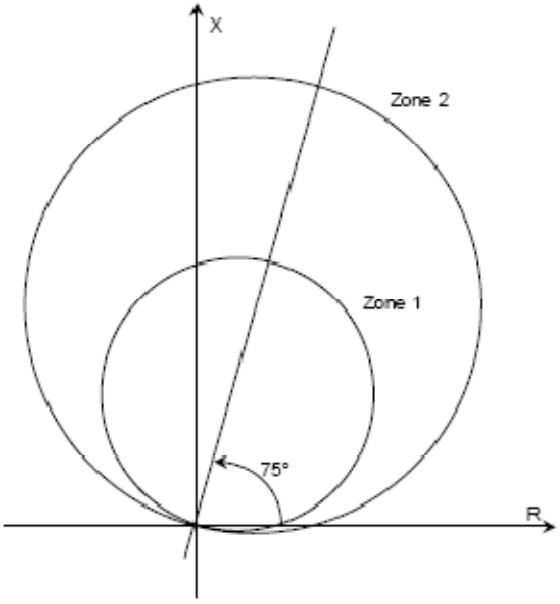

Figure A. 2 Distance Relay Diagram

The impedance and distance relays could be equivalent by adjusting the settings of Zone1 and Zone2. Therefore, only impedance relay models are set up (set ITYPE=1) in this project. The line impedance values (R+jX) in pu on the system MVA base are read directly from the output file in PSAT. Zone1 is set to reach 80% of the apparent impedance, with angle setting equal to the line angle itself. Similarly, Zone2 is set to reach 120% of the monitored line. As a result, each impedance relay in the Entergy system has the following settings:

DT1- 40% of the line impedance in pu, on system MVA base, calculated from apparent impedance value in PSAT.

DT2- Angle of the monitored line in degrees.
DT3- 80% of the line impedance in pu, on system MVA base.
DT4- Set to 0 cycles. This timer indicates that if the impedance locus of the monitored line stays in Zone1 for 'DT4' cycles after entering Zone1, the circuit breaker will trip the line.
DT5- 60% of the line apparent impedance in pu, on system MVA base.
DT6- Angle of the monitored line in degrees, same as DT2.
DT7- 120% of the line apparent impedance in pu, on system MVA base.
DT8- set to 20 cycles. This timer means if the impedance locus of the line stays in Zone 2 for 20 cycles after entering Zone 2, the circuit breaker will trip the line.
TRC is set to zero, assuming there is no reclosing device.

This is the main principle of impedance relay settings in TSAT, however, this model itself does not have the capability of setting the circuit breaker operation time. Therefore, a user defined model is set up to accomplish this goal. This UDM model is given in Figure A-3. Only Zone1 (reach 80%) and Zone2 (reach 120%) settings of a transmission line are considered. The timers for Zone1 and Zone2 are set to be 0 cycles and 20 cycles respectively. The Zone3 setting is ignored. The circuit breaker (CB) operation time is set to be 5 cycles uniformly across the whole Entergy area.

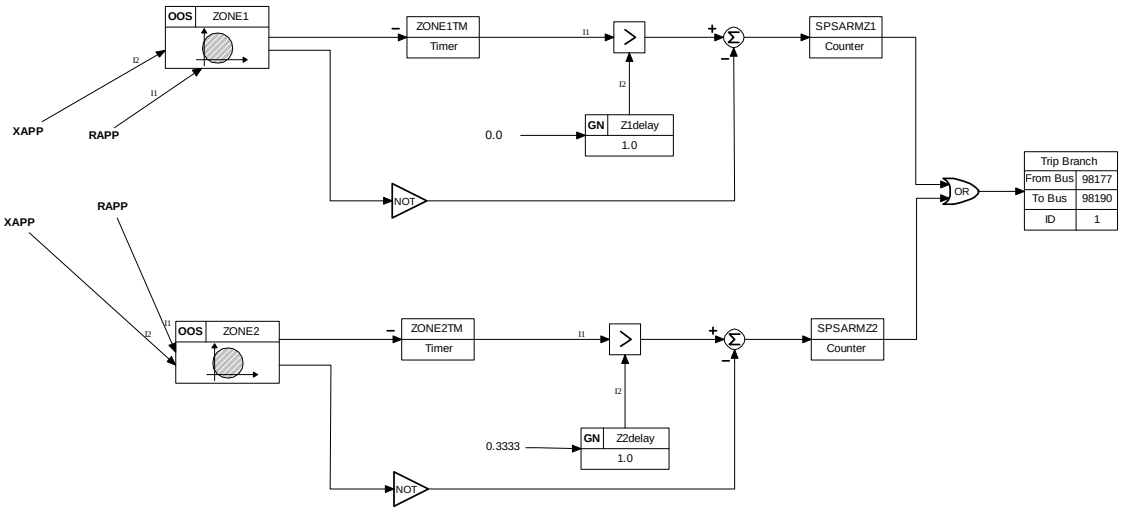

Figure A. 3 UDM model for Impedance Relays with Circuit Breaker Time

The two inputs are the real time R and X values of the monitored line, RAPP and XAPP respectively. The output is a signal to trip the line. The monitored line will be tripped once any of the following two requirements is met:

1) Impedance locus (R+jX) enters Zone1 (for 0 seconds);
2) Impedance locus enters Zone2 and stays in Zone2 for 20 cycles.